THESIS

Investigation of the Role of Intra-Abdominal Pressure and Lifting Velocity in Spine Stability: A Finite Element Study

Sean Murray

Department of Biological and Biomedical Engineering

McGill University

Montreal, Quebec, Canada

April, 2025

A Thesis submitted to McGill University in partial fulfillment of the requirements of the degree of Master of Engineering (M.Eng.) in Biological and Biomedical Engineering.

Acknowledgements

First, I would like to acknowledge the support of my friends and colleagues in the Musculoskeletal Biomechanics Research Lab. It has been a transitional period within the lab, with many students moving on during my time here. Looking back on it, I see my master's in three phases. My first year was heavily focused on learning and understanding what it means to be a graduate student. For this part, I would especially like to acknowledge Brittany Stott, who set the best example by her knowledge, organization, time management, writing, professionalism, and all else. The second phase, my second year, was marked by fewer numbers in the lab and a lot more stress. I thank Siril Dukkipati for helping me work through this tougher phase with his guidance, insight, motivation, and by simply being a great desk neighbour. Finally, the closing few months have been a period of excitement marked by an incredible trip to Austria to present my research, more social outings as a lab group, and most notably the end of my thesis. For this last phase, I thank everyone in the lab for being a friend. These are the moments I will remember when I look back on my master's degree.

Ahead of it all, my supervisor, Professor Mark Driscoll, believed in my potential as a researcher and engineer. I extend my sincere gratitude for the opportunities provided and continued professional guidance. Our conversations sparked ideas that go beyond the work presented in this thesis and the work could not be done without his expertise and guidance.

I would also like to acknowledge the financial support provided by the Fonds de Recherches du Québec – Nature et Technologies (FRQNT). Their support on this project has allowed me to focus on my research without financial worries. In addition, I acknowledge the early support from the McCall MacBain Foundation. In no small way, their process and Finalist Award made me inquisitive and motivated about pursuing a master's degree to begin with.

Lastly, I would like to acknowledge and express gratitude to my family who helped to get me to this stage and get through it. My parents set the example for pursuing success in their professional and personal worlds simultaneously and achieving both. More than anyone, my girlfriend, Bianca, has been by my side through all of it and much, much more, including many late working nights during both my bachelor's and master's degrees. It is possible that I would have never left my desk had she not encouraged me to play tennis, go on an exciting trip, take a walk, or simply enjoy a movie night.

Contents

List of Figures

List of Tables

Acronyms

AF Annulus fibrosus.

EMG Electromyography.

FE Finite element.

FEM Finite element method.

FSU Functional spine unit.

IAP Intra-abdominal pressure.

IDP Intervertebral disc pressure.

IVD Intervertebral disc.

IVR Intervertebral rotation.

LBP Low back pain.

MVC Maximum voluntary contraction.

NP Nucleus pulposus.

ROM Range of motion.

TLF Thoracolumbar fascia.

WSACS World Society of the Abdominal Compartment Syndrome.

Abstract

Low back pain is a major health and economic burden, affecting up to 84% of people and raising costs of treatment for back conditions to over $315B per year in the USA. In the workplace, faster lifting is associated with greater risk of injury and intra-abdominal pressure (IAP), the pressure concealed within the abdominal cavity, is known to fluctuate transiently during lifting. The contribution of IAP toward spine stability at different loading rates remains largely unaddressed in biomechanical models, despite its apparent relevance in the multifactorial pathomechanism of LBP. This thesis models IAP's effects on spine stiffness during lifting at different speeds and extends the results to low back injury mechanics.

The thesis takes a two-part approach. In the first part, a non-linear finite element spine model, encompassing soft tissue and bone of the abdominal compartment, was developed and validated within the context of use against *in vivo*, *ex vivo*, and *in silico* comparators. In a transient simulation, lumbar stiffness is quantified, from the angular deviation from baseline trajectory in response to a perturbation moment, at varying IAP and movement speeds during lifting motion. The results showed that stability was more sensitive to IAP than movement speed, but that the relative importance of this effect grows with movement speed.

In the second part, a limitation of the model is addressed. By directly controlling IAP, force transfer from abdominal muscles through the thoracolumbar fascia (TLF) was neglected. TLF model form was investigated on its own by first addressing the lack of suitable anatomy-derived model via segmentation. Employing the finite element method, a fiber-embedded posterior TLF model was compared to an isotropic variation for its influence on lumbar spine stiffness. The effect of abdominal muscle force was analyzed to simulate lifting conditions. Results showed that the TLF contributes markedly to spine stiffness and, further, its composite construction facilitates myofascial force transfer through its continuities with abdominal muscles and effectively maximizes its stabilizing potential.

No model has captured all pathways by which IAP can impact spine stability. This thesis has advanced the state of modelling IAP and its interaction with the spine with a high-fidelity abdominal compartment. Different IAP-induced stability mechanisms are investigated but more work is needed to capture their biomechanics simultaneously. The virtual twin study showed that IAP creates a dynamic stability potential, by extension of its beneficial effects toward lumbar stiffness during lifting motion, and behaves like an airbag to limit displacements. Further, care should be taken to avoid altering TLF fiber structure in clinical practice and future modelling should capture the fiber mechanics. Ineffective abdominal muscle activation to generate IAP or poor timing during a lift could increase low back injury risk due to insufficient lumbar spine stability.

Résumé

La lombalgie représente un fardeau majeur sur les plans médical et économique, affectant jusqu'à 84% des individus et engendrant des coûts de traitement des pathologies dorsales dépassant 315 milliards de dollars par an aux États-Unis. Sur le lieu de travail, les mouvements de levée rapides sont associés à un risque accru de blessure, et la pression intra-abdominale (PIA), la pression exercée à l'intérieur de la cavité abdominale, est connue pour fluctuer de manière transitoire lors des levées. La contribution de la PIA à la stabilité de la colonne vertébrale à différents taux de chargement reste en grande partie inexplorée dans les modèles biomécaniques, malgré sa pertinence apparente dans le mécanisme pathomécanique multifactoriel de la lombalgie. Cette thèse modélise les effets de la PIA sur la rigidité de la colonne vertébrale lors des levées à différentes vitesses et étend les résultats à la mécanique des blessures lombaires.

La thèse adopte une approche en deux parties. Dans la première partie, un modèle non linéaire par éléments finis de la colonne vertébrale, intégrant les tissus mous et les os du compartiment abdominal, a été développé et validé dans le cadre de son utilisation à l'aide de comparateurs *in vivo*, *ex vivo* et *in silico*. Lors d'une simulation transitoire, la rigidité lombaire est quantifiée en mesurant la déviation angulaire par rapport à la trajectoire de base en réponse à un moment perturbateur, pour des valeurs variables de PIA et de vitesse de mouvement pendant les levées. Les résultats ont montré que la stabilité est plus sensible à la PIA qu'à la vitesse de mouvement, bien que l'importance relative de cet effet augmente avec la vitesse.

Dans la deuxième partie, une limitation du modèle est abordée : en contrôlant directement la PIA, le transfert de force des muscles abdominaux à travers le fascia thoraco-lombaire (FTL) a été négligé. La forme du modèle de FTL a été étudiée séparément en traitant d'abord l'absence d'un modèle anatomique adapté via une segmentation. À l'aide de la méthode des éléments finis, un modèle de la couche postérieure du FTL incorporant des fibres a été comparé à une variante isotrope pour évaluer son influence sur la rigidité lombaire dans des conditions de levée simulées. Les résultats ont révélé que le FTL contribue de manière significative à la rigidité de la colonne vertébrale et que sa structure composite facilite le transfert de force myofasciale par ses continuités avec les muscles abdominaux, maximisant ainsi son potentiel stabilisateur.

Aucun modèle existant n'a capturé tous les mécanismes par lesquels la PIA peut influencer la stabilité de la colonne vertébrale. Cette thèse fait progresser la modélisation de la PIA et de son interaction avec la colonne vertébrale grâce à un compartiment abdominal à haute fidélité. Différents mécanismes de stabilité induits par la PIA sont étudiés, mais des travaux supplémentaires sont nécessaires pour en saisir la biomécanique simultanément. L'étude virtuelle de cas-témoins a montré que la PIA crée un potentiel de stabilité dynamique, renforçant ses effets

bénéfiques sur la rigidité lombaire pendant les levées et agissant comme un coussin gonflable pour limiter les déplacements. Par ailleurs, il est crucial de préserver la structure des fibres du FTL en pratique clinique, et les modèles futurs devraient intégrer la mécanique des fibres. Une activation inefficace des muscles abdominaux pour générer la PIA ou un mauvais synchronisme lors d'une levée pourrait augmenter le risque de blessure lombaire en raison d'une stabilité insuffisante de la colonne vertébrale.

Author's Contribution

I, Sean Murray, certify that I am the primary author of all the material included in the manuscripts and chapters of this dissertation. Under the supervision of Professor Mark Driscoll, I designed, modeled, and validated the three-dimensional finite element models presented in each of the main chapters of the thesis and applied these models to address the study objectives. The manuscript-style thesis includes one manuscript currently under review in the journal Computers in Biology and Medicine. The second manuscript is an additional study that that has not yet been submitted to any journal. With supervisory support from Professor Mark Driscoll, I further contributed to conceptualization, investigation, test execution, data curation, analysis, and design of methodology for both manuscripts. Professor Mark Driscoll is co-author of both manuscripts and, in addition to the aforementioned support, contributed to review and editing, funding and resources, and project administration.

This dissertation contributes to a deeper understanding in the literature of the stabilizing potential of intra-abdominal pressure through various force transfer pathways. The research expands from an isolated view of the spine to include physiological context including the abdominal wall and thoracolumbar fascia. This could lead to more effective treatment and prevention options for low back pain patients and improved modeling techniques for engineers to build upon.

1 Introduction

As the leading cause of disability globally [1], low back pain (LBP) affects as many as 84% of people at some point in their lifetime [2]–[4]. According to the most recent Global Burden of Disease Study, approximately 619 million people reported symptoms of LBP worldwide and this number is expected to grow to 843 million by 2050 [1]. Clearly, it is a major health burden, but in addition to impacting quality of life, it has severe economic consequences. The direct costs of treatment for musculoskeletal back conditions has surpassed $315 billion per year in the USA and an estimated 30% is accredited to LBP [5]. The direct costs of care are surpassed by the indirect costs attributed mainly to lost labour. Much of this is attributable to LBP that is non-specific in nature.

Diagnostic tools can be effective when an injury mechanism is clearly identifiable with structural change, but often this is not the case. Pain and loss of function occur as symptoms without any identifiable musculoskeletal fault. This has led to only one in ten patients successfully associating a cause to their pain, while the remainder are tagged non-specific. Physical stress at work is cited as one of the main risk factors for non-specific LBP [3], [6]. Despite a consistent effort over many decades to address safe lifting practice and establish clear guidelines [7]–[9], LBP remains a primary cause for lost working days due to injury [10].

LBP is multifactorial and instability, clinical and mechanical in nature, is commonly cited in non-specific cases. The spine is a complex biomechanical structure with the freedom to move in any plane or axis. The passive, active, and neurological systems of the human body keep the structure stable by finely controlling its stiffness within the healthy range of motion and under large loads, which are highest in the lumbar region [11].

Intra-abdominal pressure (IAP), the pressure concealed within the abdominal compartment, is believed to have potential for significant contributions to spine stability. By extension, it has the potential to reduce injury risk during lifting. However, its role is still debated. Competing factors affect its perceived net mechanics. While the pressure itself is believed to have supportive capabilities, contraction of abdominal muscles could offset this gain by increasing compression and pressure in the intervertebral disc. No single model has accounted for all three hypothesized stability mechanisms, namely the effects of offloading the spine, buttressing reinforcement, and tension relayed to the spine as hoop-stresses through the lateral abdominal wall and thoracolumbar fascia. The dynamic behaviour of IAP is poorly understood, with prior computational studies neglecting it or only investigating the effects of IAP statically. Lifting velocity is, however, a high-risk factor for LBP in occupational settings and IAP is known to fluctuate transiently during lifting.

The role of IAP in transient lifting remains largely unaddressed in biomechanical models, despite its known contribution to spine stability and apparent relevance in the pathomechanism of LBP.

Properties of the thoracolumbar fascia (TLF) tend to be altered with LBP due to physiological changes or treatments. Analysis of its properties and role in the pathomechanism of LBP has been hindered by various challenges. Consequently, clinical practice has minimally accounted for its biomechanical influence. Often, in clinical settings, the TLF is cut to access the posterior spinal column. Spine biomechanics are significantly affected by surgical intervention through the TLF [12] and this could have important consequences on stability. Biomechanical roles of the TLF have been studied, but the challenges inherent to investigating the thin, stiff but flexible, deep, and fibrous tissue are often unavoidable. Particularly, the complex boundary conditions, continuities with adjacent musculature, and long fiber-based structure. Computational approaches could be effective to study the tissue mechanics without these hindrances, but difficulties in segmenting the tissue have created an obstacle to this experimental methodology. As a result, the few existing *in silico* studies have not fully considered model form [13], [14] and *ex vivo* studies present mixed results with important limitations [15], [16].

The overarching interest of this thesis was to quantify stability of the lumbar spine with a comprehensive and physiological representation of the role of IAP. This yielded two specific objectives:

Objective #1: Develop and validate a nonlinear and transient finite element model of the spine and trunk to accurately capture the biomechanics of spine and IAP. Then, apply the model to quantify stiffness under the combined contributions of IAP and velocity, providing insight into injury risk and stability.

Objective #2: Address current obstacles in modelling the hoop-stress pathway for IAP to augment spine stiffness. Then, quantify the potential stiffness contributions of the TLF and how this may change with engineering assumptions on model form as well as with tension force from abdominal muscle contraction relevant to IAP.

Figure 1.0.1 visually clarifies the research rationale and links between the topics of this thesis by chapter. Both objectives were addressed using the finite element method as a computational approach offers the highest level of control over test cases and input variables, including IAP and velocity. Simultaneously, this research approach provides the most quantifiable results and greatest accuracy in measurements. However, verification and validation (V&V) were central to the interpretation of results to raise confidence in the model as a faithful comparator to a physiological spine and trunk.

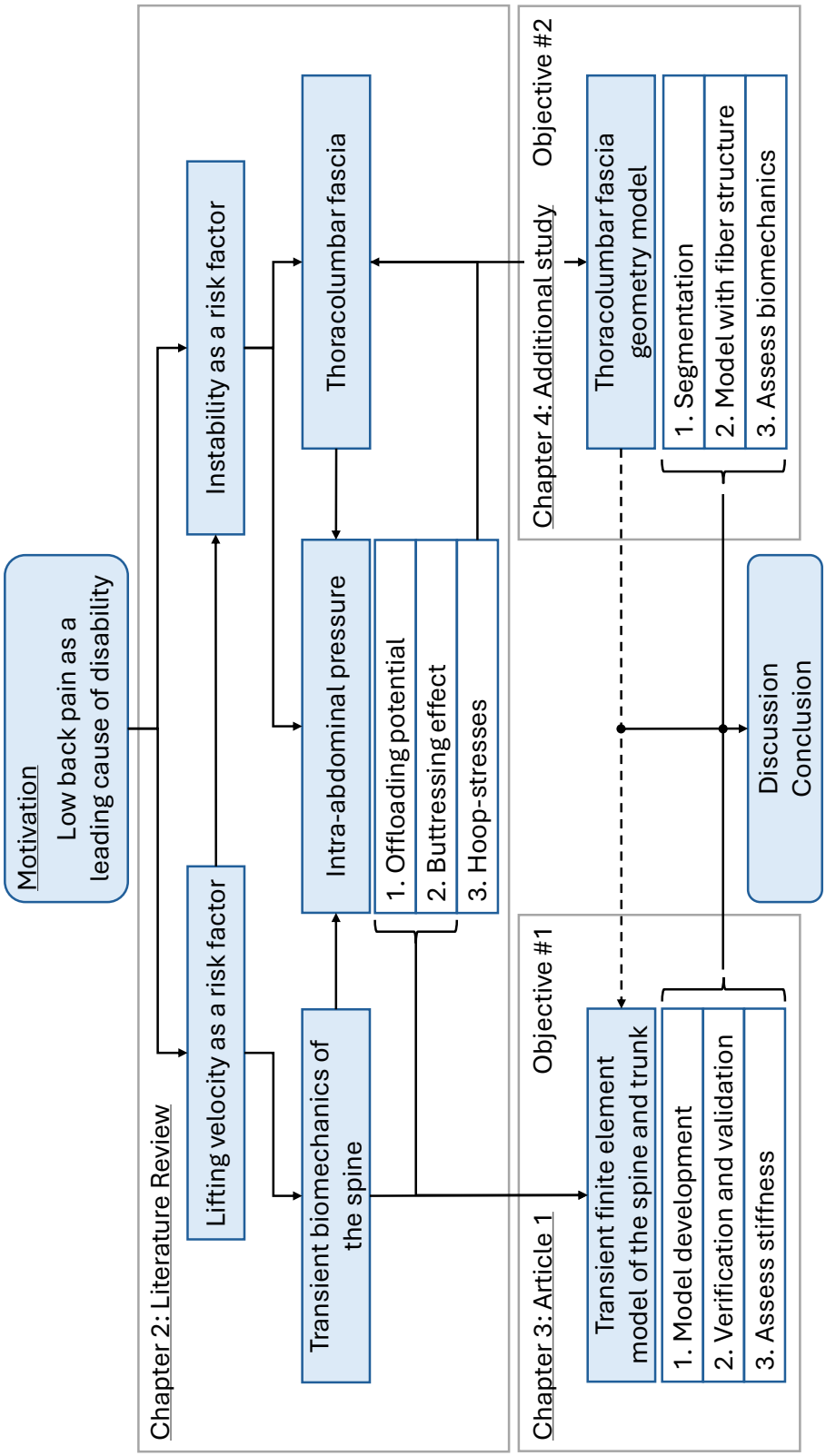

Figure 1.0.1: Flow diagram indicating the relations of motivation, rationale, and objectives, and how these fit into the outline of the thesis. The dotted line indicates a connection exists but was not integrated in the current iteration of the model.

2 Literature Review

2.1 Functional Anatomy and Biomechanics of the Spine

2.1.1 Anatomical Reference

Human body movements and anatomical geometry are not aligned in any consistent global frame of reference. For example in a moving body, up, down, left, and right are descriptors that are relative to the current body position. To mitigate this, the field of biomechanics employs a standard anatomical reference frame that is intrinsic to the anatomy in question. Figure 2.1.1 establishes these anatomical reference planes overlaid on the trunk to ensure discussion is clear and consistent throughout this document.

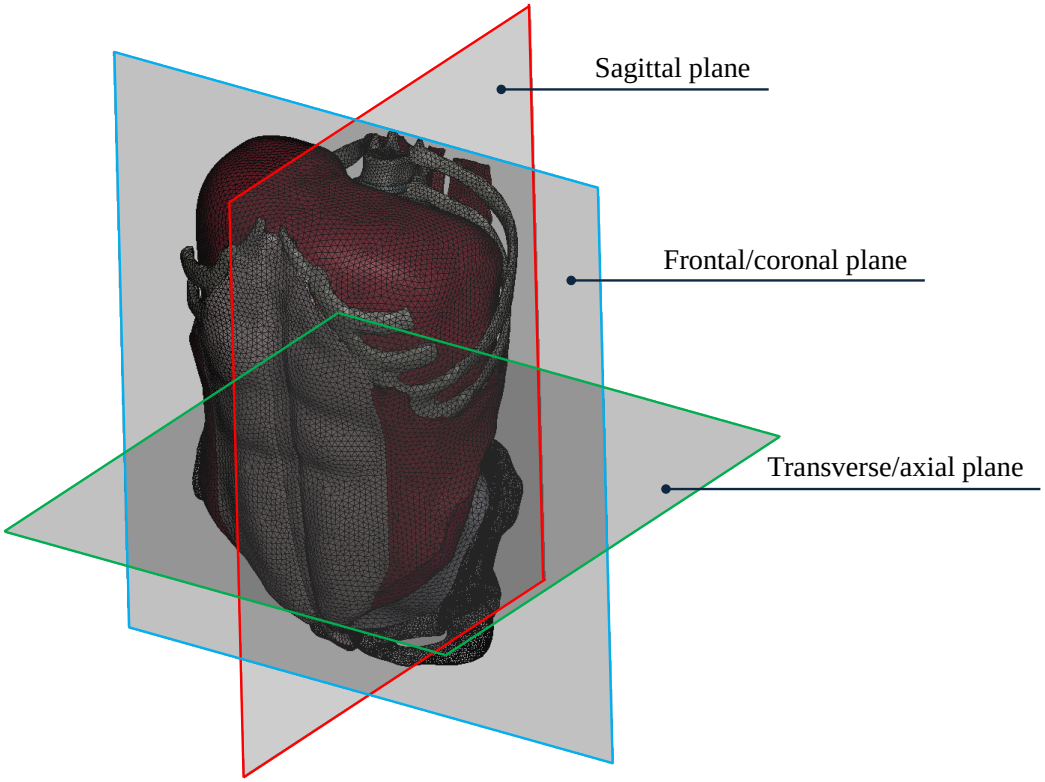

Figure 2.1.1: Anatomical reference planes with the respect to the trunk and spine.

Three axes can be identified from these reference planes. Normal to the transverse plane, in green, is the craniocaudal or superior-inferior axis, with the superior direction being toward the head (cranial) and inferior referencing the direction of the lower extremity (caudal). Normal to the frontal plane, in blue, is the anteroposterior axis with anterior indicating the direction of the chest

relative to the thoracic spine, for example. Finally, the mediolateral axis is normal to the sagittal plane, with medial referencing the midline, or a direction toward the midline, and lateral indicating a direction away from the midline toward the left or right extremities. For the spine, rotations about each of the three axes are assigned distinct functional nomenclature: flexion-extension about the mediolateral axis, lateral bending about the anteroposterior axis, and axial twist about the craniocaudal axis.

2.1.2 Spine and the Functional Spine Unit

The human spine is a complex anatomical structure, formed by a vertical column of vertebrae and intervertebral discs (IVDs). The alternating pattern of rigid bony vertebrae and softer, elastic IVDs creates flexibility in the structure, allowing it to accomodate everyday movements. The spine originates inferiorly at the sacrum (S1), rising superiorly through five lumbar verterbae (L1-L5), then twelve thoracic vertebrae (T1-T12), inserting superiorly at the base of the skull through seven cervical vertebrae (C1-C7). A schematic is provided in Figure 2.1.2(a). A principal distinguishing factor of the three sections highlighted is attachments to the rib cage. Between the cervical and lumbar spine, the thoracic spine suspends the twelve ribs [17]. On the whole, the sections are also geometrically distinct. The cervical vertebrae are small and wide, mediolaterally, facilitating large flexion-extension rotations of the neck. At the other extreme, lumbar vertebrae are the largest and are similarly characterized by mediolateral-to-anteroposterior length ratios greater than one. This anatomy is adapted to absorb the largest compressive forces in the lumbar region [18]. The thoracic vertebrae are distinct in their need for costal facets to articulate with the posterior ends of each rib. Beyond this, they can be considered to have transitional geometry, narrowing in width from T1 in caudal progression toward an equal length ratio. Closer to the lumbar region, they transition again, widening transversely [19].

As indicated in Figure 2.1.2(b), a functional spine unit (FSU) consists of a single IVD with its adjoining inferior and superior vertebrae. An FSU will have six degrees of freedom. These include three in translation, namely axial compression, lateral shear, and anterior-posterior shear. The remaining three in rotation are flexion-extension, lateral bending, and axial rotation. The complete vertebral column is a superposition of the degrees of freedom of all FSUs.

As illustrated and labelled in Figure 2.1.2(c), a single vertebra is further subdivided into its vertebral body and posterior arch, with a foramen creating space for the central nervous system. The vertebral bodies tend to increase in cross-sectional area in the lumbar spine and progressing caudally toward the sacrum. A stiff cortical bone shell encapsulates a softer matrix of trabecular, or cancellous bone within the vertebral body. The lamina and processes of the spine tend be more densely structured with cortical tissue to sustain the muscle forces applied in these regions via

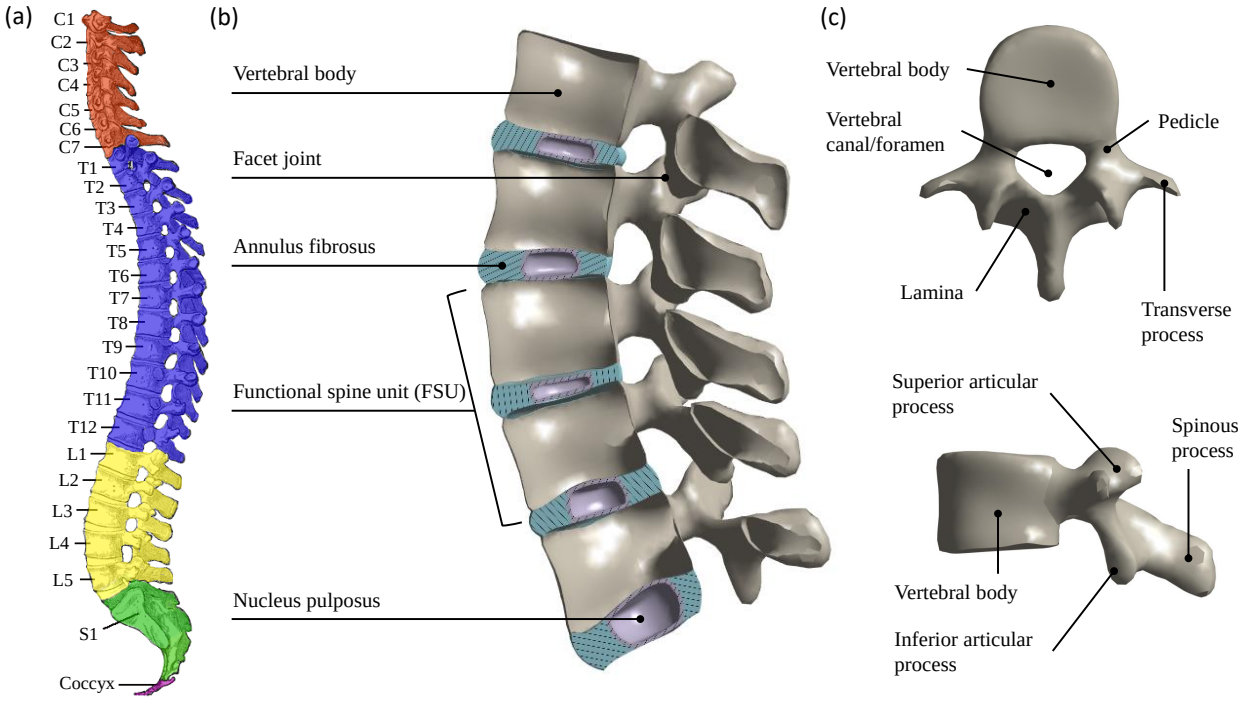

Figure 2.1.2: Anatomy of the vertebral column. (a) The complete vertebral column with labelled vertebral levels and color coded by section: cervical in orange, thoracic in blue, lumbar in yellow, and sacrum in green. Adapted from [20]. (b) A sagittal plane sectioned view of the lumbar spine, with relevant anatomy identified. (c) A focused anatomical identification of a lumbar vertebra from a top view (top) and a side view (bottom)

tendinous insertions [21]. A layer of cartilage divides each vertebral body from its adjoining IVD, acting as a transition zone between the rigid and more elastic materials. These cartilaginous end plates are approximately 1 mm in thickness [22] and their concavity aligns with the concavity of the nucleus pulposus (NP) of the IVD [19]. Yeni *et al.* (2022) calculated cortical bone shell thickness in L1 at 0.715 mm [23]. This is similar to cortical thickness in ribs, at approximately 0.7 mm [24]–[26]. Palepu *et al.* (2019) estimates a lower thickness in the lumbar spine, calculating an average across all side walls of the vertebral bodies in the range of 0.27–0.44 mm [21]. Despite its thin nature, the cortical bone in the ribs and vertebrae has markedly higher stiffness, with an elastic modulus around 14–17 GPa [27]–[30], than its trabecular counterpart. Öhman-Mägi (2021) thoroughly reviewed studies on trabecular bone properties in vertebrae. Studies have reported moduli in the range of 301–450 MPa in tension and 165–344 MPa in compression, from high-quality testing methods in mixed-sex samples [31]. Since the lattice structure of isolated trabecular bone creates large isotropy at the macro scale, the above ranges are limited to craniocaudal testing directions.

2.1.3 Intervertebral disc

The IVD is a more complex anatomical structure by composition. It is subdivided between the gelatinous NP in its core, the collagenous annulus fibrosus (AF), and a transition zone between the two. The annulus itself is composed of a ground substance, or matrix material, with imbedded collagen fibers arranged in a criss-cross pattern in concentric bands around the nucleus. The IVD contains around 15–25 layers, called lamellae, with collagen fiber bundles angled at $+/-$ 20–45° alternating in successive lamellae [32], [33]. On the whole, the IVD acts as a shock absorber in the spine, absorbing compressive loads and reducing peaks in force exerted directly on the vertebrae and end plates. The biphasic structure is effective in handling different types of loading. The collagen fibers embedded in the AF will not resist compression, but will limit bulging of the disc, maintaining disc geometry under large loads and spine rotations. Resistance to compression is mainly handled by the gelatinous NP, having a large water content of 70–90% [33]–[36], which decreases with age and varies osmotically with load history [37], to make it near incompressible. This way, it develops hydrostatic pressure in response to compressive loads. Due to this same incompressibility, the NP will act as a sliding pivot in spinal rotations. Thus, the superposition of these structures enables each FSU to rotate or translate in six degrees of freedom, while also absorbing forces in the spine [22], [33], [38] and exhibiting ligamentous behavior in resisting excessive displacements [39].

Various groups have employed the finite element (FE) method to investigate the role of the NP in supporting stability and compressive loading in the lumbar spine. It is expected that IVD pressure (IDP) will decrease as the average cross-sectional area of the NP increases. This is because pressure, and average stress on the surface, will be be proportional to the compressive force divided by the cross-sectional area. Yang *et al.* (2019) have investigated further by varying anterior-posterior centroid location, as well as NP-to-IVD area ratio, finding that the centroid location has a large effect on pressure distribution in the disc, and a slight effect on average and maximum pressure. An anterior shift of 5% of the anterior-posterior length of the disc resulted in a 40% increase in high-pressure area in flexion while a 5% posterior shift led to the same parameter increasing by 60% in extension. Despite the effects on pressure distributions, IVD joint stiffness was not affected by centroid position of the NP [40]. Du *et al.* (2021) confirmed that realistic modelling of IVD physiology, including fiber angles, material properties, and area ratios, affects the calculated response [41].

The IVD biomechanics discussed above suggest knowledge of disc and NP geometry is important for any applications involving the disc. Many studies have investigated this at various levels in the lumbar spine. O'Connell *et al.* (2007) established a reference for interpretation of IVD

results from animal studies by comparing disc geometries as normalized values between human and various animal species [42]. In doing so, O'Connell *et al.* established a standard method for approximating NP geometry according to NP:disc area ratios. This has been employed by multiple groups to model the IVD's core at all levels of the lumbar spine [27], [41], [43], [44]. Table 2.1.1 summarizes NP-to-IVD area and length ratios reported in literature as well as average NP length values. Where studies reported values by level, they were averaged across all levels. Perey (1957) measured NP areas from dissection of eleven cadavers, reporting a similar average area ratio to O'Connell *et al.* and Showalter *et al.* (2012) [36], [42], [45]. Pooni *et al.* (1986) also analyzed four cadaveric spines by serial sectioning, presenting larger area ratio at each level. The average is carried higher by a disproportionately large L5/S1 NP:IVD area ratio of 46% [38]. The larger ratios may be the result of the different measurement methodologies. Zhong *et al.* (2014) also found the L5/S1 NP length to be significantly larger than the rest. While reported average NP lengths are similar to other studies, the NP:IVD length ratio is markedly higher, driven by smaller IVD length measurements [46]. These variations of measurement may again be attributable to methodological differences as this was the only reported study to use live subjects and magnetic resonance imaging (MRI). Little *et al.* (2007) reported partial results for area ratio with large variability in measured values [47].

Table 2.1.1: Characteristic geometry of the intervertebral disc and nucleus pulposus.

	Level	N	A_{NP}/A_{IVD}	L_{NP}/L_{IVD}[a]	NP length [mm][a]
O'Connell (2007) [42]	L4/L5	3	0.28	0.56	20.8
Showalter (2012) [36]	L3/L4	3	0.31	0.55	20.8
Zhong (2014) [46]	Mixed	41	-	0.7	20.23
Perey (1957) [45]	Mixed	11	0.29	-	-
Pooni (1986) [38]	Mixed	4	0.38		
Little (2007) [47]	L4/L5	6	0.23	-	-

[a] Lengths in the anterior-posterior direction through disc midline.

In addition to the geometric properties reported in Table 2.1.1, O'Connell *et al.*, Little *et al.*, and Sharma *et al.* (2022) each reported data on posterior offset of the NP relative to the IVD centroid. Pooling and averaging the offsets yielded 4.2% of the anterior-posterior IVD length, though NP offset can be as high as 10% [40], [42], [47], [48].

2.1.4 Ligaments

Passive stiffness of the spine is in part influenced by seven ligaments, namely the anterior and posterior longitudinal ligaments (ALL and PLL), intertransverse ligaments (ITL), supraspinous ligament (SSL), interspinsous ligaments (ISL), capsular ligament (CL), and ligamenta flava (LF).

Each of these is annotated in Figure 2.1.3, depicting the ligaments of the lumbar spine.

Bogduk (2012) and Stranding (2021) both cite an oblique posterocranial orientation of the the ISL fibers from origin at the inferior vertebra to insertion at the superior vertebra [19][39]. This definition conflicts with many depictions of the ISL in the lumbar spine which may be shown have an anterocranial oblique orientation [49], as illustrated in Figure 2.1.3. To the authors' knowledge, no consensus exists in literature on the orientation of this ligament. In spine modelling, the difference would be expected to have a small effect on the force exerted on the spinous process during flexion.

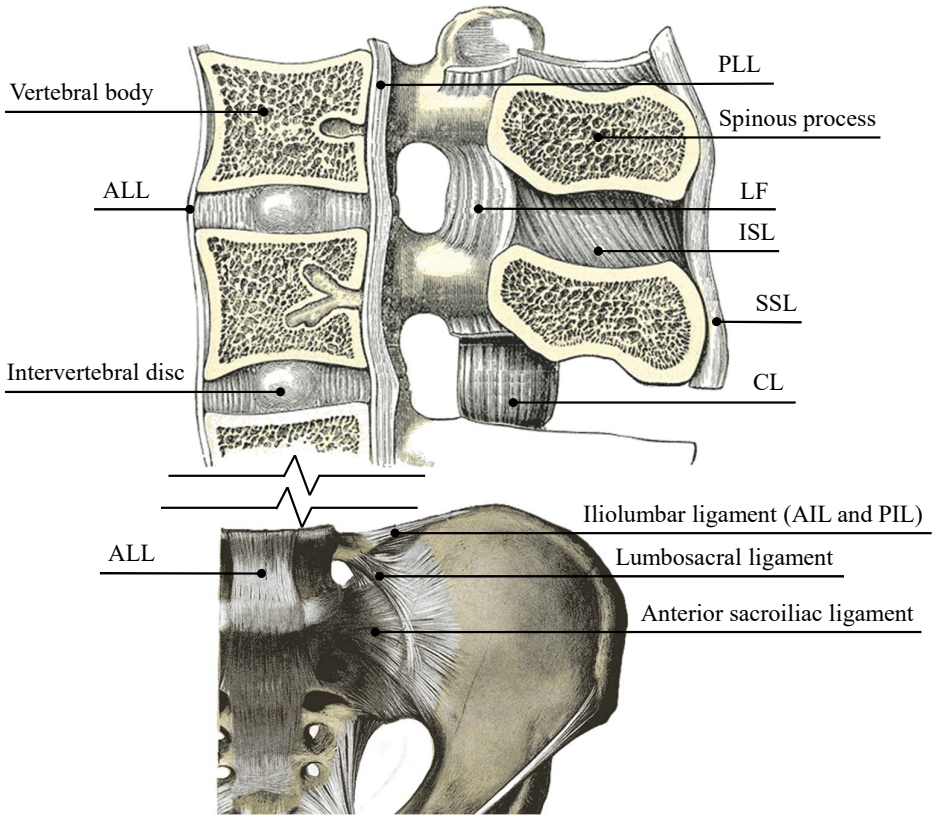

.

Figure 2.1.3: Ligaments of the lumbar spine and sacroiliac joint. Not shown is the ITL, spanning craniocaudally between the transverse processes of adjacent vertebrae. The vertebral body, IVD, and spinous process are indicated for reference. A break line shows the gap in continuity between the lumbar section and sacroiliac section. Adapted from [50], [51].

In addition to the above-mentioned lumbar spine ligaments, the anterior and posterior iliolumbar ligaments (AIL and PIL) stretch from the iliac crest to the transverse process of L5. Figure 2.1.3 also depicts the generalized iliolumbar ligament in its anatomical location. While the sacroil-

iac joint, which connects the sacrum of the spine to the pelvis, is a common source of LBP [52], it is not a main focus of this thesis. However, the AIL and PIL have important roles in stability and movement of the lumbar spine, originating on the transverse process of L5 and inserting to the iliac crest. Its geometry is well described by Hammer *et al.* (2010) using MRI and virtual reconstruction, as well as by Hanson and Sonesson (1994) from cadaveric studies. Some geometric differences between the two groups were reported, with Hanson and Sonesson claiming 30–40 mm and 10–12 mm lengths for the AIL and PIL, respectively, compared to more consistent average lengths of 30 mm and 25 mm reported by Hammer *et al.* [53][54]. The difference, particularly of the PIL, is likely due to methodological differences between groups as they both agree on origin and insertion locations. To the authors' knowledge, no characterization of material properties has been done on the iliolumbar ligaments. Hammer *et al.* (2013), however, have substituted Young's modulus of the iliotibial tract, 397 $\mathrm{N/mm^2}$, for the AIL and PIL in an FE study of the pelvis and sacrum. The model was minimally sensitive to large variations in this value between 50% (198 $\mathrm{N/mm^2}$) and 200% (794 $\mathrm{N/mm^2}$) of the target ligament stiffness.

The importance of the AIL and PIL can be well understood by comparing spine movement between *ex vivo* and *in vivo* studies. In the former method, intervertebral rotations are measured after the spine has been excised from the pelvis, removing any iliolumbar ligaments [55]–[57]. Possibly the best insight into segmental rotation patterns in the lumbar spine was provided by Wong *et al.* (2004), who used video x-ray to break down net L1-S1 rotation in a relatively large sample of 100 subjects [58]. This indicated a nearly opposite trend to the excised spine, with the largest intersegmental rotation at the most cranial level. The L5 vertebra, relative to S1, exhibited only small angular displacements in comparison. The sacroiliac joint and its ligamentous connections are therefore likely key to stiffening the caudal end of the spine, forcing a near-linear growth in intersegmental rotations moving sequentially cranial.

2.1.5 Abdomen

While abdominal muscles do not have a direct attachment to the spine, they contribute nevertheless to its movement, loading, and stability [59], [60]. The main muscles of the abdomen include the rectus abdominis (RA), obliquus externus (OE), obliquus internus (OI), and transversus abdominis (TrA). Each of these are related to each other through their aponeuroses and each is related to the spine through the ribs or fascia.

The RA is generally considered an important flexor muscle of the spine [61], originating at the pubic symphysis, or anterior aspect of the pelvis, and inserting at the xiphoid process and costal cartilage of the ribs, or more broadly the anterior aspect of the chest. Its fibers run approximately longitudinal along the craniocaudal axis. The muscle is separated, visually and functionally, into

compartments by tendinous intersections, approximately at the levels of the umbilicus, xiphoid process, and mid-way between the two. Occasionally there is an additional intersection below the umbilicus, though there is significant variability in the anatomy of the tendinous intersections [62][63]. The RA muscle is thicker at the mid-sections between intersections and reduces in thickness approaching them. Broyles *et al.* (2018) dissected 30 cadavers finding 94% of subjects had three pairs (left and right) of tendinous intersections, while the remaining had four. These did not typically cross the entire anteroposterior width of the RA, but 42% of subjects had at least one tendinous intersection spanning from anterior rectus sheath to posterior rectus sheath [63]. This thin, fibrous sheath is an extension of the aponeuroses—organized tendon-like fibrous endings of flat muscles—of the lateral abdominal wall muscles and compartmentalizes the RA, allowing it to contract more freely without adhesions. Similarly, many of the tendinous intersections do not span the entire mediolateral width of the muscle, as reported by Rai *et al.* (2018) [62]. Further, Lehman and McGill (2001) reported the RA behaves as a single functional muscle unit, showing no signs of functional separation. Electromyography (EMG) of the RA was consistent throughout the muscle [64]. The anatomical insight from Broyles *et al.* and Rai *et al.* offers an explanation, as a continuous pathway for electrical stimulus is created by the incomplete intersections.

As illustrated in Figure 2.1.4, the left and right RA muscles are joined medially by the linea alba, where the rectus sheath and muscle tissue blend into a long strip of fibrous tissue. Laterally, the rectus sheath is contiguous with the aponeuroses of the TrA, OI, and OE to complete the anterolateral abdominal wall. The aponeurosis of the TrA passes posterior to the RA above the arcuate line in Figure 2.1.4(a), but below the line all lateral wall aponeuroses merge anterior to the RA. Recently, Punekar *et al.* (2018) proposed a more complete anatomical model of the abdominal wall, with the TrA extending medially into the rectus sheath such that the muscles do not transition as abruptly as suggested by Figure 2.1.4 [59].

Fibers of the lateral abdominal wall muscles run oblique to the transverse plane. The contractile force capacity of a muscle is proportional to its cross-sectional area which should be evaluated along the effective fiber direction for these oblique muscles. Orientation of the muscle fascicles is regionally dependent [66], but Jourdan *et al.* (2024) considered effective angles of 52°, 21°, and 10°, for the OE, OI, and TrA, respectively [67]. Stokes and Gardner-Morse (1999) quantified physiological cross-sectional area of abdominal muscles based on fascicle orientation, reporting an effective area of 1575 mm^2, 1345 mm^2, and 567 mm^2 for the OE, OI, and RA, respectively [68]. McGill previously proposed 500 mm^2 for the TrA muscle [69]. The relatively large physiological cross-sectional area and fiber angle of the OE creates a notable flexion force potential on the spine. The force vector could induce compressive loading on the spine as well. Abdominal

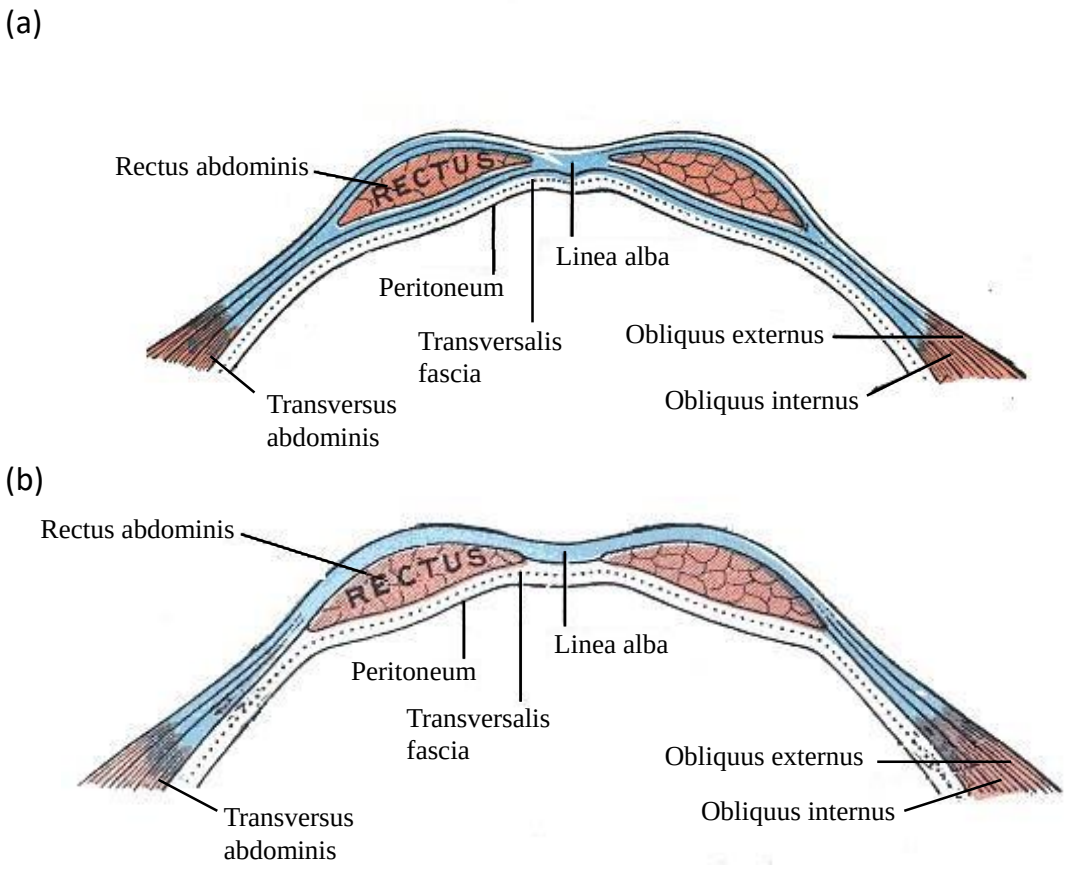

Figure 2.1.4: Anatomy of the abdominal wall forming the anterior and lateral abdominal compartment: (a) above the arcuate line and (b) below the arcuate line. Adapted from [65].

muscles have attachments to the pelvis and rib cage. Therefore, flexion of the spine will translate the ribs, causing displacement of the abdomen and its muscles.

Finally, the abdominal compartment is enclosed by the pelvic floor inferiorly and the diaphragm caps it superiorly. The posterior abdominal wall is bounded by stabilizer muscles of the spine including the psoas major and quadratus lumborum, as well as the spine itself. For women, the pelvic floor is particularly relevant due to the adjacency of the abdominal compartment, and its internal pressure, with important reproductive organs and compartments [70], [71]. The diaphragm contracts with breathing, affecting IAP [72]. Around 20% of the diaphragm surface area is occupied by its central tendon and another 35%, comprised of muscle tissue, is apposed to the lungs [73]. Seok *et al.* (2017) found that its thickness increased from 2.2 to 4.6 mm in men during maximal inspiration, further supporting pressurization [74].

2.1.6 Fascial Connections

Various fascial tissues are relevant to the biomechanics of the spine, mainly by transferring forces from surrounding tissues. Broadly, fascia has received a marked increase in research attention in recent years [60], [75]. The TLF is particularly relevant to spine biomechanics for its fibrous connections to the spine and contiguous interface with the paraspinal muscles. It is also important in the context of IAP as it blends with the posterior aponeuroses of the abdominal muscles. It contributes to the hydraulic pressurization of both the abdominal and paraspinal muscle compartments. For the former, it resists displacement of the posterior aspect of the lateral abdominal wall muscles, enabling them to expand radially toward the midline. For the latter, its tension contains radial expansion of during contraction of the erector spinae muscle group to amplify paraspinal pressure [76].

The fascial network spans the human body broadly, forming fibrous connections, in various forms, from head to toe. The TLF, highlighted in Figure 2.1.5 within the broad low back, is a specific nomenclature for the fascial tissue spanning the lumbar region from the sacrum to approximately the T9 vertebra. It is continuous with fascia superior to this level, but becomes too thin to consider as part of the functionally important connective tissue. Moving laterally, the multiple layers of the TLF blend with the aponeuroses of abdominal muscles, latissimus dorsi (LD), and gluteal muscles. The posterior lumbar fascia (PLF) is the most superficial layer, containing within itself two laminae—the deep lamina and the superficial lamina—which blend below the level of L5 into a single undifferentiated layer of organized fibrous tissue in a criss-cross pattern. Using the three-layer model, as accepted in the comprehensive review of Willard *et al.* (2012), the posterior and middle layers, together with the transverse process and spinous process of the vertebrae, enclose the paraspinal muscle compartment. With possible exceptions, the aponeuroses of the serratus posterior inferior and abdominal wall muscles blend into the deep lamina of the PLF, which wraps the paraspinal muscles, while LD muscle fibers transition from their respective aponeurosis into the superficial lamina [76]. According to the descriptions of Barker and Briggs (1999) the angle of fibers from the midline above horizontal, relative to the transverse plane, generally decreases from L5 in the cranial direction [77].

Abdominal fascia, namely the transversalis fascia in Figure 2.1.4, is relevant to the spine as well, through at least two pathways. First, it encloses the abdominal compartment, maintaining IAP. In this way it contributes to amplifying the hydraulic pressure, similar to the role of the TLF for the paraspinal muscle compartment. Second, gliding between abdominal layers facilitates bilateral movement in dynamic activities, such as walking. Contracting muscles are thus able to relay tension to more distal motion segments. This gliding behaviour would benefit from further

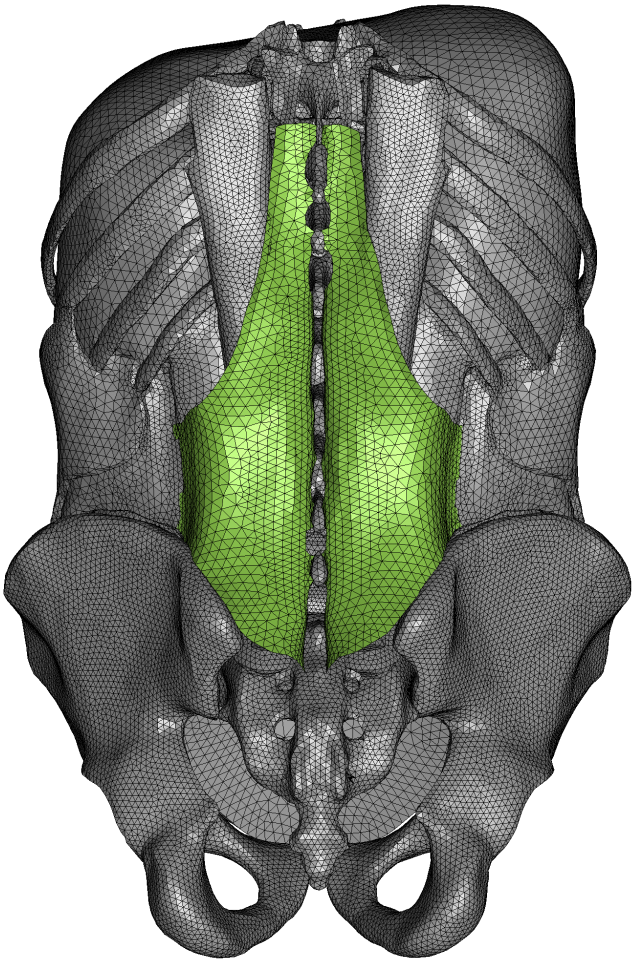

Figure 2.1.5: Thoracolumbar fascia highlighted green on a torso model to indicate its general location with respect to the surrounding anatomy.

biomechanical investigation. Further, it has been shown to connect various adjacent tissues to the spine. Passing anterior to the quadratus lumborum muscle, this fascia forms the anterior layer of the TLF, in the three layer model. These observations suggest it could have an important role in spine stability.

Fibers of the thoracolumbar fascia appear to be significantly stiffer than those of the transversalis fascia, with differences in the order of magnitude range. Newell and Driscoll (2024) recently reported TLF Young's modulus of 150 MPa [78] in the fiber direction. Conversely, tensile testing from abdominal region samples by Kirilova *et al.* (2011) yielded only 9 MPa and 3 MPa in the fiber and transverse directions, respectively [79]. Focusing on anisotropy along the anatomical axes, Berardo *et al.* (2024) have reported elastic moduli of 1.6 MPa and 3.2 MPa in the craniocaudal and mediolateral directions, respectively [80].

2.2 Intra-Abdominal Pressure

IAP is defined by the World Society of the Abdominal Compartment Syndrome (WSACS) as the steady-state pressure concealed within the abdominal cavity. However, the term is also commonly used in literature and scientific discourse to identify the any momentary pressure value, or transient pressure, within the compartment [81]. Normal IAP is maintained at a 5–7 mm Hg baseline in healthy patients [81][82]. This internal pressure helps maintain the natural hoop-like geometry of the abdomen. A pressure reaching 12 mm Hg repeatedly or sustained over a period of time is considered intra-abdominal hypertension and abdominal compartment syndrome is defined by WSACS as IAP surpassing 20 mm Hg. Abdominal compartment syndrome is associated with organ dysfunction or failure due to the sustained elevated pressure exerted on organs within the viscera [81].

Figure 2.2.1 represents the hydraulic pressure mechanism of IAP. Due to the high water content in the human body, IAP functionally behaves as a force-transfer mechanism. Some compressibility and volume change is achievable where there may be air in the stomach and intestines, but forces are for the most part translated through hydraulic effects [83]. A baseline pressure is augmented through abdominal muscle or diaphragm contraction and relays the applied forces to surrounding tissues including the spine or viscera.

The WSACS lists measurement of IAP via urinary bladder catheter as the reference standard [81]. This measurement has a very strong correlation with IAP due to the near-incompressible nature of the high-water content tissues in the abdomen, resulting in a nearly ideal hydrostatic pressure relationship.

Many studies have reported large transient variations in IAP during activity and lifting. Kawabata *et al.* (2014) studied patterns of breathing and IAP generation during lifting at various weights as a percentage of the subjects' maximal isometric lifting capacity. The authors found the time at which the rate of increasing IAP peaks consistently occurred before onset of lifting motion, while maximum IAP magnitude occurred after some delay. This delay was observed to reduce with increasing load. There was also a significant correlation between IAP and lifting load, with IAP increasing from 36.8 mm Hg at 30% of maximum isometric capacity to 90.3 mm Hg at 75%. These patterns, supported by Hagins *et al.* [84], suggest a preparatory role for IAP as a transient biophysical signal during dynamic lifting tasks [85]. The precise reason for this observed preparatory IAP behaviour remains unanswered, however, as it is unclear whether IAP is modulated by the neuromuscular control system or varies as a byproduct of other controlled parameters [72]. This gap in understanding is in part due to challenges associated with evaluating the net gain or cost of potential offloading and stability versus additional loading. Contraction of

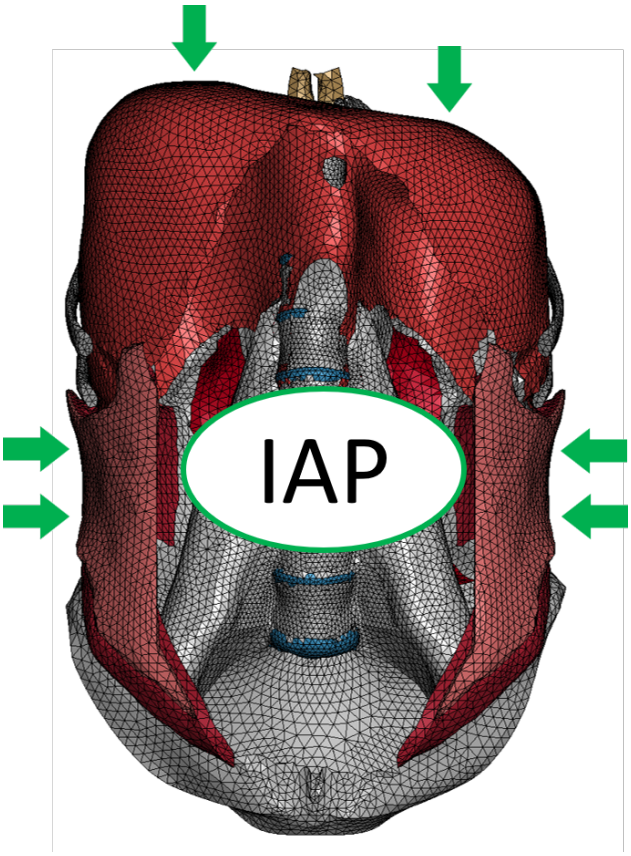

Figure 2.2.1: Hydraulic pressure mechanism of intra-abdominal pressure from contraction of abdominal muscles and the diaphragm. The rectus abdominis, rectus sheath, and anterior segments of the ribs are hidden for clarity.

flexor muscles concurrent with generation of IAP may induce additional loads on the spine [86], [87]. The balance of these competing effects, with the preparatory behaviour observed, remains unclear in literature.

IAP values recorded during various studies of lifting and Valsalva maneuver tasks are presented in Table 2.2.1. Valsalva is a voluntary maximal abdominal bracing contraction with breath control aimed to maximize IAP. McGill and Sharratt (1990) observed similar transient peaks in IAP to Cresswell *et al.* (1992) when lifting heavy weights. Each group simultaneously evaluated the EMG activity of muscles in the trunk during various tasks [88], [89]. The two groups observed similar timing of peak IAP occuring within 60 ms of muscle activation, further supporting the association with neuromuscular control. However, McGill and Sharratt suggest IAP was not strongly correlated with any particular pattern of trunk muscle activation. Rather, pressure magnitude was task-specific. In lifting, targeting maximal IAP, as in the Valsalva maneuver, could also affect blood pressure. Though, it is not clear whether this pulse pressurization could lead to any adverse health effects if a longer duration is targeted [90].

Similarly, Essendrop and Schibye (2004) measured IAP and muscle EMG in trained athletes during lifting and sudden loading of the trunk. Sudden loading was induced by simulating unpredictable patient fall events, a common risk in patient handling scenarios wherein healthcare workers must attempt to prevent the fall, exposing themselves to sudden loads on the spine. Higher IAP was recorded in sudden loading over lifting tasks, with respective magnitudes of 137 mm Hg versus 62.5 mm Hg [91]. Contrary to some similar studies, EMG activity of the RA muscle was recorded at an average 3% of maximal voluntary contraction (%MVC) during lifting and 6% during sudden loading. Large IAP peaks were generated mainly from TrA and OI activity (38% average), as well as OE to a lesser extent [91]. These findings oppose those from Juker and McGill (1998), who observed greater RA activation on average (14%) than TrA and OI when lifting light weights [92]. The differences are possibly attributable to experience levels of the subjects or EMG measurement techniques and study protocols. Juker and McGill used intramuscular probes for TrA and OI while Essendrop employed surface electrodes everywhere. Further, by simultaneously measuring IAP, Essendrop and Schibye likely made their subjects more aware of their abdominal muscle control, introducing bias. Essendrop and Schibye also noted the airbag-like contribution of IAP under sudden trunk loading. There was no significant RA activity to oppose extension of the spine [91], but the induced flexural load is resisted by the pressure of the abdomen. These findings combine to highlight how neuromuscular control mechanisms for IAP can vary with different tasks, but the pressure is consistently apparent, in large magnitude, when the trunk is loaded [90]. Cresswell *et al.* (1994) also found that IAP increases with lifting velocity, along with TrA EMG [93]. This could result from a subconscious effort to bolster stability as velocity increases.

Table 2.2.1: Average IAP during lifting.

	Lift		Valsalva
	Avg. Mass (range) [kg]	Avg. IAP (SD) [mm Hg]	Avg. IAP (SD) [mm Hg]
Kawabata (2014) [85]	75.9 (60.0–92.5)[a]	90.3 (11.2)	140 (86–226)[c]
Kawabata (2014) [85]	30.7 (25.0–37.5)[a]	36.8 (8.4)	
McGill (1990)[b] [88]	78.2 (72.7–81.8)[a]	99.6 (21.3)	192 (27.3)
Essendrop (2004) [91]	15	62.5 (16.9)	241 (32.8)
Hagins (2004) [84]	70% max	50.2 (23.2)	-
Hagins (2004) [84]	35% max	34.3 (8.1)	-
Cresswell (1992) [89]	-	-	82.5–112.5[c]
Cobb (2005) [94]	-	-	64.9 (22)

[a] Variable load per subject is expressed as an average mass across all subjects.
[b] National-level expert powerlifter (subject F) excluded
[c] Range of values provided.

2.3 Spine stability

2.3.1 Clinical Stability

In biomechanics there are differing context-specific definitions of stability that lead to varying interpretations. In clinical discussion, the term 'stability' is often used in reference to a patient's ability to remain at a state of homeostasis, around a healthy baseline, and without pain. Ghezelbash *et al.* (2023) have recently attempted to unify definitions of stability, particularly for application to computational modelling. The authors describe clinical stability as follows [95],

> *"Stability appears as the ability to maintain and control, within safe limits, joint positions and motions in submaximal activities under voluntary tasks and suddenly applied internal-external disturbances."*

Specific to the spine, Panjabi has defined the alternative, clinical instability, as the loss of this ability to maintain a healthy range of intervertebral rotations when the spine is subject to loads expected within the normal activity of the specific subject [18], [96]. Further, the vertebrae should retain their form without inducing painful irritations to the nervous system. Thus, clinical stability is associated with subject-specific physiological limits and resistance to joint buckling [97].

2.3.2 Mechanical Stability

From an engineering perspective, stability usually refers to a system's ability to return to equilibrium upon perturbation [98], [99]. To understand the complexity of defining stability in the spine, consider that mechanically, a rigid structure which does not move or buckle under any reasonable force would be maximally stable. Obviously, this would not be a useful criterion for any joint. The criterion could then be extended, so that a joint should not move outside of its physiological range of motion. This is useful for pivot joints in the human body. The knee and elbow have clearly defined physiological motion. Clinical instability is characterized, then, by patient-reported pain as well as increased varus-valgus rotations or hyperextensions. The spine, conversely, is intended to move in six degrees of freedom per FSU. Panjabi described a useful thought experiment to visualize stability in the spine. Placing a ball in a bowl, it will tend to rest at the bottom. Spine stability is analogous to the bowl, where the spine itself is the ball. If pushed, the ball will move up the sides of the bowl and then fall back to equilibrium. A narrow bowl with steep walls, like the shape of a champagne glass, exhibits high stability because a large force is needed to move the ball out of the bowl. From this analogy, the relation between clinical and mechanical descriptions of stability can be easily identified [11], [97]. The ball-in-a-bowl analogy describes mechanical stability based on the potential energy of a system. It does so by exploring critical points of the energy balance to gauge the response to a perturbation. The description falls

short in that the deep and narrow bowl, with the ball resting within a large potential energy well, is only the optimal stability case if the system is not pushed to its tissue tolerance limits within a healthy range of motion. The ball alone does not fully represent the spine because it fails to consider clinical stability, pain and tissue failure.

The nonlinear force-displacement response of the spine creates what is referred to in the literature as a neutral zone. This region corresponds with the basin of the potential energy well, or stability bowl, where the spine is relatively uninhibited in its displacements. Beyond the neutral zone of the spine, studies on the excised spine have shown that passive tissues rapidly increase joint stiffness to oppose hypermobility [55], [56], [100], [101].

Panjabi (2003) has described three units working together to mechanically stabilize the spine: the passive vertebral column, the active musculature, and the neurological control system [11], [96]. These three are captured within the two pathways of joint stiffness, namely the intrinsic and reflex response [102]. The intrinsic stiffness pathway reflects the nonlinear force-displacement constitutive laws of all passive materials in the spinal column including the IVDs, ligaments, muscles, tendons, fascia, and adjacent compartment pressures such as IAP. The body is in a constant state of pre-stress from body weight and muscle contraction. Thus, the stiffness of the muscles varies and stiffness measured about some operating point will encompass the active contribution of a stiffened musculoskeletal system. The neurological control system, meanwhile, reads nerve input from mechanoreceptors or nociceptors in biological tissues including muscle and fascia [60], [76]. These efferent stimuli report mechanical stresses to the central processing of the nervous system, which then makes small adjustments to stability, via reflexive stiffness. Granata *et al.* (2004) have estimated a delay of approximately 50 ms for the afferent and efferent nervous signals to alter the mechanical baseline of a joint [103], [104]. Maaswinkel *et al.* (2016) highlighted how the three mechanical stability units function simultaneously and cannot be evaluated independently in a live subject [105].

Adding to this, a component that narrows the width of the neutral zone, by increasing stiffness, without drawing the biological system nearer to its tissue failure limits, increases the stability of that system. It becomes, therefore, most practical to define the baseline state of operation of a system and quantify stability based on deviations from this state. Ghezelbash *et al.* formulated a more comprehensive definition as follows [95],

> *"Stability of a mechanical or biological structure during regular operations may be defined as its ability to withstand small (internal and/or external) disturbances without hypermobility or excessive motions that could potentially cause malfunction, damage, or pain."*

This bridges the gap between clinical and mechanical perspectives on spine stability and establishes a clear objective in which computational studies can explore this concept. It is also aligned with the definition put forward by Solomonow (2011) [106],

> *"Stability, therefore, is an assessment of the robustness of the spine functioning within its physiological range of motion and loads without the risk of buckling, fracturing, displacing out of range and incurring additional damage to associated structures."*

Robustness may be quantified in engineering by the system's deviation from baseline under some perturbation. In a dynamic system, the baseline may be a moving trajectory [99]. The perturbation can be internal or external. Relating this back to tissue tolerance involves quantifying the perturbation response within the range of motion and loading context of the spine. For example, in spine flexion, stiffness can be quantified as a function of flexion angle, indicating the change in robustness through normal movement. Alternatively, quantifying the stiffness contribution of IAP should consider the cost of additional compression on the spine.

2.3.3 Experimental Approaches

Based on these conceptual definitions of stability, various attempts at mathematical formulations have been proposed. For static analysis, the ball-in-a-bowl analogy is intuitively translated to a potential energy formulation for stability. Cholewicki and McGill (1996) extended this to an EMG-assisted multibody dynamic model. Stability was quantified over time using the determinant of the second derivative of minimum potential energy across all directions [107]. This was evaluated at quasi-static freeze-frames and does not consider kinetic energy in the system.

Ghezelbash *et al.* (2022) quantified stability at quasi-static postures by measuring forces required to cause instability by buckling [108]. This approach could be considered most directly tied to the definition of mechanical stability, but the conclusions are also tied to the stress state and loading profile of the system, rather than characterizing the system. The authors modeled the active muscle unit of mechanical stability using the equivalent spring approach originally described by Bergmark (1989) [109]. The method estimates muscles forces according to an EMG-assisted optimization criterion and then replaces the muscles with a spring defined by $K = q\frac{F}{L}$, where the spring stiffness, K [N/m], is a function of the force-to-length ratio (F/L) [N/m], and a dimensionless coefficient, q [95]. Bazrgari *et al.* (2008) used this formulation directly as the stability margin of the spine, by quantifying the minimum coefficient needed to maintain stability, for all equivalent muscle springs [110], [111]. This formulation of stability is less intuitive, but captures the active unit and its role in stability, albeit indirectly via optimization. However, most multibody dynamic models fall short in physiological representation of the passive unit, which could lead

to overestimates of the active role in this approach. Also, it is still limited to freeze-frames and moving operating points.

The comprehensive definition of mechanical stability from Ghezelbash *et al.* can be naturally tied to stiffness. In the ball-in-a-bowl conceptualization, steeper walls represent greater joint stiffness. Most simply, quasi-joint stiffness evaluates this as the torque-rotation response. More complex, a system identification process—named the parallel cascade nonlinear system identification technique—can identify the intrinsic and reflex responses individually and was first applied to the knee and elbow joints by Kearney *et al.* (1997) [102]. It has since been extended to the lumbar spine [112]. For *in vivo* characterization of dynamic joint stiffness, the two pathways must be identified simultaneously as the they are not independent of each other [105]. In muscles, the reflex pathway can recruit additional fibers, changing the elasticity of muscles even under isometric loading when some perturbation is imposed. In benchtop testing and simulation, however, intrinsic stiffness is effectively isolated from the reflex pathway. This could be leveraged to simplify the system identification process. This experimental approach characterizes the system's dynamic response about an operating point and can be extended to time-varying dynamics to evaluate stability over a moving trajectory [113], [114]. A drawback to this method is that it can be difficult to relate the parameters back to physiologically meaningful variables. Stiffness is identified as a whole, without regard to specific contributors.

Finally, Ghezelbash *et al.* highlighted that dynamic stability can be evaluated by considering the state of decay or expansion of its eigenvalues [95]. This ties directly to the kinematic variance approach, where Lyapunov exponents are used to quantify stability. Briefly, the Lyapunov exponent is a measure of the variance in repeated movement, representing divergence of the trajectory. A large positive Lyapunov exponent indicates instability, as small perturbations in joint movements grow exponentially, causing divergence from the baseline or expected trajectory. This has been applied to *in vivo* spine stability analysis in movement [98], [115] and lifting [116], but may be less applicable to computational studies without repeated movement trials. This approach shares the drawback of dynamic joint stiffness proposed above.

Many of the previous methods lump the passive and active units together as an intrinsic component differentiated only from reflex stiffness, or the neurological unit. Focusing on the passive unit, experimental and computational studies have explored individual contributions to passive mechanical stability by sequentially resecting tissues that contribute to stability and evaluating the change in range of motion and related intrinsic stiffness [100], [117], [118]. The passive and active units can be conceptualized by the inverted cone analogy. Inherently, the cone would be an unstable system, but by attaching taught wires around its perimeter, it can become conditionally stable

[107], [119], [120]. Passive tissues create a baseline stability and active tension in muscles adjust the neutral zone according to loading. This is demonstrated experimentally by the spine's intrinsic resistance to buckling, which is dependent on loading mechanism. Patwardhan *et al.* (1999) was the first to define the concept of the follower load, initially as a tool for more accurately reflecting the compressive tolerance of the spine in *ex vivo* testing [121]. This has been used in many isolated lumbar spine models to approximate the aggregate active muscle activity [122], [123]. To maintain stability in the human body, flexural forces and body weight are supplemented by co-contraction of extensor and stabilizing muscles. The vector sum of the lines of action of extensor and stabilizing muscles of the spine direct forces tangentially along its curvature. Patwardhan *et al.* showed that applying compression through the centers of mass of vertebral bodies, via tensioned cables, greatly increased buckling tolerance to more than 1200 N, from 100 N for a simple vertical load. Rolhmann *et al.* (2001) supported this, indicating the addition of a follower produced more realistic rotations in the excised spine [101]. This highlights the important role of the active unit in adjusting intrinsic stiffness according to net external and internal forces on the spine. Rohlmann *et al.* (2009) later applied this this concept in FEM, showing that best agreement with *in vivo* data is obtained by combining rotation with the follower load. They added that 1175 N compression created the most realistic loading profile [123].

Two studies have attempted to evaluate the stiffness contribution of the TLF by isolating an *ex vivo* FSU. Excising samples of only a single FSU with ligaments and a section of the middle layer of TLF, Barker *et al.* (2006) showed a lateral force of 20 N on the lateral raphe increased stiffness in flexion and decreased it in extension. This force was estimated to represent approximately 50% TrA activity, assumed from myoelectric patterns related to IAP [16]. Contrarily, Ranger *et al.* (2017) found no consequence of this same TLF force vector on FSU stiffness in any of the three anatomical axes of rotation [15]. Both studies used similar methodology and equal lateral force magnitude. They each faced a major limitation likely affecting conclusions about the TLF's role in spine stiffness. By isolating individual FSUs, the TLF loses its continuities to adjacent vertebrae as well as caudal and lateral muscle attachments such as the gluteal muscles and LD. Similarly, by isolating the TLF from its interface with the paraspinal compartment, it loses a critical boundary condition affecting its line of action to the spine and its ability to maintain form. These notable absences in experimental set up create unrealistic freedom of motion for the segmental TLF tissue, and likely underestimate its effect on rotational displacement of the spine with and without abdominal force.

2.3.4 Intra-Abdominal Pressure and Stability

IAP, specifically, is considered to be involved in, at least, the passive and active units of the spine stability system. This is possible through three mechanisms. The first mechanism, offloading, was demonstrated first with a practical benchtop analogue by Cholewicki *et al.* (1999a) and then, more concretely, via direct stimulation of the diaphragm to incite contraction by Hodges *et al.* (2001). The benchtop experiment used a simple pivot joint with parallel springs to represent muscle tension from RA and the erector spinae, at realistic moment arms. A parallel pneumatic piston represented IAP [124]. By including only the pressurized IAP piston with the RA spring at a pre-tension to reach equilibrium, the joint could handle higher loads before buckling. Greater IAP led to greater critical loads. In this setup, the spring pre-tension is antagonistic to the IAP piston's offloading effect. Thus, the combined loading of RA tension with offloading from the IAP piston raises the stability margin, by deepening the potential energy well. It can be inferred that any additional pressure created without adding to the equal and opposite RA force would further benefit stability by consideration of tissue loading. Essendrop and Schibye showed this inequilibrium condition could exist *in vivo* by evaluating sudden trunk loading. In these conditions, IAP was increased rapidly, without tension in the RA [91]. More directly, diaphragm stimulation produced a net extensor moment on the spine, despite not having any line of action to induce this rotation [72].

By supplementing IAP with a lumbosacral orthosis, Larivière *et al.* (2019) and Cholewicki *et al.* (1999b) showed that stiffness was increased, despite no reliance on muscle contraction [125], [126]. This provided valuable insight into the presence of a buttressing effect, the second mechanism, given the absence of a role for the active unit. Under internal or external loads, displacements cause the vertebrae to abut against the internal compartment pressure.

The third mechanism, hoop-stress relayed as tension through the TLF, has been supported experimentally. Tesh *et al.* (1987) did so by inflating balloons in the abdominal compartment of whole cadavers up to realistic IAP magnitudes of 60 mm Hg and 120 mm Hg. This tensed the middle and posterior layers of the TLF, adding stiffness to the system [127]. This may have also supported the buttressing effect, as the compartment was pressurized in a manner independent of abdominal muscle contraction. Vleeming *et al.* (2014) directly tensed the abdominal aponeuroses connecting with the TLF, simulating lateral abdominal wall muscle contraction. The authors showed that with pressure in the paraspinal muscle compartment, tension mostly bypassed the middle layer, relaying force to the spine through the PLF [128]. The experiment also showed the importance of muscle pressure in the erector spinae to maintain a line of action necessary for tension to influence the spine. This was confirmed *in silico* by El-Monajjed and Driscoll (2020)

[129]. In the absence of sufficient muscle compartment pressure, the TLF is free to displace laterally and anteriorly [128], affecting the internal reaction force [129]. These findings support the importance of accurately reflecting boundary conditions and tissue interactions when investigating TLF behaviour through *ex vivo* and *in silico* experimental approaches. These studies have led in to the experimental approaches on TLF tension discussed in the previous section, which focused in on this reported tension.

The baseline IAP magnitude (5–7 mm Hg) is considered a passive stabilizer. Muscle contraction in the diaphragm and abdominal wall would represent active stability which, as discussed, may be targeted through preparatory behaviour before lifting. It is also unclear whether IAP can be modulated through the neurological unit as a contributor to reflex stiffness. The sudden loading trials by Essendrop *et al.*, in which subjects experienced unpredictable disturbances accompanied by significant changes in IAP, suggest the involvement of a reflexive pathway [91].

2.4 Low Back Pain Risk Factors

2.4.1 Stability as a Risk Factor

An example from McGill (2001) underlines the importance of understanding the biomechanical mechanism of spine stability within the context of LBP. Mechanical testing shows the spine may buckle at high loads, but patients can experience LBP from bending over to pick up a pencil [97]. A more intrinsically stable system is less vulnerable to neurological control error. Excess muscle forces from reflex response in a sudden absence of stability or prolonged dependence on the active unit to enhance stiffness through elevated muscle activity, even by small EMG increases [99], could cause clinically significant stress on the spinal column and lead to pain [107]. Low-magnitude motor activity could cascade toward tissue inflammation if sustained over long periods [106]. By characterizing the baseline stability of a healthy spine, it becomes possible to evaluate factors that alter the system stability, positively or negatively. Thus, studying the dynamic intrinsic stiffness of the system, which is isolated in a FE model, provides valuable insight into the injury mechanisms of the low back. Further, with up to 90% of patients unable to identify the cause of their LBP [3], identifying the factors that affect stability could be essential toward minimizing risk in daily activities.

2.4.2 Occupational Risk

Many retrospective studies have looked at risk factors for LBP, tying historical records to job-specific trends. Similarly, prospective studies have used worker reports to evaluate risk [130]. Fewer have specifically quantified biomechanical motion factors and even fewer have done so in their native occupational settings.

Marras *et al.* (1993) reviewed risk factors in occupational settings. Through biomechanical

data analysis of worker kinematics during lifting between historically high- versus low-risk occupations, the authors were able to identify movement patterns that increased probability of LBP. Workers wore a lumbar motion monitoring device on the job. Of the trunk motion factors studied, those having to do with dynamic effects appeared to most significantly raise the risk of LBP, with trunk average trunk velocity leading the way. Odds ratios—the relative increase in chance of LBP due to a certain factor, with a value of 1 being equal chance—were 3.33, 1.73, and 1.70 for average sagittal plane velocity, maximum velocity, and maximum acceleration, respectively. The previous factors were followed, in odds ratios, by maximum flexion position, maximum range of motion, and maximum extension position. Increases to these variables raised the risk by factors of 1.60, 1.48, and 1.36, respectively. Thus, while many biomechanical factors could affect low back injury in the workplace, Marras *et al.* indicate that the most likely individual candidate, nearly doubling any other, is average trunk velocity [131].

While velocity stands out from the kinematic variables within the worker's control, other workplace factors are believed to have a greater probability of injury. Most notably, load in the hands and its intercorrelated low back moment [8], [131], [132]. Marras quantified odds ratios of 2.76, 3.17, 4.08, and 5.17 for average and maximum load in the hands, and average and maximum low back moment, respectively. Similarly, Norman *et al.* (1998) calculated the odds of low back injury are as much as 10.5 and 4.8 times higher when lifting at the extremes of load and velocity, respectively, as measured over a two year period [8]. Low back moment can be influenced by the lifter, but is most appropriately considered a workplace factor out of their control since load distance is usually a function of the job requirements [133].

From a different perspective, and outside the workplace, McGregor *et al.* (1995) indicated that mean velocity in the flexion range of motion (ROM) is affected by LBP, proportionally more so than ROM itself. This shows a two-way relationship for velocity as a risk factor in LBP. Lifting at greater velocity raises the odds of injury and having the injury, patients are more inclined to move at lower velocity [134]. These motion characteristic differences between healthy and LBP patients have also been supported by McIntyre *et al.* (1991) [135]. Functionally, the dynamic effects are believed to influence spinal loads. According to the equations of motion, greater acceleration leading to higher velocity induces larger reaction forces in the spine, whereas a constant velocity, regardless of its magnitude, does not generate such forces. A faster lift overall will include larger accelerations as the spine always starts and finishes at rest.

Norman *et al.* further proposed cumulative loading as an indicator of risk in the workplace. More recently, this has been supported by Johnen *et al.* (2022) [136]. This approach accounts for loading integrated over a work day. While it can statistically differentiate low and high risk, it has

not differentiated itself from the individual factors [8].

2.5 Finite Element Method and Existing Models

Overarchingly, the FE method (FEM) discretizes a continuum into finite elements to solve for nodal displacements by balancing forces within a stiffness matrix framework. This formulation receives input from material properties and element shape functions. The solution space is constrained by problem-specific inputs like boundary and initial conditions.

More relevant to the topic of this thesis are applications of FEM toward spine biomechanics and IAP modelling. Some FE investigations have been previously reviewed where relevant to the functional biomechanics. Static models are most efficient at taking peak loads and evaluating stresses, strains, displacements, or pressures at specific areas of interest. Dreischarf *et al.* (2014) compared current industry-recognized osseoligamentous lumbar spine models to establish a reference point and evaluate variability between published models. There was notable variability in predicted rotations, IVD pressures, and facet joint reactions forces between models, though they generally do well in representing the physiological range of values. The study proposes that there is strength in pooling models to improve statistical power and more accurately reflect biomechanics with inter-subject variability [57].

Despite the elevated risk associated with dynamic effects, elegantly highlighted by Marras *et al.*, few models have considered viscoelastic, time-varying properties in the IVD, a tissue characterized by its high water content in the NP. Two studies have modelled this behaviour using different approaches. Wagnac *et al.* (2012) did so by defining two sets of hyperelastic constitutive laws, representative of fast and slow compressive loading rates [137]. Conversely, Wang *et al.* (1997) characterized a hyper-viscolelastic material law for the nucleus and annulus by inputting stress-relaxation and volume-relaxation parameters [138]. The latter approach is more suited to general applications where load rate may not be a precisely known parameter or may be a function of combined loading effects.

Biomechanical models can and have been used to investigate cause and effect relationships from risk factors identified by epidemiological studies highlighted in the previous section. Focusing on subject-controlled variables with the greatest consequence on LBP risk—velocity and posture—computational studies have related these factors to stability [110], [139]–[141] and resultant low back moment [142]. Generally, these have found increasing trends, remarking gains in loads and stability with faster lifting speed and larger flexion angle. As discussed, these velocity observations are understood to be attributed to larger acceleration and deceleration at each respective end of the ROM during a lift. Arjmand *et al.* (2006) specify that load in the hands has a much larger effect on internal stresses compared to posture [139]. These trends also indicate that

stability increases with flexion angle. This is intuitive from the mechanical stability perspective as deep flexion brings the system out of the its neutral zone, where stiffness rises sharply [110], [139]. However, this analysis does not consider tissue tolerance and whether this movement brings the passive stabilizers, such as the ligaments, closer to failure or micro-failure.

Historically, EMG- or optimization-assisted rigid-body dynamic models have been used to quantify muscle forces as well as compressive and shear forces in the spine associated with certain dynamic movements and external loads [143]. These kinetic models treat IVDs as rigid joints and are efficient in estimating reaction forces, but do not factor in deformations. Further, advances in computing and parametric geometry inputs facilitate efficient patient-specific modelling in this approach [142].

More recently, models have combined the depth of information retrievable from fully deformable FE models with the efficiency of rigid multibody models. These flexible multibody dynamic models can incorporate soft tissue effects, such as IAP. Three studies have employed varying approaches to abdominal muscle-IAP-spine coupling. Remus *et al.* (2023) relied on mathematical assumptions to directly quantify IAP forces from abdominal muscle contraction [144]. Guo *et al.* (2021) and Stokes *et al.* (2010) represented the abdominal wall with simplified geometry. Stokes *et al.* directly control IAP, exerting outward radial force to the abdominal wall [145], while Guo converts volume reduction in the compartment from abdominal muscle contraction to pressure changes [146]. Normal forces acting on the diaphragm, pelvic floor, and simplified abdominal walls are described. However, neither model description has clearly outlined how the compartment pressure exerts force directly on the spine, posteriorly. Each model, to varying degrees, sacrificed accuracy in modelling the abdominal wall geometry, favoring dynamic effects.

Favoring physiological accuracy in the abdominal wall geometry, Jourdan *et al.* (2024) have recently validated a high fidelity abdominal wall model for application to hernia repair [67]. Their approach should establish a target, moving forward, for capturing the interaction of abdominal musculature with IAP. Radial expansion from contraction of volumetric abdominal wall muscles compresses the hydrostatic abdominal compartment volume, pressurizing the cavity without relying on assumptions in the muscle-IAP pressure relationship. The lateral abdominal wall is subdivided into the three muscle layers, capturing individual contributions. The problem becomes significantly more complex, computationally, when extending to the spine. El Bojairami *et al.* (2020) and Bernier and Driscoll (2024) have integrated anatomy-derived abdominal compartment models with a FE model of the spine [147], [148]. However, El Bojairami *et al.* excluded the abdominal wall, modelling only the compartment. As a result, the behaviour of IAP is not fully represented as there is no anterior or lateral restriction to pressurization of the compartment.

Bernier and Driscoll advanced this further, adding a passive abdominal wall, but with all muscles blended into a combined elastic component.

2.5.1 Thoracolumbar Fascia Modelling

The previously discussed experimental investigations of TLF as a passive element contributing to spine stiffness underline, through their limitations and inconsistent results, the inherent difficulties of studying this stiff, but flexible tissue via benchtop testing. Relatively few studies have capitalized on the advantages of the *in silico* experimental approach to maneuver around the challenges posed by the complex boundary conditions and continuities between abdominal, paraspinal, and upper back musculature.

The model of El Bojairami *et al.* introduced above also benefits from including the TLF and its attachment to the LD. The fascia was isotropic and its geometry was approximated, rather than derived from segmentation and appeared to be an overestimate of the tissue's true thickness. However, no model has captured its contribution to spine mechanics with anatomically-representative geometry. By virtual sequential resection of tissues in a spine model inclusive of major stabilizing muscles and connective tissues, with IAP, the TLF was shown to contribute up to 75% of the flexural stiffness of the spine [149]. It also served as a lead-off point for further studies, including an investigation of stress-shielding in the TLF by Newell and Driscoll (2021), a phenomenon propagated by tissue remodelling in LBP patients [14]. Specifically, TLF thickness tends to increase with LBP due to tissue fibrosis from reduced movement [150]. In a cascading effect, this could reduce stress in the erector spinae [151], potentially leading to muscle atrophy [14].

Choi and Kim (2017) employed a similar study design to those of Barker *et al.* and Ranger *et al.* by applying a virtual lateral force to the spinous process in an osseoligamentous FE spine model representing L4–S1 [13]. However, the authors abandoned TLF geometry altogether, opting to apply the lateral PLF tension directly to the spine. The authors identified a nonlinear curve, with increasing TLF force up to 40 N having a growing effect on augmenting bending stiffness of each of the L4/L5 and L5/S1 segments. Their approach is likely a result of the lack of anatomy-derived TLF geometry to deploy in FEM. This limitation forced the assumption that contractile forces from TrA are perfectly transmitted through the TLF as tension on spinous process angled along the fiber directions. These *ex vivo* and *in silico* studies motivate the need for a more physiologically representative approach to investigate the TLF biomechanics outside the live human body, particularly within the context of abdominal muscle forces related to IAP.

2.6 Conclusion

The relevant literature pertaining to the functional biomechanics of the lumbar spine was reviewed. Key factors playing a part in the multifactorial pathomechanism of LBP were discussed

in detail, including IAP, stability, and occupational risk. Particularly, the interplay of these factors was underlined and the transient nature of their effective loading was identified. A description of the relevant anatomy was provided to support the reader's interpretation of the content of this thesis, as well as to describe the most important physiology influencing some of the engineering decisions and assumptions leaned on during development of a spine and trunk model. In developing a comprehensive FE model of the trunk, including abdominal musculature and connective tissue, sources of image data alone cannot always provide the entire basis for a computational model. Further quantifiable insight into the typical geometry of an average human is needed to build a converging model. To understand the role of IAP in spine stability, it is necessary to understand the pathways by which the abdominal compartment can exert forces on the spine, which in turn requires an understanding of its fascial connections to the spine. This is in addition to the pathways by which abdominal muscle contraction can pressurize the abdominal compartment. Finally, these descriptions were tied to computational studies that have laid a foundation for the current FE analysis. The FE model developed and discussed in this thesis relies on this foundation to conform with established best practice in the field while building beyond the spine to represent the behaviour and loading of IAP. The following chapter will discuss the effects of IAP and lifting velocity, as a key occupational risk, toward intrinsic spine stiffness to provide insight into the stability mechanisms of the low back. An additional study will then focus on the TLF to generate an anatomy-derived model, define its intrinsic stiffness contribution, and evaluate the effect of abdominal muscle force.

3 Finite element evaluation of the contribution of intra-abdominal pressure toward dynamic spine stability

3.1 Framework for Article 1

The first manuscript addresses the first objective of the thesis using the steps listed in this Chapter's respective block in Figure 1.0.1. Occupational lifting is, in itself, a risk factor for low back injury contributing to the high prevalence and burden of the musculoskeletal condition. IAP and lifting velocity have been identified, through the content of Chapter 2 as dynamic factors with important roles in spine stability. It is hypothesized that the baseline stability during lifting movement is altered by the these two input variables to the musculoskeletal system of the trunk. Thus, through the study of Chapter 3.2, the dynamic intrinsic stiffness of the spine along a moving trajectory with these inputs, individually and combined, is quantified. By comparing stiffness between each load case, insight is provided into the relation between the intrinsic stiffness and the mechanical stability potential among the three units of the spine stability system.

To accomplish this, a FE model of the spine and trunk was developed. Widening focus from an isolated spine, a physiologically representative abdominal compartment was included, along with paraspinal musculature, to represent the passive mechanisms of IAP while minimizing assumptions. The model captures two of the three pathways for IAP contribution to stiffness, specifically offloading and buttressing. Limitations of the model are discussed, particularly as they relate to the third pathway, hoop-stress and tension through the TLF.

A graphical overview of the article is provided in Figure 3.1.1. The manuscript has been submitted for publication in Computers in Biology and Medicine is currently under review. The content of the manuscript was also presented at the Eurospine congress in Vienna, Austria, on October 2nd, 2024.

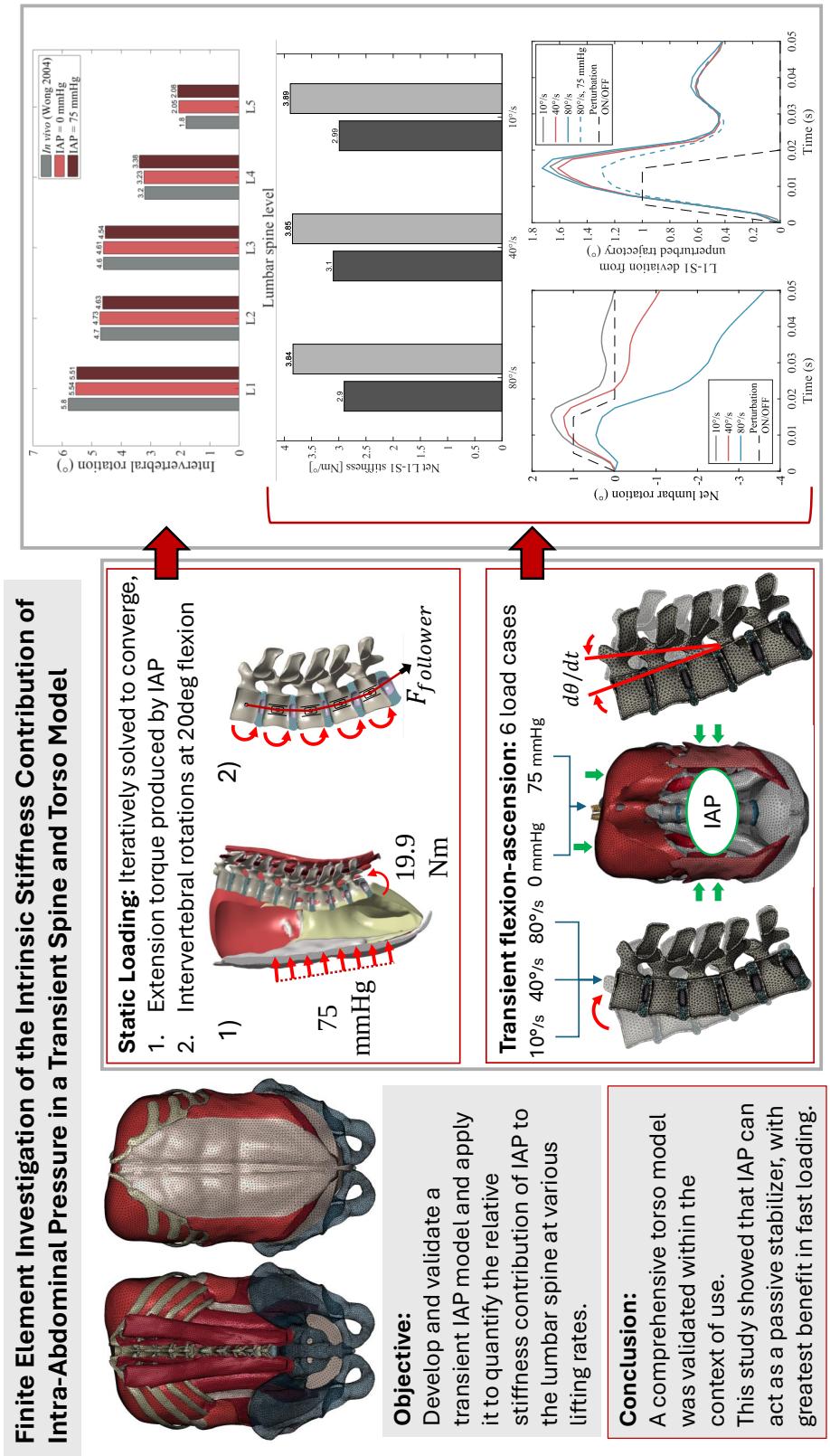

Figure 3.1.1: Graphical abstract summarizing the content and flow of Article 1.

3.2 Article 1: Finite element evaluation of the contribution of intra-abdominal pressure toward dynamic spine stability

Sean Murray[1,2], Mark Driscoll[1,2]

[1]Musculoskeletal Biomechanics Research Lab, Department of Mechanical Engineering, McGill University, Montreal, QC, Canada

[2]Orthopaedic Research Lab, Montreal General Hospital, Montreal, QC, Canada

Address for notification, correspondence, and reprints:

Mark Driscoll, Ph.D., P.Eng.

Associate Professor, Department of Mechanical Engineering

Canada NSERC Chair Design Eng. for Interdisciplinary Innovation of Medical Technologies

Associate Member, Biomedical Engineering

Associate Member, Department of Surgery

Investigator, Research Institute MUHC, Injury Repair Recovery Program

McGill University, Department of Mechanical Engineering

817 Sherbrooke St. West, Montreal, QC H3A 0C3, Canada

Macdonald Eng. Bldg., office #153

T: +1 (514) 398-6299

F: +1 (514) 398-7365

E-mail: mark.driscoll@mcgill.ca

3.2.1 Abstract

Lifting velocity is a high-risk factor for low back pain in occupational settings and intra-abdominal pressure (IAP) is known to fluctuate transiently during lifting. The contribution of IAP toward spinal stability at different loading rates remains largely unaddressed in biomechanical models. This could provide insight into how lifting velocity can affect low back injury mechanics.

A nonlinear, transient finite element model of the lumbar spine and surrounding anatomy was developed, including an anatomically accurate abdominal compartment. In combined loading, the spine was flexed to target *in vivo* intervertebral rotation patterns at 20° net L1-S1 rotation. Six load cases were then simulated transiently, driving extension back to standing posture at $80°/s$, $40°/s$, and $10°/s$ velocities, for IAP magnitudes of 0 mmHg and 75 mmHg.

Statically, 75 mmHg IAP introduced a 19.9 Nm extension moment. Transiently, 75 mmHg IAP increased lumbar stiffness at all rates, with a maximum gain of 0.948 $Nm/°$ (33%) at $80°/s$. Without IAP, intrinsic stiffness was maximized at $40°/s$, with 3.1 $Nm/°$. Between lift velocities, stiffness increased proportionally to velocity when calculated relative to the starting angle. The differences were small when offsetting the effect of faster baseline trajectories.

An intrinsic stability potential for IAP was identified during lifting movement. Since faster lifting is induced by larger loads, the passive displacement-limiting gain of IAP holds greater weight with increasing velocity. Ineffective abdominal muscle activation to generate IAP or poor timing during a lift could increase low back injury risk due to insufficient lumbar spine stability.

3.3 Introduction

In occupational settings, workers are often required to lift objects repeatedly over many hours in a work day. As many as 84% of people experience low back pain (LBP) in their lifetime and these injuries have significant quality of life and economic consequences [1]–[3]. The health-care system in Canada suffers a $12B annual loss due to patients seeking medical attention for LBP [4] while in the USA, $315B was spent per year between 2012 and 2014 on direct medical costs for treatment of back conditions [5], with non-specific LBP as the global leading cause for disability [6]. Greater sagittal trunk velocity during ascension from flexion back to neutral posture has been associated with greater incidence of LBP in the workplace [7], [8]. In response, Davis and Marras (2000) identified the need for a broader understanding of risk factors related to spine movement and their role in the multifactorial pathomechanism of LBP [9]. However, there has been little account of trunk motion in modeling studies.

The effects of loading rate on the spine are important to consider for traumatic injury resulting from sudden loading events such as crashes or falls [10]. It is somewhat less obvious to consider it in the context of LBP. Yet, it is well known that occupational lifting is a high-risk factor for LBP [7]–[9], [11]–[13]. Marras *et al.* (1993) noted that lifting velocity had the highest risk factor among parameters relating to trunk motion, with a higher average magnitude observed in high-risk occupations [7]. Biomechanical measures such as low back moment, compressive load, muscle activity, and intra-abdominal pressure (IAP)–the internal pressure within the abdominal cavity–tend to increase with the rate of ascension [9], [14]–[19].

The claim that faster lifting is inherently riskier is challenged in some ways. Notably, the dynamic model of Bazrgari *et al.* (2008) was employed to support notions of larger loads induced by faster movement speeds, but it was additionally concluded that stability increases with velocity [18]. This is likely attributable in part to the nature of viscoelastic materials to be stiffer when loaded at a higher rate [20] and a stiffness-based definition of stability will reflect this. A kinematic-variance approach to spine stability, as employed by Granata and England (2006), suggests the inverse trend [19]. In a review of trunk dynamics studies, Davis and Marras note trunk strength tends to decrease with increasing dynamics, but this trend was disputed by some [9]. Lin and Cheng (2017) offered a more nuanced view, proposing there may be an optimized lifting speed at which capacity is maximized [21]. There appears to be no consensus on the best practice for controlling velocity during the ascending phase of a lift, despite its obvious relevance to occupational tasks.

Just as lifting velocity appears to be intimately tied to LBP through spinal loads and stability, IAP is believed to be a principal contributor to those same biomechanical outcome measures

of the spine, particularly affecting net lumbar moment and stability [22]–[25]. Proportionality between IAP and movement speed [9], [15] or load [26], [27] during lifting has also been reported. These monotonic trends hint at the importance of effective IAP control in the context of occupational lifting. Timing factors of IAP also play a role in dynamic lifting. Rate of development of IAP is known to peak before lifting motion onset [26], [28], while peak IAP occurs shortly after [26], [27], [29]. Since IAP appears to employ a supportive role in lifting tasks [15], [22], [28], [30]–[32], the timing and magnitude of IAP generation could have functional importance as there may be risk in ill-timed IAP modulation.

In vivo studies have been used to identify trends in IAP with movement [14], [22], but lack the ability to push safe tolerance limits or directly control IAP [33]. Further, it is difficult to safely evaluate internal stresses during extreme loading. The finite element method (FEM) presents itself as a suitable alternative for studying the effects of IAP in dynamic lifting conditions.

Few studies have evaluated transient behavior in FE models of the spine and none have considered IAP in flexion-ascension of the spine. Flexible multibody dynamic trunk models have recently included IAP while sacrificing geometrical representation of the abdominal compartment and muscles in efforts to efficiently compute spinal loads [34]–[36]. Flexible FE models of the spine have captured the behavior of IAP with anatomically representative abdominal compartments, but not during movement [25], [37], [38]. Specifically, El Bojairami and Driscoll (2022) noted IAP accounted for 25% of static spine stability [25]. Jourdan *et al.* (2024) created a high fidelity EMG-driven dynamic model of the abdominal wall to capture its interaction with IAP. However, the spine was neglected with a focus on implications for hernia repair [39].

Engineering systems are often optimized for stability. The spine is similar, except humans have control over system parameters and inputs, such as IAP, during voluntary tasks. By expanding our understanding of the intrinsic properties of IAP as it relates to the biomechanics of the spine, stability can be optimized via training, lifting strategy or external devices [38]. Ghezelbash *et al.* (2023) consolidated definitions of stability in musculoskeletal systems, defining a stable system as one that will not reach tissue or mobility limits upon relatively small perturbation [40]. A system that passively limits displacements in response to perturbation is considered more intrinsically stable [41].

Maaswinkel *et al.* (2016) proposed a framework for assessing *in vivo* trunk stability from its response to perturbation. The authors suggest that *in vivo* stability must be assessed with simultaneous contributions of reflexive and intrinsic stiffness due to interplay between the two contributors. The reflexive contribution to perturbation response comes with a latency of around 50 ms [42]. However, in a FE model, the contribution of intrinsic stiffness to trunk stability can be

isolated [43].

To the authors' knowledge, no FE study has investigated the effect of IAP on the spine as a function of movement speed. The objective of this study was to develop and validate a physiologically representative FE model of the spine that accurately captures the behavior and contributions of IAP toward spine stability. Subsequently, the study aimed to apply the novel FE model to quantify the relative stiffness contribution of IAP to the lumbar spine at fast and slow lifting rates.

3.4 Methods

3.4.1 Model

A nonlinear, time-dependent model of the lumbar spine and surrounding anatomy was developed and validated in the FE software Ansys Mechanical (V23.1, Ansys Inc., Canonsburg, PA, USA). The FE model geometry was developed from an anatomography database (BodyParts3D) of volumetric bodies constructed from MRI images of a 22-year old, healthy male subject. The geometry includes the lumbar spine and musculature as well as muscle tissue and bone enclosing the abdomen. It is an expanded and modified iteration of the model developed and validated by El Bojairami *et al.* (2020) [24]. Figure 3.4.1 displays the trunk model with an exploded view listing the included geometry. Anatomic structures were included on the basis of their accepted role in generating or transferring IAP and stabilizing forces to the spine. Thus, abdominal muscles included in the model are rectus abdominis (RA), obliquus externus (OE), and a combined transversus abdominis (TrA) and obliquus internus (OI), along with connective tissues including the rectus sheath, linea alba, and tendons. Ribs 9 to 12 were added with the costal cartilage to transfer IAP forces from the abdomen through the diaphragm.

In alignment with comparable models in literature, muscle forces from paraspinals were not applied individually to the lumbar spine, but rather combined and imposed as a follower load. The follower load method proposed by Patwardhan *et al.* (1999) [44] was adapted for nonlinear analysis in Ansys Parametric Design Language (APDL) as illustrated in Figure 3.4.2. Tension-only linear elements (LINK180) representing a 1 mm^2 steel cable connected slider joints (MPC180) at the centers of mass (COMs) of vertebrae L2-L5 and a rigid remote point at L1. A follower load force directed from the slider at L5 to the fixed COM of S1 creates tension in the cable, compressing the structure while maintaining stability through joint reaction forces in the sliders. Initial slider positions were manually adjusted through iteration to minimize intervertebral rotations in pure compression [45].

Also visible in Figure 3.4.2 is the biphasic structure of the intervertebral disc (IVD) with nucleus pulposus (NP) modeled as an incompressible fluid-filled cavity using hydrostatic pressure elements (HSFLD242). The geometry of the NP was approximated from the outer disc surface

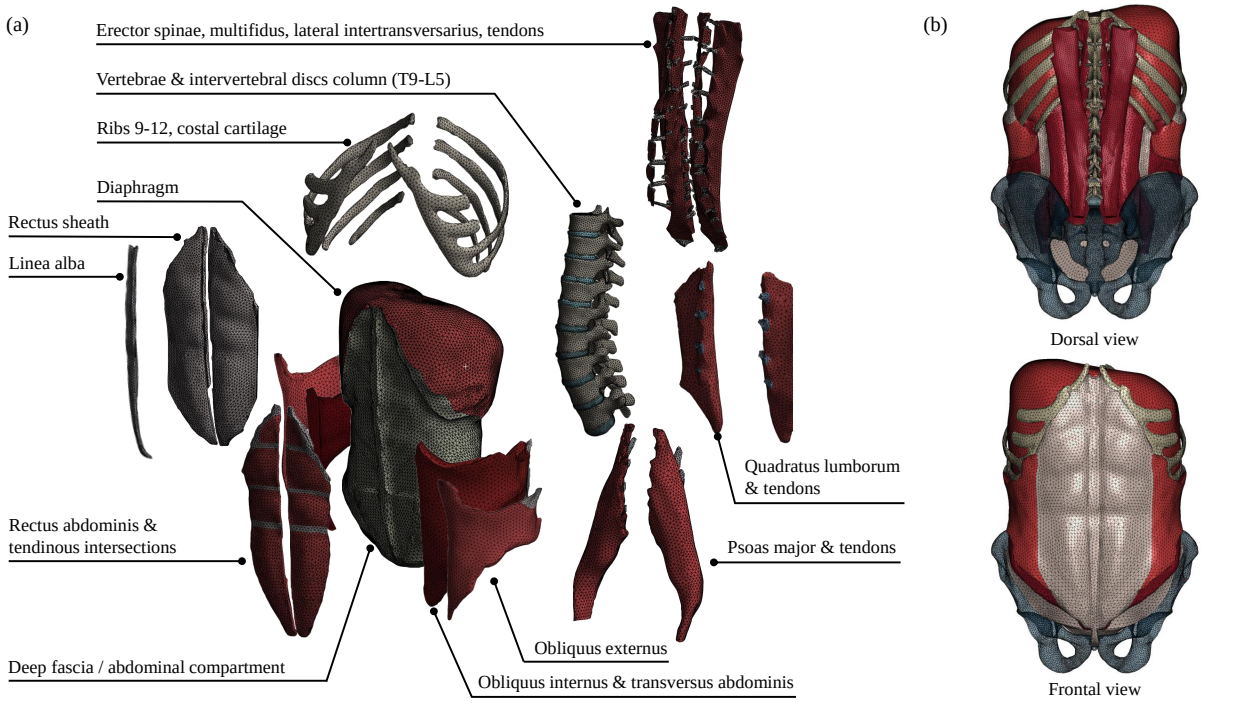

Figure 3.4.1: Model geometry and FE mesh. (a) Exploded view with annotations identifying each anatomic structure. (b) Full trunk model in dorsal and frontal views. The sacrum and pelvis are shown in translucent blue to indicate the fixed boundary conditions where the deformable model meets these bony tissues.

curvature [46], with geometrical properties as listed in Table 3.4.1. NP-to-IVD area ratios were set according to published data on a per-level basis, where available. Limited data was available at L5/S1. Instead, NP length was set to match the data of Zhong *et al.* (2014) [47], following trends indicating larger morphological ratios at this level [48]. The NP was offset posteriorly such that its curvature was best aligned with the concavity of the adjacent vertebrae [49] in the cranial-caudal axis, while remaining within one standard deviation of the average offset percentage of anterior-posterior IVD length reported by Sharma *et al.* (2022) [50]. Since intervertebral rotations (IVRs) in the thoracic spine are not of interest, these IVDs were modeled as uniform structures, as in El Bojairami *et al.* [24].

Six ligaments of the lumbar spine were modeled using tension-only nonlinear spring elements (COMBIN39). These included the supraspinous ligaments (SSL), interspinous ligaments (ISL), intertransverse ligaments (ITL), ligamentum flava (LF), posterior longitudinal ligaments (PLL), and anterior and posterior iliolumbar ligaments (AIL and PIL, respectively). The anterior longitudinal ligament was excluded as it would be in compression during flexion-ascension of the spine. Each ligament was represented by a number of spring-type elements corresponding with Shirazi-Adl *et al.* (1986) [54], except PLL which was discretized by 4 elements. The AIL and PIL connected the ilium to L5 with geometry estimated from the quantitative descriptions of Hammer

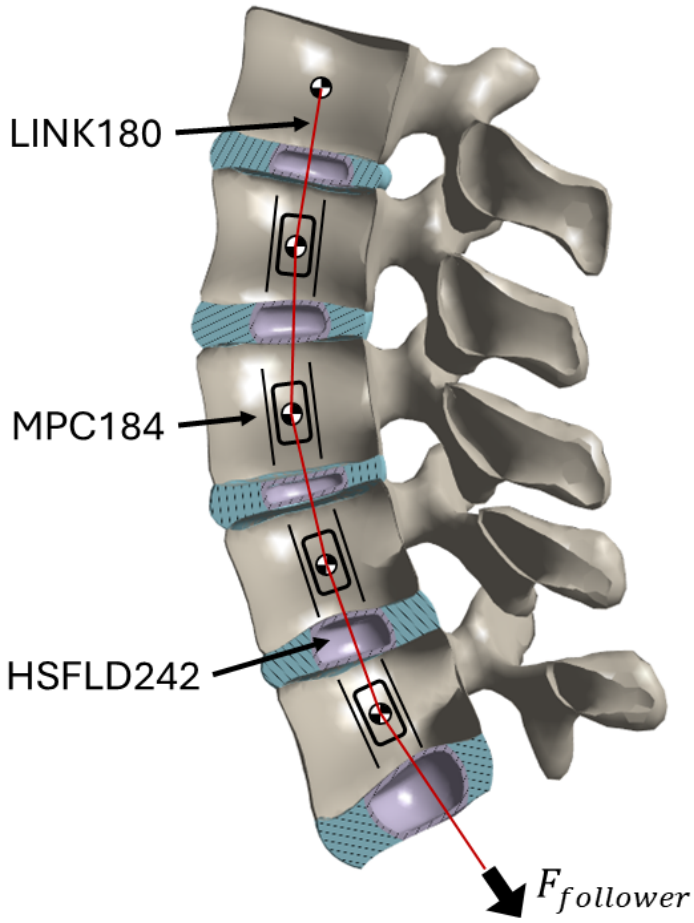

Figure 3.4.2: Graphical representation of the follower load adaption in APDL with annotation of the non-structural element types employed in the model. Not shown are the lumbar spine ligaments, implemented using COMBIN39 nonlinear spring-type elements.

Table 3.4.1: Nucleus pulposus geometric modeling properties and verification by comparison to experimental NP lengths.

IVD level	L1/L2	L2/L3	L3/L4	L4/L5	L5/S1
NP:IVD area ratio	29%[a]	29%[a]	31% [51]	28% [52]	37%
NP offset	6.7	6.7	4.2	1.9	6.7
NP length [mm] (model)	17.5	16.8	18.2	18.2	21.58 [47]
NP length [mm] (literature)[b]	19.7 (2.94)	20.5 (3.14)	20.0 (3.02)	19.32 (2.98)	21.58 (3.10)

[a] Averaged from [52][51][53].
[b] Average (standard deviation) as reported by Zhong *et al.* [47].

et al. (2010) [55] and Hanson and Sonesson (1994) [56]. The total cross-sectional area for each of AIL and PIL was defined at 72 mm^2 [55]. The AIL and PIL are believed to contribute to differences in IVR patterns observed between *in vivo* [57] and *ex vivo* [58] studies of lumbar spine flexion.

3.4.2 Materials

Table 3.4.2 summarizes the constitutive models of the NP and annulus in the IVDs of the lumbar spine. The NP was modeled as an incompressible fluid-filled cavity enclosed within a 1 mm thick outer layer [59] to capture its gelatinous, hydrostatic behavior [60]. Load rate-dependencies were modeled by prescribing viscoelastic Prony series shear stress relaxation, $G(t)$, and volumetric (bulk modulus) relaxation, $K(t)$, constants for Equations 3.4.1 and 3.4.2, respectively.

$$G(t) = G_0 \left[g_\infty + \sum_{i=1}^{n} g_i e^{-\frac{t}{\tau_i}} \right] \tag{3.4.1}$$

$$K(t) = K_0 \left[k_\infty + \sum_{i=1}^{n} k_i e^{-\frac{t}{\tau_i}} \right], \tag{3.4.2}$$

where G_0/K_0 [MPa] is the instantaneous response–defined here by a Neo-Hookean hyperelastic model in the annulus and a linear elastic model in the outer shell of the NP–and g_∞/k_∞ [MPa] is the steady-state value, and g_i/k_i are the prescribed moduli, ranging 0–1, which define the relative relaxation for corresponding time constant τ_i [s]. Relaxation moduli were adopted from Wang *et al.* (1997) [20]. The hyperelastic model of the annulus was adopted from Newell *et al.* (2019), who fit a Neo-Hookean model to the average of stress-strain relationships used across FE model publications [61]. The Neo-Hookean model parameters given in Table 3.4.2 are used by the FE solver, ANSYS Transient Structural, to calculate the strain-energy potential per unit volume, W, according to Equation 3.4.3.

$$W = \frac{\mu}{2}(\bar{I}_1 - 3) + \frac{1}{d}(J-1)^2, \tag{3.4.3}$$

where $\bar{I}_1$ is the first invariant of the isochoric left or right Cauchy-Green deformation tensor, μ [MPa] is the initial shear modulus, d [MPa] is the instantaneous incompressibility parameter, and J is the determinant of the elastic deformation gradient. The parameter d is related to the instantaneous bulk modulus, K_0 by the relationship $K_0 = \frac{2}{d}$.

Material properties of the remaining anatomical components are summarized in Table 3.4.3. To maximize IAP force transfer to the spine, the diaphragm was assumed to be entirely composed of its most stiff tissue, the central tendon, with thickness in the upper range of maximal inspiration.

Table 3.4.2: Constitutive models assigned to the NP annulus of the IVD.

Component	Elastic Coefficients	Viscoelastic Coefficients [20]		
		Shear Relaxation	Bulk Relaxation	Time Constants [sec]
Annulus fibrosus	$\mu = 0.872$ MPa [61], $d = 0.3$ MPa	$g_1 = .399$ $g_2 = 0$ $g_3 = 0.361$ $g_4 = 0.108$	$k_1 = .399$ $k_2 = 0.300$ $k_3 = 0.149$ $k_4 = 0.150$	$\tau_1 = 3.45$ $\tau_2 = 100$ $\tau_3 = 1000$ $\tau_4 = 5000$
Nucleus pulposus	$E = 1$ MPa, $\nu = 0.495$[a]	$g_1 = 0.638$ $g_2 = 0.156$ $g_3 = 0.120$ $g_4 = 0.038$ $g_5 = 0$	-[a]	$\tau_1 = 0.141$ $\tau_2 = 2.21$ $\tau_3 = 39.9$ $\tau_4 = 266$ $\tau_5 = 500$

[a] Material is considered incompressible.

As stresses or deformations in the vertebrae or ribs themselves are not of interest in the present study, these were modeled as shell bodies consisting only of cortical bone with mesh thickness 1.5 mm and 0.7 mm, respectively. The thickness of the cortical bone layer in the vertebrae is artificially increased to account for the stiffness contribution of trabecular bone. Mass of the vertebrae were then adjusted to match average values from Lowrance (1967) [72].

Ligaments of the lumbar spine were assigned discretized force-displacement relationships derived from nonlinear stress-strain curves published by Shirazi-Adl *et al.* (1986) [54] and average cross-sectional areas of the ligaments from Eberlein *et al.* (2004) [73]. Strain magnitudes were converted to displacements using lengths measured directly in the FE model.

3.4.3 Loading and Boundary Conditions

The trunk model was prescribed zero-displacement Dirichlet boundary conditions where the flexible model meets the sacrum and pelvis, highlighted in blue in Figure 3.4.1(b).

A preliminary simulation was done to determine the lumbar torque created across L1-S1 by IAP. The internal pressure was directly controlled and de-coupled from abdominal muscle activation such that a rotation of the spine in extension was created. A force perpendicular to the vector connecting the COMs of IVD L5/S1 and L1 vertebral body was increased iteratively until inter-vertebral rotations in the lumbar spine remained below 0.5°, under the IAP load. The torque about L5/S1 required to balance the extension moment induced by IAP was recorded and maintained throughout the subsequent movement simulation to equate the extension torques used to move the spine with and without IAP.

Table 3.4.3: Properties of linear materials used in the FE model.

Component	Young's Modulus [MPa]	Poisson's Ratio	Thickness [mm]
Vertebrae	17,420 [61]	0.3 [61]	1.5
Ribs & costal cartilage	14,700 [62]	0.3	0.7[63]
Tendons	200 [64][38]	0.495	-
Erector spinae	0.041 [65]	0.495	-
Multifidus	0.091 [65]	0.495	-
Psoas major	0.52 [24]	0.495	2.7[a]
Quadratus lumborum	0.091[b]	0.495	-
Longitudinal intertransversarii	0.037 [24]	0.495	-
Transversus abdominis & obliquus internus[c]	0.84[d] [66]	0.495	4 [24]
Rectus abdominis	0.52 [66]	0.495	3 [24]
Obliquus externus	1 [66]	0.495	-
Peritoneum of abdominal wall / Transversalis fascia	8.9 [66]	0.495	2
Rectus sheath	30.3 [67]	0.495	-
Linea alba	72 [68]	0.495	-
Central tendon of diaphragm	33 [69]	0.33 [69]	5 [70]
Iliolumbar ligaments	397 [71]	-	-

[a] Modeled as a shell with given thickness, enclosing a fluid-filled cavity, representing intra-muscular fluid pressure.
[b] Mechanical properties of quadratus lumborum were approximated by those of multifidus.
[c] Muscle geometry was combined into one blended part.
[d] Averaged Young's Modulus of OI and TrA.

With resultant torques determined as described, the lumbar spine flexion-ascension simulation was run in four load steps, summarized in Table 3.4.4. In a static step, the model was loaded to a realistic but arbitrary stress state of 20° net lumbar rotation in flexion [12] in combination with 1175 N follower load [74]. Simultaneously, IAP was ramped using the direct control method to its target value. Matching the approaches of Bernier and Driscoll [38] and Goel *et al.* (2005) [75], a large flexion moment was applied to L1 and small magnitude intersegmental moments were iteratively adjusted to closely approximate *in vivo* IVR angles reported by Wong *et al.* (2004) [57]. The method of applying and tuning IVRs best matches the force-control strategy of the neuromuscular control system to target a certain spinal displacement. Figure 3.4.3 compares IVRs at 20° between the current study in Load Step 1 and Wong *et al.*

In subsequent transient steps, the spine was moved in ascension through its range of motion (ROM) back to neutral standing posture. A 20 ms duration, 5 Nm magnitude step perturbation force was applied to T9 at 25% of movement trajectory [26]. The step perturbation could represent any arbitrary disturbance during movement including, for example, irregular contraction from an abdominal muscle or external force.

The process was repeated at fast (80°/s), medium (40°/s) and slow (10°/s) ascension velocities, for zero IAP and high (75 mm Hg) IAP magnitudes. Comparison of these six load cases enabled characterization of spine stability as a function of movement speed and IAP.

Table 3.4.4: Description of loading stages for the flexion-ascension simulation with dynamic perturbation applied during lifting motion.

Load step	Condition	Description	Duration
1	Static	Flexion to 20° net lumbar rotation with combined 1175 N compression. In high IAP load case only, IAP is simultaneously ramped to 75 mm Hg.	1 s
2	Transient	Begin ascension from maximum flexion to neutral posture at fast, medium and slow velocities.	25%[a]
3	Transient	Dynamic perturbation force applied at 25% of lift duration.	0.02 s
4	Transient	Continue through ascension RoM.	75%[a]

[a] Percentage of the total flexion-ascension duration, being 0.25 s, 0.5 s and 2 s, for 80 °/s, 40 °/s and 10 °/s, respectively, over the 20° ROM.

3.4.4 Measurements

IVRs were calculated according to the method described by Dvořák *et al.* (1991) for fluoroscopic imaging *in vivo* [76]. This method, adopted by Wong *et al.* to quantify the movement profile of the spine during normal *in vivo* flexion and extension in a large sample of 100 subjects, measures the relative angular displacement of a tangent line connecting the inferior-posterior and superior-posterior corners of a vertebral body, after aligning its inferior adjacent vertebra in the sagittal plane fluoroscopic images [57]. An adaptation of this method for FEA was implemented by Bernier and Driscoll [38]. A similar, but time-varying approach was scripted in APDL to track IVRs during flexion-ascension movement from rotation of the tangent lines. IDP was measured directly from the hydrostatic pressure in the HSFLD242 node at the COM of each lumbar NP.

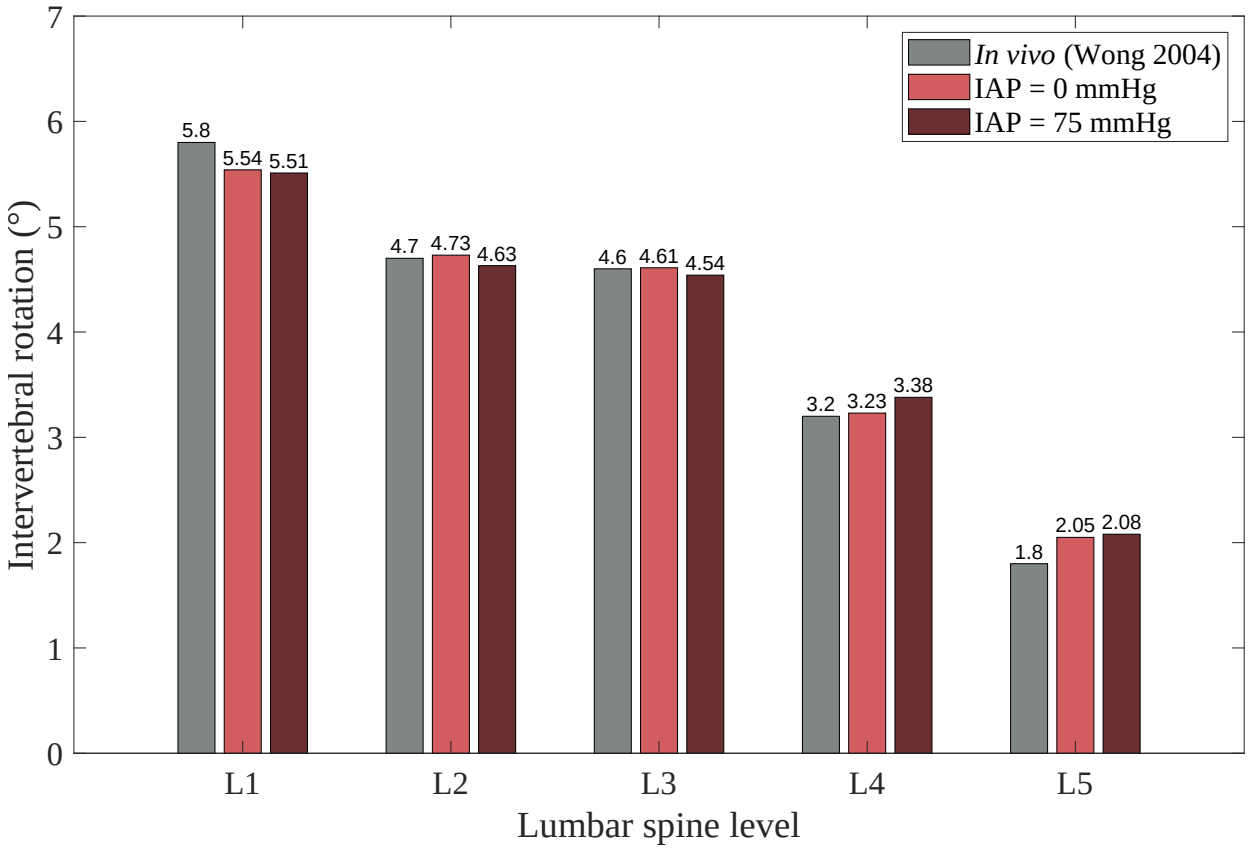

Figure 3.4.3: IVR values for zero and high IAP loading, compared to targeted in vivo rotations from Wong et al. [57]

3.4.5 Validation

3.4.5.1 Outcome Variables

The model was extensively validated in comparison to available *in vivo*, *ex vivo* and *in silico* data, establishing credibility within the context of use. IVRs were plotted against applied moment at L1. To match boundary conditions with the experimental testing of Guan *et al.* (2007) [58], iliolumbar ligaments were disabled. IDP was plotted as a function of compressive load for the full trunk model and isolated spine for comparison against a range of *in silico* models as well as *ex vivo* experimental data. Viscoelastic parameters in the material model of the IVD were validated in comparison to *in silico* flexion trials from the data source [77] over 0.3 s, 1 s and 3 s durations.

3.4.5.2 Sensitivity Analyses

Sensitivity analyses were done to quantify the dependence of outcome measures, IVR and IDP, on variable modeling decisions, specifically element mesh size and type in the IVDs and vertebrae, as well as shell thickness for IMP-based muscle models and the abdominal cavity. The measurements were also compared after varying Young's Modulus by 20% in the spine and anterior tissues. Sensitivity of the model to mesh size and Young's modulus in the posterior muscle geometry was previously done by El Bojairami *et al.* [24].

3.5 Results

3.5.1 Validation and Credibility

A mesh convergence study was done to prove validity in the discretization of the model. Further reductions in mesh element size from the baseline discretization produced, at most, 0.06° (1.7%) and 0.09° (2.5%) variation of IVR in flexion for the IVD and vertebrae, respectively. The same mesh refinements negligibly altered IDP at L4/L5 in pure compression. Sensitivity analysis was stopped at a mesh size of 1.5mm in the annulus and 1mm in the NP and vertebrae as effects were negligible. In the IVD, employing hexahedral elements, over the quadratic tetrahedrons used in this study, varied results by only 1.75%. Using linear elements altered measurements by 4.5%.

Sensitivity of the model to variable inputs was quantified under combined loading to assess robustness of results and identify areas deserving of attention in future work. Shell thickness for surface geometry enclosing fluid-filled cavities was varied by 50%, producing at most 8.9%, 8.7%, 0.03%, 1.6%, and 0.19% variation in model outputs for each of the peritoneum of the abdominal compartment, diaphragm, RA, combined TrA and OI, and psoas, respectively. Cortical bone thickness in the ribs and vertebrae was also varied by 50%, yielding 4% and 1.1% variation, respectively. Young's modulus in elastic tissues were also varied 20%, with deviation maximized in the peritoneum of the abdominal compartment at 3.4%, followed by the ribs at 3.3%.

The osseoligamentous lumbar spine was isolated for comparison to *ex vivo* data in literature, as plotted for IDP at L4/L5 as function of the imposed follower load magnitude in Figure 3.5.1 and for IVR at each intervertebral level as function of the applied flexion moment at L1 in Figure 3.5.2. IDP at L4/L5 under pure compression was linearly related to the magnitude of the follower load. The lumbar spine in isolation closely followed the linear trends of experimental data and the average of eight similar spine-only FE models [59]. When combined with the full trunk geometry, IDP was reduced by 30% at 1000 N.

IVRs were also evaluated by matching boundary conditions to the *ex vivo* experimental methods of Guan *et al.* in lumbar spine flexion [58]. The intersegmental curves in Figure 3.5.2 indicate good alignment with this experimental data. All curves lie within one standard deviation of

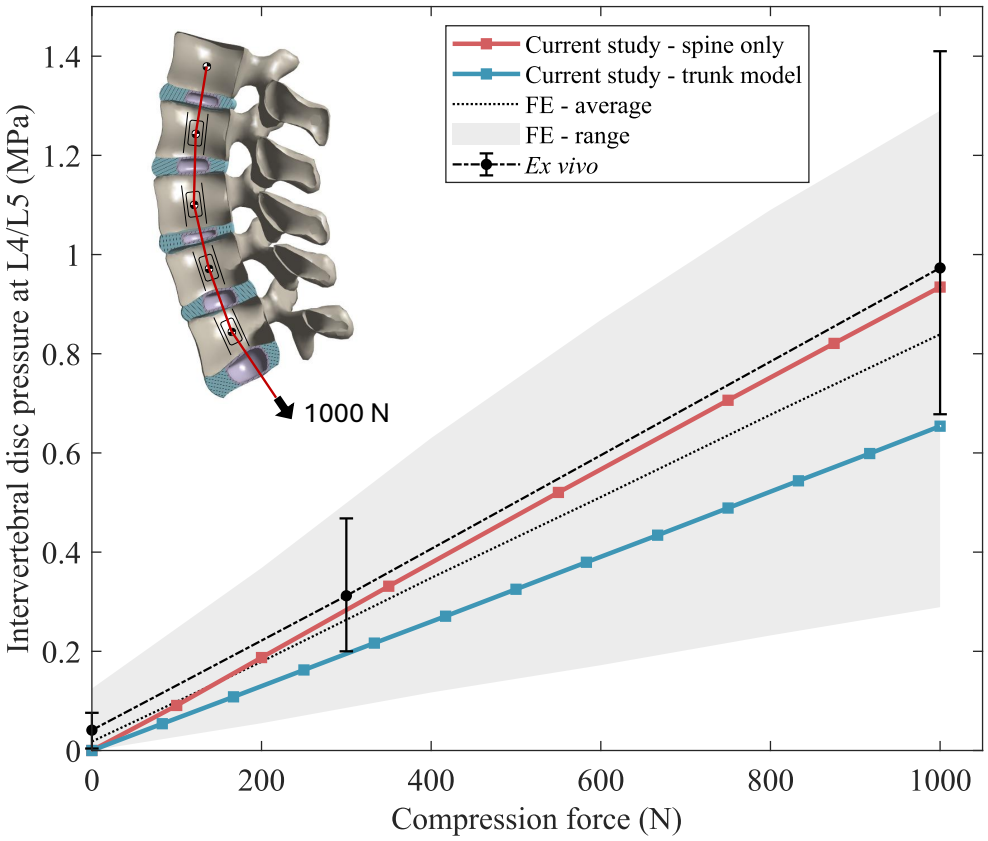

Figure 3.5.1: IDP plotted as a function of follower load magnitude, compared against the ex vivo experimental results of Brinckmann and Grootenboer (1991) [78] as well as a range of FE model results [59].

the mean, with the exception of L4/L5 which appears to fall outside this range if the experimental trends are assumed to continue at larger moments. L4/L5 rotations are better aligned with *in vivo* measurements of IVR, as represented by Figure 3.4.3. Comparing static flexion over 0.3 s, 1 s, and 3 s confirmed the viscoelastic model of the IVD matches the source data [77].

3.5.2 Static Loading

Under the direct-control method for IAP as an input to the model, the internal pressure was de-coupled from abdominal muscle activation, allowing it to produce an extension torque in the lumbar spine. A torque of 19.9 Nm at 75 mm Hg, or 0.27 Nm/mm Hg, was calculated by iteratively solving the model with the objective of minimizing forces required to balance the displacements induced by IAP. This is comparable to Hodges *et al.* (2001), who observed on average 5.7 Nm at 22 mm Hg, or 0.26 Nm/mm Hg, by direct electrical stimulation of the diaphragm [79]. IDP was unloaded by 53 kPa at high IAP.

In flexion, an iterative method was used to determine the minimum loading required to best approximate the *in vivo* IVR pattern of Wong *et al.*, as shown in Figure 3.4.3. Moments of

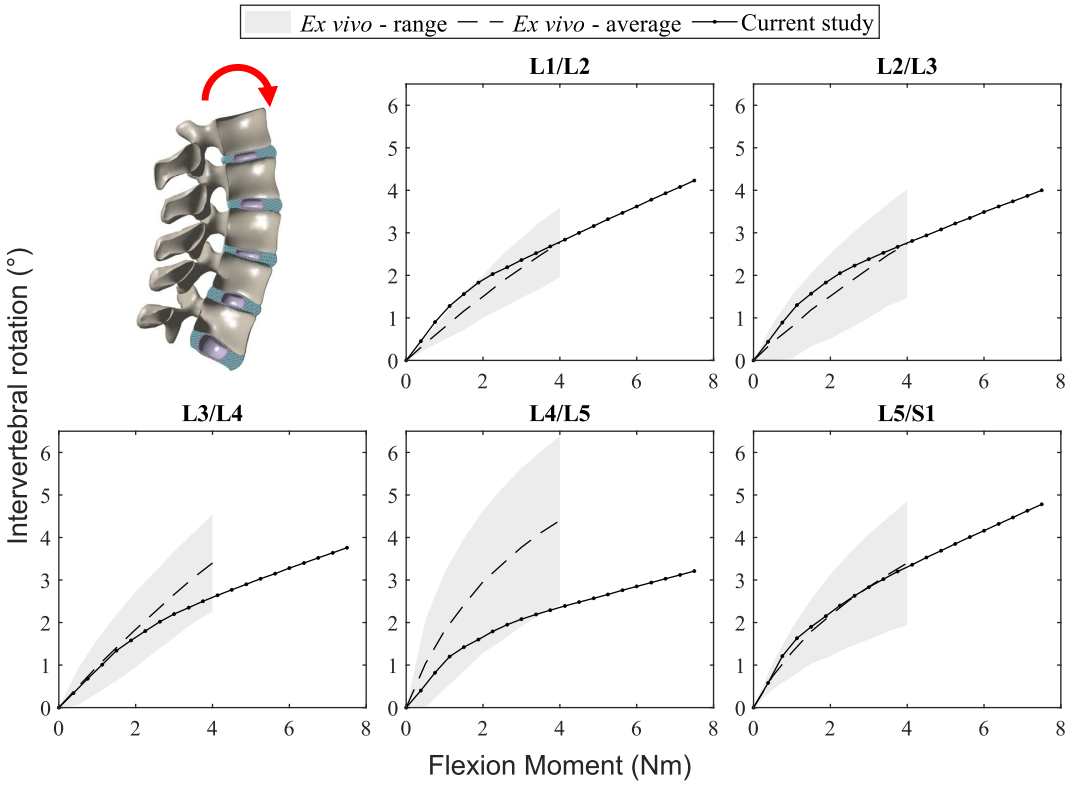

Figure 3.5.2: IVR as a function of pure flexion moment in the isolated spine, compared against the ex vivo experimental results of Guan et al., with matched boundary conditions [58].

magnitude 42 Nm at L1 and T9, with 4.5 Nm and 3.0 Nm at L2 and L3, were calculated. In static equilibrium at 20° flexion, this loading is comparable to Plamondon *et al.* who estimated, via a rigid body dynamic model, extension moments in the range (within one standard deviation) of 80–146 Nm in subjects lifting light 15 kg weights from lumbar flexion angles 0°–29° [12]. After offsetting the extensor torque produced by IAP, flexional stiffness of the spine was increased by 13.6%. Flexion moments at each level were increased accordingly to equate the angular profiles after the first load step with and without IAP: 44 Nm, 5 Nm, and 3.5 Nm at L1 and T9, L2, and L3, respectively.

3.5.3 Flexion-Ascension Trials

Figure 3.5.3 summarizes results from the six flexion-ascension lumbar stiffness trials, extending the trunk back to standing posture from 20° lumbar flexion at different velocities and IAP magnitudes. High IAP (75 mm Hg) increased lumbar stiffness at fast, medium and slow movement rates by 0.948 Nm/° (33%), 0.749 Nm/° (24%) and 0.898 Nm/° (30%), respectively. At high IAP there was no apparent difference between movement rates. IAP appeared to limit displacements, with displacements converging between 1.28° and 1.3° at all velocities. With IAP turned

off, there were small variations in stiffness at the three movement rates. Of the three tested load cases, stiffness during movement without IAP was maximized at $40°/s$, though the small magnitude of change invites the need for further investigation. The stiffnesses presented in Figure 3.5.3 are representative of deviation from the moving trajectory of the spine. The effect of trajectory can be understood by inspection of Figure 3.5.4. Evaluating absolute deviations from the angle at the time of perturbation, plotted in Figure 3.5.4(a), yields 1.11°, 0.87°, and 0.14° for slow, medium, and fast velocities, respectively. Comparing instead the deviations from the moving trajectory, as in Figure 3.5.4(b), notably alters the intrinsic stiffness patterns. The effect of attenuating angular deviation at high IAP grew from L1/L2 to L5/S1. Attenuation magnitudes and percentages relative to the angular deviation at zero IAP were 0.003° (0.4%), 0.031° (7.5%), 0.085° (32.2%), 0.129° (79.4%), and 0.171° (74.0%), at each lumbar level, moving caudally from L1/L2.

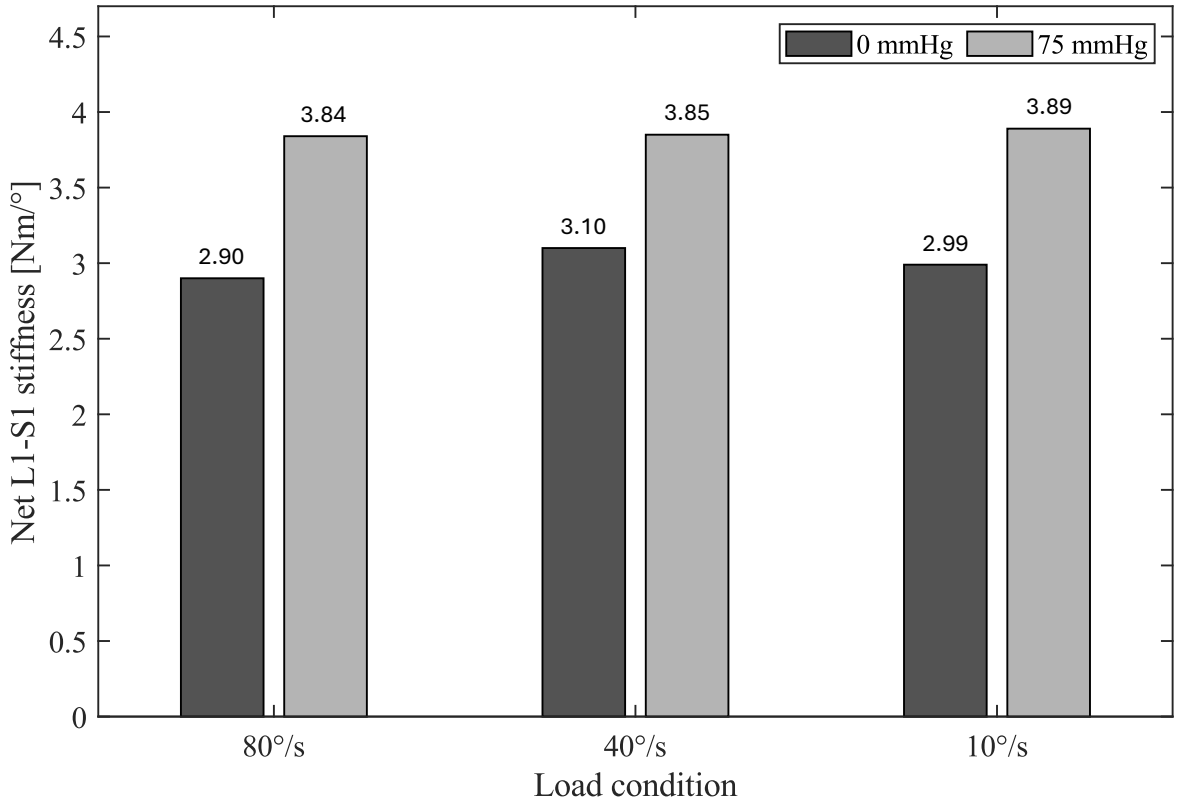

Figure 3.5.3: Lumbar spine stiffness for each ascension velocity, with and without IAP.

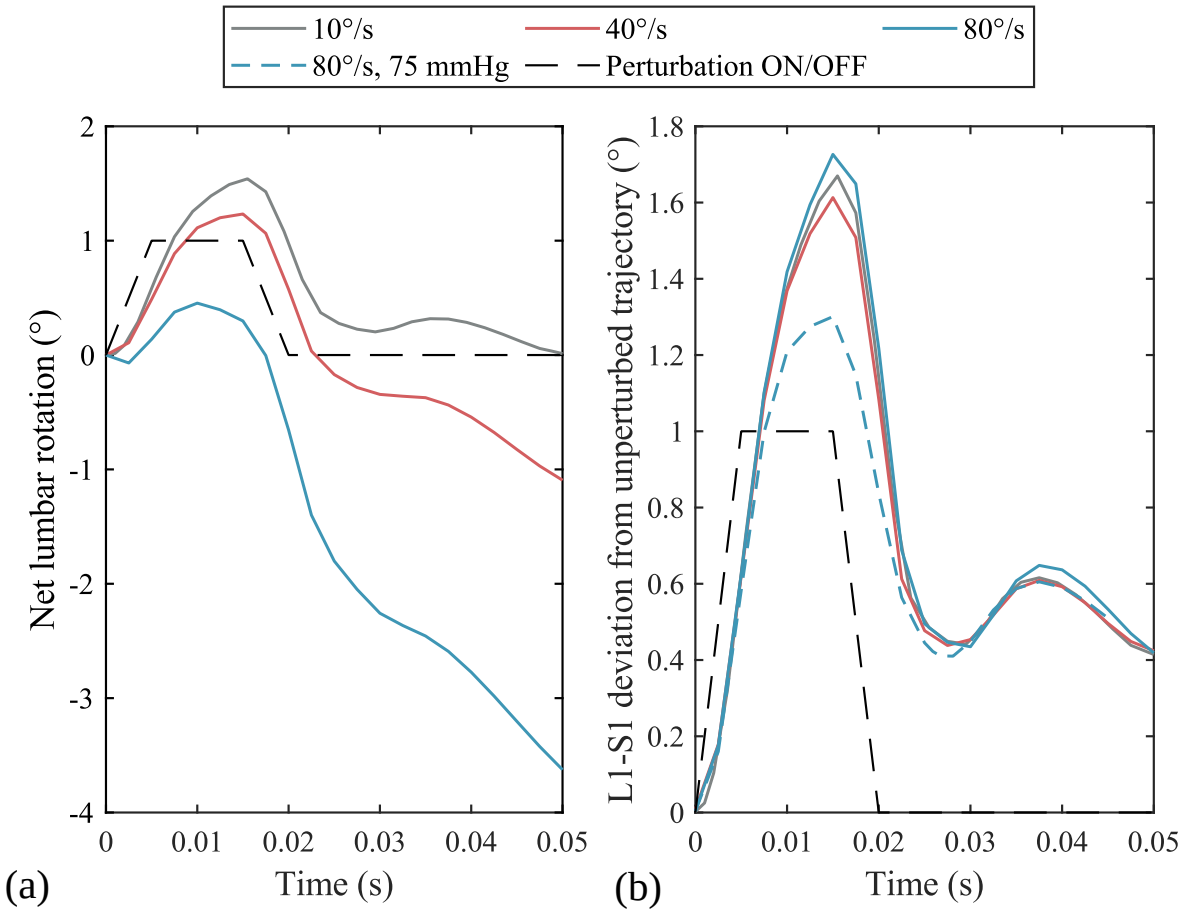

Figure 3.5.4: Time curves of angular displacement of L1-S1 angular displacement during lifting motion over the duration of the perturbation event, for each ascension velocity. (a) Lumbar rotation relative to the angle at the time of perturbation. (b) Deviation from the baseline, unperturbed trajectory.

3.6 Discussion

The present computational study employed a case-control methodology to evaluate the transient effects of IAP in lifting motion at different speeds. This is a notable advantage of using FEM to study spine movement biomechanics as it allows the creation of virtual twins, identical in properties and anatomy, and differing only in loading. In the present study, one twin was incapable of generating IAP, and another was able to generate optimal IAP during flexion-ascension movement. It is unclear whether IAP is a subconsciously or reflexively controlled biomechanical system or, rather, a by-product of neuromuscular controls targeting other factors. Alternative IAP targets could be movement or stability via increasing tension to the spine through soft tissues such as fascia. The presence of pressure mechanoreceptors in the mesentery and viscera of the abdomen [80] could indicate the ability to modulate IAP. This study has strength in that it is parallel to that discussion as it explores the effects of IAP on lumbar stability during movement, without dependence

on the source of pressure in the abdomen.

The results from this approach support the description by Essendrop *et al.* of IAP as an airbag-like contributor to spine stability [22], absorbing the shock of dynamic perturbation during movement to minimize deviation from the moving trajectory of the lumbar spine. While the shock-absorbing effect was largest in fast movement (33% increase in stiffness) the difference was small compared to low velocity (30%). However, it has been well established in rigid and flexible multi-body dynamic models that larger loads are associated with faster movement [18]. Thus, the passive displacement-limiting gain of IAP holds greater weight with increasing velocity. At slower lifting speeds, smaller loads leave more margin for reflexive responses to create additional tension in muscles to pull perturbed vertebrae back toward their target trajectory. However, the larger loading inherent to lifting at greater velocity would narrow this margin of tissue tolerance. It is useful to consider IAP as providing stability potential because it is possible to generate large IAP without the cost of lumbar compression. Specifically, this could be done with focused TrA activation [14], [28], [39] or external orthoses in lifting [38], [81]. This avoids generating pressure from large isometric RA contraction, which would create a flexion moment leading to compressive forces when offset by extensor moments from the erector spinae. Improving motor control of abdominal musculature to generate IAP as a protective measure during lifting is not trivial and requires training [82], [83]. The results presented here heighten the importance of this training or, more simply, widespread deployment of external orthoses in the context of occupational lifting.

These findings may bridge the gap between stiffness-based conclusions, which have suggested spine stability is increased at faster movement [18], and kinematic variance-based conclusions, which have utilized the maximum Lyapunov exponent to suggest stability is reduced at higher velocity flexion-extension [19]. The present findings, highlighted in Figure 3.5.4, show that velocity reduces angular deviation in response to external perturbation relative to its starting point, but that this effect is offset by the larger change to its target trajectory. The involuntary reflex response system is expected to activate, at around 50 ms [42], according to the movement trajectory rather than position at time of perturbation, resulting in a relatively larger correction. Though the difference was minor, intrinsic stiffness was maximized at mid-velocity. The small effect can be considered significant since the only change to loading was movement speed. It remains unclear from this study how differences in active muscle forces between load rates would affect this finding. In a level playing field with regards to loading, the results are in line with those of Lin and Cheng [21], suggesting there may be an optimized lifting speed. Active paraspinal muscles are understood to increase stiffness, but also forces on the spine [18]. Thus, targeting an optimal lifting speed at which intrinsic stiffness is maximized under level loading may be the best strategy

to optimize intrinsic stability.

The present study explored extreme cases of IAP magnitude and timing, specifically maximal IAP occuring before lifting motion onset and remaining at full magnitude throughout ascension. This behavior is different from *in vivo* observations. Although IAP onset precedes motion onset [84], it is shown to peak after motion onset [26]. Biomechanically, the results suggests it is advantageous to control IAP for the intrinsic stability gain. Physiologically, however, sustained pressure could negatively impact organ functions and blood flow [85]. Though, consequences of dynamic pressure could be offset by nervous system modulation of blood flow [80]. While the possible impacts of dynamic pressure are not well understood, it is reasonable to expect that real timing of IAP would play a meaningful role in stability during a lift, providing stiffness at the most critical moment [26]. Conversely, untrained or fatigued lifters are susceptible to poor timing and may lack sufficient IAP to maintain stability, particularly during fast lifting.

Essendrop *et al.* (2002) found that IAP tended to increase with fatigue of the extensor muscles of the spine [86]. This finding could suggest a greater reliance on IAP stability potential after repeated lifting. In occupational lifting, fatigue can set in due to the work load. If reliance on IAP increases due to fatigue, and reliance on IAP for stability increases with movement speed, then a high injury risk scenario could be created by faster lifting over the course of a working day. From Legg (1981), unlike the extensors, IAP is unaffected by abdominal muscle fatigue [87] and thus remains a reliable source of stability throughout the workday. Back injury can occur from error in the neural subsystem causing muscle misfire as well as excessive tension in muscles [88].

The FE investigation faces various limitations. Most notably, the transient study was driven by external loading patterns, rather than active muscles. The active muscle approach is used in rigid and flexible multibody dynamic models, but with simplified geometric modeling of musculature. This approach is efficient for inverse-kinematic studies. An approach similar to Jourdan *et al.* [39], using a user-defined material subroutine (UMAT) to create Hill-type elements could be adopted to confirm the expected influence of active muscle tension in case control or subject-specific loading. This way, passive and active stress components could be combined in anatomically accurate abdominal musculature. The method of external loading, via pure flexion and compressive forces, as well as direct IAP control as an input, is best aligned with existing lumbar spine studies and offers control of model inputs. This facilitates conclusions on intrinsic biomechanics of the spine in a case control approach.

The method of directly controlling IAP produced realistic offloading of the lumbar spine and the results confirm a notable buttressing effect under dynamic perturbation. Other sources of stability contribution are not investigated, such as stiffness increase via activation of transverse

abdominal muscles, relaying tensional forces through the thoracolumbar fascia. This would be expected to limit displacements of the lumbar vertebrae, but the effect may be less prominent for flexional disturbances. The investigation focused on the intrinsic contribution of IAP to show how it may have an important role in limiting displacements, even if de-coupled from active muscle control.

The complex time-varying loading patterns, geometrical nonlinearities, and multiple controlled load cases introduce computational challenges in the form of long simulation times. The approach is additionally limited by the introduction of linearized material properties. Though human tissues are generally anistropic and hyper-viscoelastic in nature, the simplified stress-strain properties have been shown to generate accurate results with faster computing. Nonlinear and viscoelastic properties were considered in the critical region of the lumbar spine with an anatomically accurate biphasic structure of the IVD. Future work may gradually introduce nonlinear and viscoelastic material properties of human soft tissues as they become more readily available in literature and as computational power becomes more cost effective.

To conclude, IAP was shown, via transient analysis in a FE model of the lumbar spine and surrounding soft and bone tissue relevant toward spine stability and IAP-spine interaction, to augment lumbar spine stability. In flexion-ascension, IAP limited angular displacements in response to external perturbation. At different speeds, deviation form target trajectory remained consistent, but the value of this passive shock-absorber would grow with greater loading observed in fast lifting. To the authors' knowledge, this is the first study to explore the functional relationship between the two contributing variables toward spine stability–IAP and movement velocity–in a fully deformable FE model. The results offer nuanced insight into the contribution of IAP, which has been proposed as creating intrinsic stability potential. *In vivo* studies should build off these findings by controlling both IAP and lift velocity to observe the combined contribution of these related factors, with the variability of real loading in live subjects. This may be facilitated, in terms of ethics, cost and feasibility, through improvements in non-invasive measurement tools for continuous IAP monitoring.

3.7 Declarations

3.7.1 Funding

This study was funded by the Fonds de Recherche du Québec – Nature et Technologies (FRQNT) [grant no. 335748]; the National Sciences and Engineering Research Council of Canada (NSERC) [grant no. 2024-04173]; and McGill University.

3.7.2 Conflicts of Interest

The authors declare that they have no known competing financial interests or personal relationships that could have appeared to influence the work reported in this paper.

3.8 References

[1] G. B. J. Andersson, "Epidemiology in low back pain," *Acta. Orthop. Scand.*, vol. 69, no. 281, pp. 28–31, 1998.

[2] D. P. Gross *et al.*, "A population-based survey of back pain beliefs in canada," *Spine (Phila Pa 1976)*, vol. 31, no. 18, pp. 2142–2145, 2006. DOI: 10.1097/01.brs.0000231771.14965.e4.

[3] M. Laffont *et al.*, "The non-silent epidemic: Low back pain as a primary cause of hospitalisation," *Rheumatol. Int.*, vol. 36, pp. 673–677, 2016. DOI: 10.1007/s00296-015-3421-z.

[4] A. E. Bussières *et al.*, "Spinal manipulative therapy and other conservative treatments for low back pain: A guideline from the canadian chiropractic guideline initiative," *J. Manip. Physiol. Ther.*, vol. 41, no. 4, pp. 265–293, 2018. DOI: 10.1016/j.jmpt.2017.12.004.

[5] E. Yelin, S. Weinstein, and T. King, "The burden of musculoskeletal diseases in the united states," *Semin. Arthritis Rheum.*, vol. 46, no. 3, pp. 259–260, 2016. DOI: 10.1016/j.semarthrit.2016.07.013.

[6] M. L. Ferreira *et al.*, "Global, regional, and national burden of low back pain, 1990–2020, its attributable risk factors, and projections to 2050: A systematic analysis of the global burden of disease study 2021," *Lancet Rheumatol.*, vol. 5, no. 6, e316–e329, 2023. DOI: 10.1016/S2665-9913(23)00098-X.

[7] W. S. Marras *et al.*, "The role of dynamic three-dimensional trunk motion in occupationally-related low back disorders," *Spine*, vol. 18, no. 5, pp. 617–628, 1993. DOI: 10.1097/00007632-199304000-00015.

[8] S. M. McGill, "Chapter 6 - lbd risk assessment," in *Low back disorders: evidence-based prevention and rehabilitation*, 3rd ed. Human Kinetics, 2016, pp. 167–175.

[9] K. G. Davis and W. S. Marras, "The effects of motion on trunk biomechanics," *Clin. Biomech.*, vol. 15, no. 10, pp. 703–717, 2000. DOI: 10.1016/s0268-0033(00)00035-8.

[10] E. Wagnac, P.-J. Arnoux, A. Garo, and C.-E. Aubin, "Finite element analysis of the influence of loading rate on a model of the full lumbar spine under dynamic loading conditions," *Med. Biol. Eng. Comput.*, vol. 50, pp. 903–915, 2012. DOI: 10.1007/s11517-012-0908-6.

[11] R. Norman *et al.*, "A comparison of peak vs cumulative physical work exposure risk factors for the reporting of low back pain in the automotive industry," *Clin. Biomech.*, vol. 13, no. 8, pp. 561–573, 1998. DOI: 10.1016/s0268-0033(98)00020-5.

[12] A. Plamondon, C. Lariviére, A. Delisle, D. Denis, and D. Gagnon, "Relative importance of expertise, lifting height and weight lifted on posture and lumbar external loading during a transfer task in manual material handling," *Ergonomics*, vol. 55, no. 1, pp. 87–102, 2012. DOI: 10.1080/00140139.2011.634031.

[13] W. E. Hoogendoorn, M. N. van Poppel, P. M. Bongers, B. W. Koes, and L. M. Bouter, "Physical load during work and leisure time as risk factors for back pain," *Scand. J. Work. Environ. Health.*, vol. 25, no. 5, pp. 387–403, 1999. DOI: 10.5271/sjweh.451.

[14] A. G. Cresswell and A. Thorstensson, "Changes in intra-abdominal pressure, trunk muscle activation," *Eur. J. Appl. Physiol. Occup. Physiol.*, vol. 68, no. 4, pp. 315–321, 1994. DOI: 10.1007/BF00571450.

[15] W. S. Marras and G. A. Mirka, "Intra-abdominal pressure during trunk extension motions," *Clin. Biomech.*, vol. 11, no. 5, pp. 267–274, 1996. DOI: 10.1016/0268-0033(96)00006-X.

[16] S. A. Lavender, G. B. Andersson, O. D. Schipplein, and H. J. Fuentes, "The effects of initial lifting height, load magnitude, and lifting speed on the peak dynamic l5/s1 moments," *Int. J. Ind. Ergon.*, vol. 31, no. 1, pp. 51–59, 2003. DOI: 10.1016/S0169-8141(02)00174-9.

[17] M. Gagnon and G. Smyth, "Biomechanical exploration on dynamic modes of lifting," *Ergonomics*, vol. 35, no. 3, pp. 329–345, 1992. DOI: 10.1080/00140139208967817.

[18] B. Bazrgari, A. Shirazi-Adl, M. Trottier, and P. Mathieu, "Computation of trunk equilibrium and stability in free flexion-extension movements at different velocities," *J. Biomech.*, vol. 41, no. 2, pp. 412–421, 2008. DOI: 10.1016/j.jbiomech.2007.08.010.

[19] K. P. Granata and S. A. England, "Stability of dynamic trunk movement," *Spine*, vol. 31, no. 10, E271–E276, 2006. DOI: 10.1097/01.brs.0000216445.28943.d1.

[20] J. L. Wang, M. Parnianpour, A. Shirazi-Adl, A. E. Engin, S. Li, and A. Patwardhan, "Development and validation of a viscoelastic finite element model of an l2/l3 motion segment," *Theor. Appl. Fract. Mec.*, vol. 28, pp. 81–93, 1997.

[21] C. J. Lin and C.-F. Cheng, "Lifting speed preferences and their effects on the maximal lifting capacity," *Ind. Health*, vol. 55, no. 1, pp. 27–34, 2017. DOI: 10.2486/indhealth.2016-0032.

[22] M. Essendrop and B. Schibye, "Intra-abdominal pressure and activation of abdominal muscles in highly trained participants during sudden heavy trunk loading," *Spine*, vol. 29, no. 21, pp. 2445–2451, 2004. DOI: 10.1097/01.brs.0000143622.80004.bf.

[23] K. El-Monajjed and M. Driscoll, "A finite element analysis of the intra-abdominal pressure and paraspinalmuscle compartment pressure interaction through the thoracolumbar fascia," *Comput. Methods Biomech. Biomed. Eng.*, vol. 23, no. 10, pp. 585–596, 2020. DOI: 10.1080/10255842.2020.1752682.

[24] I. El Bojairami, K. El-Monajjed, and M. Driscoll, "Development and validation of a timely and representative finite element human spine model for biomechanical simulations," *Sci. Rep.*, vol. 20, no. 21519, Dec. 2020. DOI: 10.1038/s41598-020-77469-1.

[25] I. El Bojairami and M. Driscoll, "Coordination between trunk muscles, thoracolumbar fascia, and intra-abdominal pressure toward static spine stability," *Spine*, vol. 47, no. 9, E423–E431, 2022. DOI: 10.1097/BRS.0000000000004223.

[26] M. Kawabata, N. Shima, and H. Nishizono, "Regular change in spontaneous preparative behaviour on intra-abdominal pressure and breathing during dynamic lifting," *Eur. J. Appl. Physiol.*, vol. 114, no. 11, pp. 2233–2239, 2014. DOI: 10.1007/s00421-014-2944-4.

[27] M. Hagins, M. Pietrek, A. Sheikhzadeh, M. Nordin, and K. Axen, "The effects of breath control on intra-abdominal pressure during lifting tasks," *Spine*, vol. 29, no. 4, pp. 464–469, 2004. DOI: 10.1097/01.brs.0000092368.90019.d8.

[28] A. G. Cresswell, H. Grundström, and A. Thorstensson, "Observations on intra-abdominal pressure and patterns of abdominal intra-muscular activity in man," *Acta. Physiol. Scand.*, vol. 144, pp. 409–418, 1992.

[29] S. M. McGill and M. T. Sharratt, "Relationship between intra-abdominal pressure and trunk emg," *Clin. Biomech.*, vol. 5, pp. 59–67, 1990.

[30] J. Cholewicki, P. C. Ivancic, and A. Radebold, "Can increased intra-abdominal pressure in humans be decoupled from trunk muscle cocontraction during steady state isometric exertions?" *Eur. J. Appl. Physiol.*, vol. 87, no. 2, pp. 127–133, Jun. 2002. DOI: 10.1007/s00421-002-0598-0.

[31] S. M. McGill and R. Norman, "Reassessment of the role of intra-abdominal pressure in spinal compression," *Ergonomics*, vol. 30, no. 11, pp. 1565–1588, 1987. DOI: 10.1080/00140138708966048.

[32] J. Cholewicki, K. Juluru, and S. M. McGill, "Intra-abdominal pressure mechanism for stabilizing the lumbar spine," *J. Biomech.*, vol. 32, no. 1, pp. 13–17, 1999. DOI: 10.1016/S0021-9290(98)00129-8.

[33] P. Hodges, A. E. Martin Eriksson, D. Shirley, and S. C. Gandevia, "Intra-abdominal pressure increases stiffness of the lumbar spine," *J. Biomech.*, vol. 38, pp. 1873–1880, 2005. DOI: 10.1016/j.jbiomech.2004.08.016.

[34] R. Remus, S. Selkmann, A. Lipphaus, M. Neumann, and B. Bender, "Muscle-driven forward dynamic active hybrid model of the lumbosacral spine: Combined fem and multibody simulation," *Front. Bioeng. Biotechnol.*, vol. 11, pp. 1–23, 2023. DOI: 10.3389/fbioe.2023.1223007.

[35] J. Guo, W. Duo, and G. Ren, "Embodiment of intra-abdominal pressure in flexible multibody model of the trunk and the spinal unloading effects during static lifting tasks," *Biomech. Model. Mechanobiol.*, vol. 20, pp. 1599–1626, 2021. DOI: 10.1007/s10237-021-01465-1.

[36] A. A. Stokes, M. Gardner-Morse, and S. M. Henry, "Intra-abdominal pressure and abdominal wall muscular function: Spinal unloading mechanism," *Clin. Biomech.*, vol. 25, pp. 859–866, 2010. DOI: 10.1016/j.clinbiomech.2010.06.018.

[37] I. El Bojairami, N. Jacobson, and M. Driscoll, "Development and evaluation of a numerical spine model comprising intra-abdominal pressure for use in assessing physiological changes on abdominal compliance and spinal stability," *Clin. Biomech.*, vol. 97, no. 105689, 2022. DOI: 10.1016/j.clinbiomech.2022.105689.

[38] E. Bernier and M. Driscoll, "Numerical investigation of intra-abdominal pressure and spinal load-sharing upon the application of an abdominal belt," *J. Biomech.*, vol. 161, no. 111863, 2023. DOI: 10.1016/j.jbiomech.2023.111863.

[39] A. Jourdan *et al.*, "Numerical investigation of a finite element abdominal wall model during breathing and muscular contration," *Comput. Methods Programs Biomed.*, vol. 244, no. 107985, 2024. DOI: 10.1016/j.cmpb.2023.107985.

[40] F. Ghezelbash, A. Shirazi-Adl, M. Sharifi, N. Arjmand, and B. Bazrgari, "Chapter 4 - computational stability of human musculoskeletal systems," in *Digital Human Modeling and Medicine*, G. Paul and M. Hamdy Doweidar, Eds., Acad. Press, 2023, pp. 85–105. DOI: 10.1016/B978-0-12-823913-1.00025-7.

[41] I. El Bojairami, "Assessment of static spinal stability and muscle activation strategies: A comprehensive approach via a novel validated finite element spine model inclusive of thoracolumbar fascia, intramuscular pressure, and intra-abdominal pressure," Ph.D. dissertation, McGill University, 2021.

[42] K. P. Granata, G. P. Slota, and B. C. Bennett, "Paraspinal muscle reflex dynamics," *J. Biomech.*, vol. 37, no. 2, pp. 241–247, 2004. DOI: 10.1016/s0021-9290(03)00249-5.

[43] E. Maaswinkel, M. Griffioen, R. S. G. M. Perez, and J. H. van Dieën, "Methods for assessment of trunk stabilization, a systematic review," *J. Electromyogr. Kinesiol.*, vol. 26, pp. 18–35, 2016. DOI: 10.1016/j.jelekin.2015.12.010.

[44] A. G. Patwardhan, R. M. Havey, K. P. Meade, B. Lee, and B. Dunlap, "A follower load increases the load-carrying capacity of the lumbar spine in compression," *Spine*, vol. 24, no. 10, pp. 1003–1009, 1999.

[45] M. Rao, "Explicit finite element modeling of the human lumbar spine," Ph.D. dissertation, University of Denver, 2012.

[46] P. Little J, M. J. Pearcy, and G. J. Pettet, "Parametric equations to represent the profile of the human intervertebral disc in the transverse plane," *Med. Biol. Eng. Comput.*, vol. 45, pp. 939–945, 2007. DOI: 10.1007/s11517-007-0242-6.

[47] W. Zhong *et al.*, "In vivo morphological features of human lumbar discs," *Medicine (Baltimore)*, vol. 93, no. 28, e333, 2014. DOI: 10.1097/MD.0000000000000333.

[48] J. S. Pooni, D. W. L. Hukins, P. F. Harris, R. C. Hilton, and K. E. Davies, "Comparison of the structure of human intervertebral discs in the cervical, thoracic and lumbar regions of the spine," *Surgical and Radiologic Anatomy*, vol. 8, pp. 175–182, 1986.

[49] S. Stranding, *Gray's anatomy: The anatomical basis of clinical practice*. Elsevier, 2021.

[50] A. Sharma, K. Lagerstrand, H. Brisby, and H. Hebelka, "Interpretation of morphological details of nondegenerated lumbar intervertebral discs on magnetic resonance imaging: Insights from a comparison between computed tomography discograms and magnetic resonance imaging," *J. Comput. Assist. Tomogr.*, vol. 46, no. 3, pp. 487–491, 2022. DOI: 10.1097/RCT.0000000000001292.

[51] B. L. Showalter *et al.*, "Comparison of animal discs used in disc research to human lumbar disc: Torsion mechanics and collagen content," *Spine (Phila Pa 1976)*, vol. 37, no. 15, E900–E907, 2012. DOI: 10.1097/BRS.0b013e31824d911c.

[52] G. D. O'Connell, E. J. Vresilovic, and D. Elliot, "Comparison of animals used in disx research to human lumbar disc geometry," *Spine*, vol. 32, no. 3, pp. 328–333, 2007. DOI: 10.1097/01.brs.0000253961.40910.c1.

[53] O. Perey, "Fracture of the vertebral end-plate in the lumbar spine: An experimental biomechanical investigation," *Acta Orthop. Scand.*, vol. 28, no. sup25, pp. 1–101, 1957. DOI: 10.3109/ort.1957.28.suppl-25.01.

[54] A. Shirazi-Adl, A. M. Ahmed, and S. C. Shrivastava, "Mechanical response of alumbar motion segment in axial torque alone and combined with compression," *Spine*, vol. 11, no. 9, pp. 914–927, 1986.

[55] N. Hammer *et al.*, "Description of the iliolumbar ligament for computer-assisted reconstruction," *Ann. Anat.*, vol. 192, no. 3, pp. 162–167, 2010. DOI: 10.1016/j.aanat.2010.02.003.

[56] P. Hanson and B. Sonesson, "The anatomy of the iliolumbar ligament," *Arch. Phys. Med. Rehabil.*, vol. 75, no. 11, pp. 1245–1246, 1994.

[57] K. Wong, J. C. Leong, M.-k. Chan, K. D. Luk, and W. W. Lu, "The flexion-extension profile of lumbar spine in 100 healthy volunteers," *Spine*, vol. 29, no. 15, pp. 1636–1641, 2004. DOI: 10.1097/01.BRS.0000132320.39297.6C.

[58] Y. Guan *et al.*, "Moment–rotation responses of the human lumbosacral spinal column," *J. Biomech.*, vol. 40, pp. 1975–1980, 2007. DOI: 10.1016/j.jbiomech.2006.09.027.

[59] M. Dreischarf *et al.*, "Comparison of eight published static finite element models of the intact lumbar spine: Predictive power of models improves when combined together," *J. Biomech.*, vol. 47, pp. 1757–1766, 2014. DOI: 10.1016/j.jbiomech.2014.04.002.

[60] F. Alonso and D. J. Hart, "Intervertebral disk," *Encyclopedia of the Neurological Sciences*, vol. 2, pp. 724–729, 2014.

[61] N. Newell, D. Carpanen, G. Grigoriadis, J. P. Little, and S. D. Masouros, "Material properties of human lumbar intervertebral discs across strain rates," *Spine J.*, vol. 19, no. 12, pp. 2013–2014, 2019. DOI: 10.1016/j.spinee.2019.07.012.

[62] M. J. Katzenberger, D. L. Albert, A. M. Agnew, and A. R. Kemper, "Effects of age, sex, and two loading rates on the tensile properties of human rib cortical bone," *J. Mech. Behav. Biomed. Mater.*, vol. 102, no. 103410, 2020. DOI: 10.1016/j.jmbbm.2019.103410.

[63] S. A. Holcombe, Y. S. Kang, B. A. Derstine, S. C. Wang, and A. M. Agnew, "Regional maps of cortical bone thickness and cross-sectional area," *J. Anat.*, vol. 235, no. 5, pp. 883–891, 2019. DOI: 10.1111/joa.13045.

[64] K. A. Bonilla, A. M. Pardes, B. R. Freedman, and L. J. Soslowsky, "Supraspinatus tendons have different mechanical properties across sex," *J. Biomech. Eng.*, vol. 141, no. 1, pp. 0 110 021–0 110 028, 2019. DOI: 10.1115/1.4041321.

[65] M. Masaki, X. Ji, T. Yamauchi, H. Tateuchi, and N. Ichihashi, "Effects of the trunk position on muscle stiffness that reflects elongation of the lumbar erector spinae and multifidus muscles: An ultrasonic shear wave elastography study," *Eur. J. Appl. Physiol.*, vol. 119, pp. 1085–1091, 2019. DOI: 10.1007/s00421-019-04098-6.

[66] C. R. Deeken and S. P. Spencer, "Mechanical properties of the abdominal wall and biomaterials utilized for hernia repair," *J. Mech. Behav. Biomed. Mater.*, vol. 74, pp. 411–427, 2017. DOI: /10.1016/j.jmbbm.2017.05.008.

[67] P. Martins *et al.*, "Mechanical characterization and constitutive modelling of the damage process in rectus sheath," *J. Mech. Behav. Biomed. Mater.*, vol. 8, pp. 111–122, 2012. DOI: 10.1016/j.jmbbm.2011.12.005.

[68] G. M. Cooney *et al.*, "Uniaxial and biaxial tensile stress-stertch response of human linea alba," *J. Mech. Behav. Biomed. Mater.*, vol. 63, pp. 134–140, 2016. DOI: 10.1016/j.jmbbm.2016.06.015.

[69] M. P. Pato *et al.*, "Finite element studies of the mechanical behaviour of the diaphragm in normal and pathological cases," *Comput. Methods Biomech. Biomed. Eng.*, vol. 14, no. 6, pp. 505–513, 2011. DOI: 10.1080/10255842.2010.483683.

[70] J. I. Seok, S. Y. Kim, F. O. Walker, S. G. Kwak, and D. H. Kwon, "Ultrasonographic findings of the normal diaphragm: Thickness and contractility," *Ann. Clin. Neurophysiol.*, vol. 19, no. 2, pp. 131–135, 2017. DOI: 10.14253/kjcn.2017.19.2.131.

[71] N. Hammer *et al.*, "Ligamentous influence in pelvic load distribution," *Spine J.*, vol. 13, no. 10, pp. 1321–1330, 2013.

[72] E. W. Lowrance and H. B. Latimer, "Weights and variability of components of the human vertebral column," *Anat. Rec.*, vol. 159, pp. 83–88, 1967.

[73] R. Eberlein, G. A. Holzapfel, and M. Fr ohlich, "Multi-segment fea of the human lumbar spine including the heterogeneity of the annulus fibrosus," *Comp. Mechs.*, vol. 34, pp. 147–163, 2004. DOI: 10.1007/s00466-004-0563-3.

[74] A. Rohlmann, T. Zander, M. Rao, and G. Bergmann, "Realistic loading conditions for upper body bending," *J. Biomech.*, vol. 42, pp. 884–890, 2009. DOI: 10.1016/j.jbiomech.2009.01.017.

[75] V. K. Goel *et al.*, "Effects of charité artificial disc on the implanted and adjacent spinal segments mechanics using a hybrid testing protocol," *Spine*, vol. 30, no. 24, 2005. DOI: 10.1097/01.brs.0000195897.17277.67.

[76] J. Dvořák *et al.*, "Clinical validation of functional flexion-extension roetgenograms of the lumbar spine," *Spine*, vol. 16, no. 8, pp. 943–950, 1991.

[77] J.-L. Wang, M. Parnianpour, A. Shirazi-Adl, and A. E. Engin, "Viscoelastic finite-element analysis of a lumbar motion segment in combined compression and sagittal flexion: Effect of loading rate," *Spine*, vol. 25, no. 3, pp. 310–318, 2000.

[78] P. Brinckmann and H. Grootenboer, "Change of disc height, radial disc bulge, and intradiscal pressure from discectomy an in vitro investigation on human lumbar discs," *Spine*, vol. 16, no. 6, pp. 641–646, 1991.

[79] P. W. Hodges, A. G. Cresswell, K. Daggfeldt, and A. Thorstensson, "In vivo measurement of the effect of intra-abdominal pressure on the human spine," *J. Biomech.*, vol. 34, no. 3, pp. 347–353, 2001. DOI: 10.1016/s0021-9290(00)00206-2.

[80] B. F. Leek, "Abdominal and pelvic visceral receptors," *Br. Med, Bull.*, vol. 33, no. 2, pp. 163–168, 1977.

[81] E. Bernier, A. Mithani, A. Aoude, and M. Driscoll, "Feasibility of a novel back support device to improve spine stability and muscular activity during trunk flexion: A prospective cross-sectional study with healthy controls and low back pain subjects - preliminary," *Clin. Biomech.*, vol. 122, p. 106 414, 2025. DOI: 10.1016/j.clinbiomech.2024.106414.

[82] S. M. McGill, "Chapter 3 - Functional anatomy of the lumbar spine," in *Low back disorders: evidence-based prevention and rehabilitation*, 3rd ed. Human Kinetics, 2016, pp. 49–83.

[83] C. Lariviére, J.-A. Boucher, H. Mecheri, and D. Ludvig, "Maintaining lumbar spine stability: A study of the specific and combined effects of abdominal activation and lumbosacral orthosis on lumbar intrinsic stiffness," *J. Orthop. Sports. Phys. Ther.*, vol. 49, no. 4, pp. 262–271, 2019. DOI: 10.2519/jospt.2019.8565.

[84] P. Hodges, A. Cresswell, and A. Thorstensson, "Preparatory trunk motion accompanies rapid upper limb movement," *Exp. Brain. Res.*, vol. 124, pp. 69–79, 1999.

[85] G. Sánchez-Etayo, X. Borrat, B. Escobar, A. Hessheimer, G. Rodriguez-Laiz, and P. Taura, "Effect of intra-abdominal pressure on hepatic microcirculation: Implications of the endothelin-1 receptor," *J. Dig. Dis.*, vol. 13, no. 9, pp. 478–485, 2012. DOI: 10.1111/j.1751-2980.2012.00613.x.

[86] M. Essendrop, B. Schibye, and C. Hye-Knudsen, "Intra-abdominal pressure increases during exhausting back extension in humans," *Eur. J. Appl. Physiol.*, vol. 87, pp. 167–173, 2002. DOI: 10.1007/s00421-002-0620-6.

[87] S. J. Legg, "The effect of abdominal muscle fatigue and training on the intra-abdominal pressure developed during lifting," *Ergonomics*, vol. 24, no. 3, pp. 191–195, 1981. DOI: 10.1080/00140138108559233.

[88] M. M. Panjabi, "Clinical spinal instability and low back pain," *J. Electromyogr. Kinesiol.*, vol. 13, no. 4, pp. 371–379, 2003. DOI: 10.1016/S1050-6411(03)00044-0.

[89] S. M. McGill, *Low back disorders: evidence-based prevention and rehabilitation*, 3rd ed. Human Kinetics, 2016.

4 Role of Thoracolumbar Fascia Structure in Lumbar Spine Stability: A Finite Element Investigation

4.1 Framework for Article 2

The present article addresses the second objective, with key steps indicated in the Chapter 4 block of the thesis flow chart shown in Figure 1.0.1. As discussed in Chapter 3.2, the method of directly controlling IAP in the trunk model provided the desired control over IAP magnitude throughout the lifting motion, across flexion-ascension velocities. This came at the cost of losing the third pathway for IAP to build stiffness around the lumbar spine through tension in the TLF. The review of Chapter 2 underlined existing challenges in modelling the TLF, due mainly to lacking anatomy-derived geometry. Investigators have studied the tissue anatomy, noting the long fiber structure of the tissue which is hypothesized to augment its myofascial force transfer capability. However, the effect of model form on the TLF's contribution to passive spine stiffness has not been investigated. With this objective application of the novel model, future studies will be able to test theories on TLF mechanics *in silico*, while relying on both model geometry and an understanding of the potential consequences of their assumptions regarding model form.

A few studies have aimed to evaluate the active unit's role in spine stability through the TLF. Notably, these have quantified a change in observed displacements of a single FSU with a TLF section and lateral forces representing abdominal muscle contraction associated to IAP. These studies were limited in representing the complete set of boundary conditions that are believed to have important influence on its biomechanics. While still challenging, it is possible to better represent these boundary conditions and contact surfaces through simulation. To do so, an anatomy-derived geometry model of the thin tissue must first be created.

The content of this chapter has not yet been submitted to any journal for publication.

4.2 Additional Study: Role of Thoracolumbar Fascia Structure in Lumbar Spine Stability: A Finite Element Investigation

Sean Murray[1,2], Mark Driscoll[1,2]

[1]Musculoskeletal Biomechanics Research Lab, Department of Mechanical Engineering, McGill University, Montreal, QC, Canada

[2]Orthopaedic Research Lab, Montreal General Hospital, Montreal, QC, Canada

Address for notification, correspondence, and reprints:

Mark Driscoll, Ph.D., P.Eng.

Associate Professor, Department of Mechanical Engineering

Canada NSERC Chair Design Eng. for Interdisciplinary Innovation of Medical Technologies

Associate Member, Biomedical Engineering

Associate Member, Department of Surgery

Investigator, Research Institute MUHC, Injury Repair Recovery Program

McGill University, Department of Mechanical Engineering

817 Sherbrooke St. West, Montreal, QC H3A 0C3, Canada

Macdonald Eng. Bldg., office #153

T: +1 (514) 398-6299

F: +1 (514) 398-7365

E-mail: mark.driscoll@mcgill.ca

4.2.1 Abstract

Properties of the thoracolumbar fascia (TLF) tend to be variable with low back pain (LBP) due to physiological changes or treatments. Analysis of its properties and role in the multifactorial pathomechanism of LBP has been hindered by various challenges in modelling the thin, fibrous tissue. Consequently, clinical practice has minimally accounted for its biomechanical influence. This study evaluated the hypothesis that model form in the TLF would affect its contribution toward flexional stiffness in the lumbar spine.

A novel TLF model was derived from segmenting the Visible Human Project™ histological slices. The geometry was transformed to match a prior osseoligamentous spine finite element model, which was validated within the context of use. Two models were derived from the TLF geometry. Their effect on lumbar stiffness was evaluated by comparing intervertebral rotations. In the first, stiffness was allocated to discreet fibers reinforcing a low-stiffness ground substance. In the second, the ground substance was isotropic with fibers removed and was allocated the full share of TLF stiffness. In combined loading non-linear analysis, a 7.5 Nm flexion moment was applied at L1 and T9, with a 500 N follower force. Loading and boundary conditions were matched in both model forms. Next, force representing abdominal contraction was applied laterally over a range (0–90 N) associated with intra-abdominal pressure in lifting.

Without TLF, baseline L1-S1 rotation was 25.7°. Both model forms significantly increased stiffness. Sensitivity of the fiber model to stiffness of the ground substance was analyzed for Young's modulus ranging between 10 and 30 MPa. Lumbar rotation decreased from 12.7° to 8.3°, respectively. The isotropic model was notably stiffer, as L1-S1 rotation decreased to 4.8°. Under IAP-related tension, angular displacements further decreased along a linear relationship. For a 15 MPa ground substance modulus, 90 N (20 % MVC of transversus abdominis) induced a 16.1% reduction.

The results indicate particular attention is needed in accurately representing model form when evaluating the function of TLF. The biomechanical advantage of the long fiber structure is highlighted, as it can relay tensional forces from muscles, while reducing the cost of added intrinsic rotational stiffness. Evidence is provided toward a stabilizing pathway of IAP through abdominal muscle tension, relayed to the spine via the TLF. Clinically, it can also be interpreted that to regain healthy biomechanics, care should be taken to avoid altering TLF fiber structure and form during operation and suturing.

4.3 Introduction

Thoracolumbar fascia (TLF) has recently gained notable attention within low back pain (LBP) research as it becomes clear that it can significantly affect the biomechanics of movement and injury [1]. Mechanoreceptors and nerve endings in the TLF link the connective tissue to sensory feedback in movement and pain [2], while physiological changes, including increased thickness and reduced gliding, are apparent in nonspecific LBP patients [3], [4]. Despite it's steadily increasing research attention [1], inspired by its apparent crucial role in force transmission to the spine [5] and mobility [6], few studies of lumbar spine biomechanics have included fascia when evaluating spinal movements in response to applied loading [7]. Similarly, many computational models explored the role of ligaments on stiffness of the lumbar spine [8], [9], but this is typically not extended to the TLF, despite its similarity as a passive and organized fibrous tissue. The relevance extends further in that the fibers of the TLF merge in some places with those of the supraspinous ligament of the lumbar spine [10].

Ranger *et al.* (2017) and Barker *et al.* (2006) have both evaluated stiffness changes of the TLF in an *ex vivo* spine model. The two studies present many contradictory results, likely influenced by their limitations with respect to neglected boundary conditions [11], [12]. The TLF is defined by its long fibers with continuities to the lateral abdominal wall muscles, latissimus dorsi (LD), and the gluteal muscles. Willard *et al.* (2012) has extensively described the complex anatomy of this tissue [10]. It's middle layer and posterior layer (PLF) wrap the paraspinal muscle compartment, including the erector spinae and multifidus muscles. Laterally, these layers combine and merge with the aponeuroses of the abdominal muscles [13]. Medially, the middle layer and PLF insert to the transverse and spinous processes, respectively. The PLF itself is a complex of a two laminae, which become undifferentiated below the L5 vertebra. The deep lamina is an extension of abdominal muscle aponeuroses, while the superficial lamina is continuous with the LD. Barker and Briggs (1999) have described fiber angles in both lamina which, together, form a criss-cross pattern [14].

Computationally, the reasoning for having neglected the TLF in isolated spine models is obvious and may be justifiable. Origin and insertion points are complex, without direct connections between adjacent vertebrae. It is also not an isolated intrinsic tissue of the lumbar spine. Further, there are few useful comparators for validation due to absence of the TLF in most cadaveric or animal testing. Applications of spine finite element (FE) modelling have historically been limited to measurable quantities within the spine itself and the effects of implants interfacing directly with it. Fascia has also been looked over in descriptions of functional musculoskeletal anatomy [15], being considered only for its most obvious function as a containment wrap to section off muscles

into compartments [10].

Only recently have FE models expanded beyond the spine to capture the effects of surrounding anatomy on more indirectly measured variables like stiffness, stability, intra-abdominal pressure (IAP), and stress shielding. Prior rigid body dynamic models are, by definition, unable to evaluate the contributions and behaviour of a flexible, connective tissue. Moving toward flexible dynamic FE models, interactions between materials can be considered including radial forces from muscle pressurization during contraction, gliding contacts, and geometric deformations, among others. All of the previous concepts are particularly relevant to the behaviour of the TLF.

Recent research in functional anatomy has aimed to push the outdated consensus view of the TLF as a simple disorganized muscle wrap [7] toward an understanding of its broad contributions to musculoskeletal function. Notably, it is now understood to have roles in force transfer, stability, proprioception and nociception [6], [15]–[17]. Its biomechanical functions can be further investigated with advances in computational modelling. Newell and Driscoll recently explored stress shielding in the lumbar spine using both *in silico* [18] and *ex vivo* approaches [19]. They concluded that changes in TLF thickness typically associated with low back pain (LBP) patients resulted in the greatest change in stress, compared to other lumbar spine soft tissues. Computational analysis, via FE modelling in particular, has been hindered in large part by difficulties in building an anatomy-derived geometry for the thin tissue. Segmentation from magnetic resonance imaging is challenging as the tissue is difficult to track outside of the L3–L5 range, where it becomes particularly thin.

Confirming their *in silico* results with *ex vivo* observations, Newell and Driscoll (2024) also characterized TLF elasticity while investigating its potential effect in stress shielding of the erector spinae muscle [19]. From the small sample dimensions, motivated by past testing of Yahia *et al.* [20] (1993), it is not clear how this stiffness relates to the structure of the tissue. At the two extremes, the reported modulus of elasticity value could represent either the isolated fiber elasticity, or the elasticity of the whole TLF, irrespective of load direction.

The force transfer capability of the TLF is inferred from its place in myofascial chains and connective tissue linkages. It has also been demonstrated experimentally in cadaveric and animal studies, noting that force gradients within a muscle were eliminated by removing its series or parallel fascial connections to other muscles. Similarly, isolated movements can span multiple joints to induce displacement across the body [15]. The abdominal muscles may behave in this way to influence spine mobility through myofascial linkage with the TLF [16]. The transversus abdominis (TrA) and obliquus internus (OI) are understood to blend with the TLF at a lateral raphe of the posterior and middle TLF layers [15]. Going further, Fan *et al.* (2018) showed myofascial

continuity between the obliquus externus (OE) and the PLF, supporting the force transfer pathways of the oblique abdominal muscles [13].

Intra-abdominal pressure (IAP) is understood to contribute to stability, not only through offloading and buttressing effects, but also by maintaining the hoop-like geometry of the abdominal wall. By doing so, the oblique abdominal wall muscles exert force through a lateral line of action at the posterior aponeuroses and lateral raphe of the TLF. Myofascial force transfer through the PLF could therefore offer an added mechanism by which IAP can stabilize the lumbar spine [16].

This study aimed to address limitations in FE modelling of the TLF by evaluating representations of model form and analyzing their effects on the flexural stiffness of the spine. This would provide valuable insight for future computational investigations to rely on when weighing engineering decisions and assumptions in TLF models. It also contributes to a growing understanding of the importance of its fiber-based structure. A further objective was to quantify the potential for IAP to contribute to spine stability through myofascial force transfer from the abdominal muscles.

4.4 Methods

4.4.1 Fascia Segmentation

The posterior layer of the TLF was manually segmented from the histological image data set of the Visible Human Project™ (VHP, U.S. National Library of Medicine, Bethesda, MD) [21] using the software Fie (AudiLab, McGill University) [22]. The data set contains anatomical images of a single subject (38 yr-old, 1.8 m tall, 90 kg) with no pertinent medical history and is the result of serial histological slicing in the transverse plane with image spacing of 1 mm. Many challenges exist in segmenting the TLF due to its very thin nature. The software Fie was specifically created for segmentation of thin tissues in the human ear and was thus well suited to this task [22]. Figure 4.4.1(a) shows a representative slice from the VHP dataset, with relevant landmarks and tissues indicated. The PLF segmentation is highlighted in yellow. Figure 4.4.1(b) shows the end result of this process as a three-dimensional volumetric PLF geometry.

The resulting 3D PFL body was then transformed to fit a previously validated lumbar spine FE model. This was done by first roughly segmenting the L1, L4, and L5 vertebrae from the same VHP histological image stack, using 3D Slicer [23]. These were then used as reference points to orient and scale the TLF model. In Figure 4.4.2, this transformation process is visualized with the final alignment of the VHP vertebrae, highlighted in blue, overlaid on the original FE model. In Figure 4.4.2(b), this manual transformation process is further clarified, showing that the discretized TLF geometry was rotated with the vertebrae about select axes parallel to the x-axis. Relatively small scaling parameters were needed, first by 0.9 in XYZ, and then by 0.95 in the Z-direction, aligned with the superior-inferior axis.

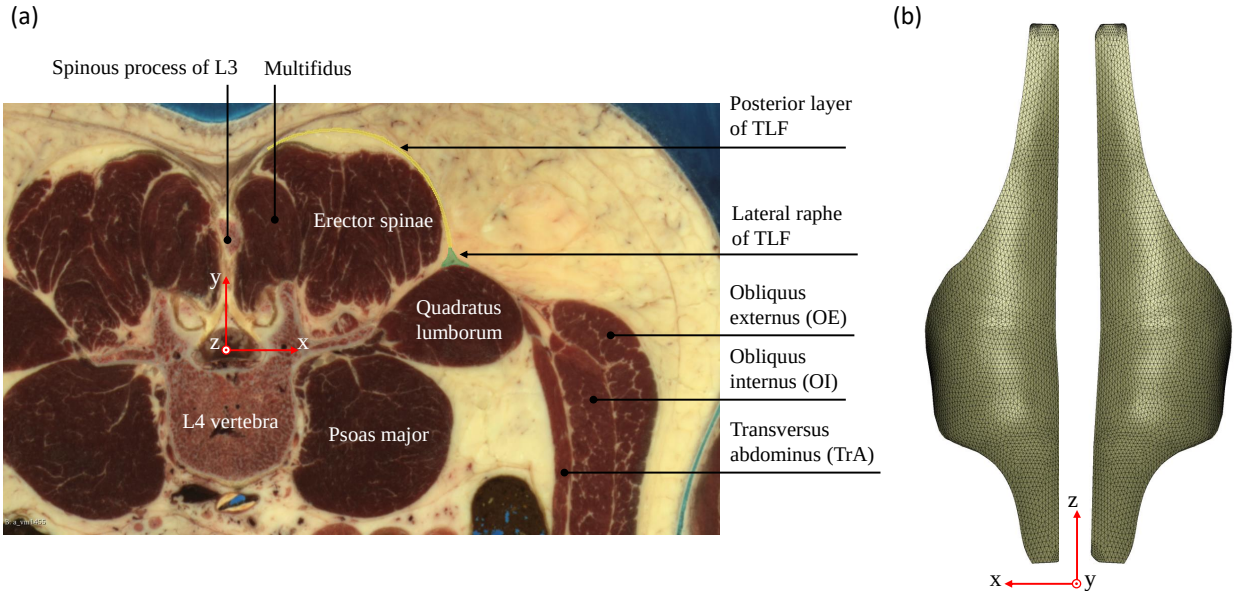

Figure 4.4.1: Segmentation of the thoracolumbar fascia showing (a) a representative histological slice with annotations indicating the visible relevant tissues, and (b) The resulting 3D geometry of the posterior layer.

The thickness of the volumetric PLF model after segmentation and transformation was compared to ultrasound measurements at the lumbar levels where this data was available. Average thickness was computed by dividing the cross-sectional area at each lumbar level by its characteristic in-plane length. The lumbar levels are identified by a plane passing through the center of mass of each vertebral body. At the TLF, the planes were rotated such that the normal vectors are aligned with the craniocaudal curvature of the thin tissue.

4.4.2 Model

A FE model of the thoracolumbar spine, from L5 to T9, was created, inclusive of the spine, intervertebral discs (IVDs), erector spinae, and thoracolumbar fascia. The complete model employs a previously validated spine model [24].

The aligned volumetric TLF is a valuable resource, enabling further modelling and simulation studies with realistic geometry for the thin, fibrous connective tissue. To address the aims of the present study, the geometry was further simplified to a uniform thickness shell and fiber geometry was superimposed onto the surface contacting the erector spinae muscle, as shown in Figure 4.4.3(c). Fiber angles above and below horizontal, directed laterally from the spine, were defined at L5, L3, T1, T12, and T10 from Barker and Briggs (1999) [14]. A gradual, linear transition was interpolated between reported levels.

Sample width and average rectangular cross-sectional area from Newell and Driscoll [19] were prescribed for the fiber spacing and circular cross-section. This created an effective fiber den-

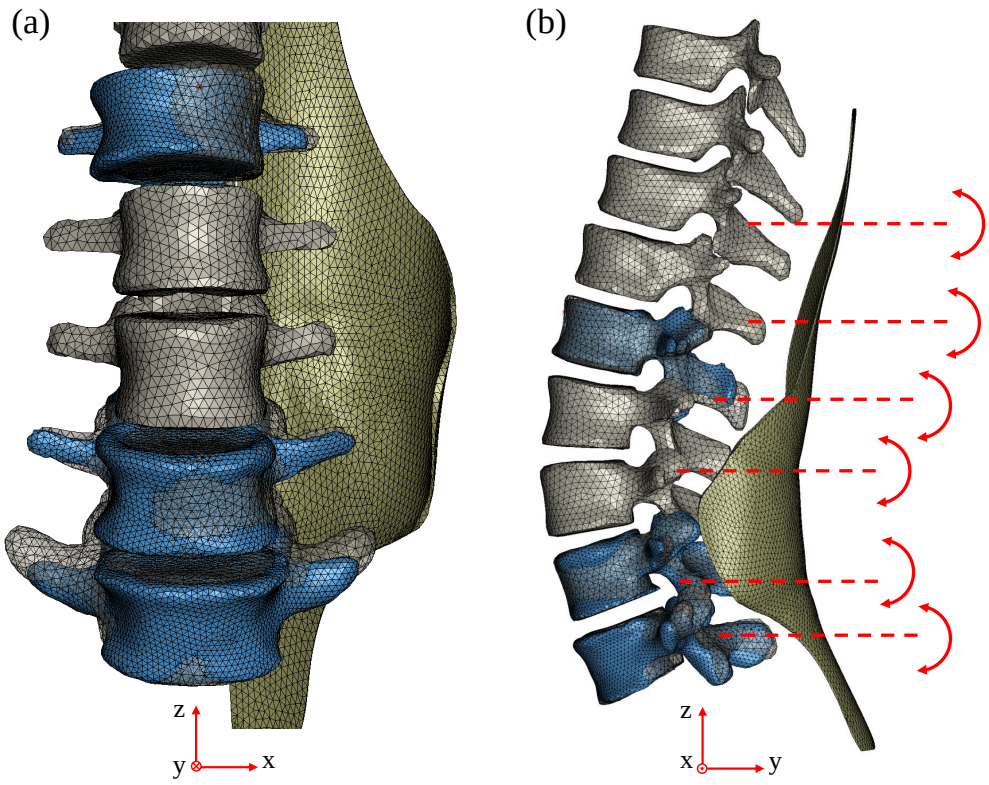

Figure 4.4.2: Visual demonstration of the transformation process to align the PLF model with the existing thoracolumbar spine. (a) Frontal view with final alignment after scaling. (b) Lateral view with key axes of rotation at inflection points along the curvature.

sity and corresponding effective fiber area in the model. This way, model form could be evaluated under conditions of equal effective high-stiffness area. True fiber density is not well characterized. The study evaluates the effect of distributing stiffness between two variations of model form; stiffness is either concentrated into effective fibers or distributed isotropically across the complete sheet.

Starting from the fiber-based model, the curvilinear fibers were discretized as beam elements with nodes at 2 mm spacing. The PLF mesh was then built around the fiber array, creating a fiber-embedded shell mesh of mixed triangle and quadrilateral elements to fit the space between fibers. The segmentation was not extended to the spine since it was not possible to distinguish the TLF from tendons and ligaments near the spinous process.

Therefore, an assumed extension of the PLF surface was created to interface with the spine. The medial end of each discreet fiber was extended linearly at its prescribed angle to merge with the spinous process. To avoid artificial stress concentration, curvature was added by smoothing the edge junction of this geometrically linear region and the segmented geometry. Shell meshing was again built around the extended fiber beam elements. In the isotropic model, the fibers were

suppressed leaving a continuous surface mesh.

The erector spinae muscle cross-sectional area was inflated from the existing model such that its posterior surface was contiguous with the PLF surface. This was necessary due to the human variability between image data sources of the PLF and the existing spine model. The erector spinae muscles were anchored to the spine by tendons. The complete FE model comprised the validated osseoligamentous spine, including vertebrae and IVDs between T9 and L5, as well as the fiber-embedded PLF shell, and erector spinae. The LD muscle was included as a virtual connection to the model its influence on the PLF.

4.4.3 Material Properties

Newell and Driscoll identified a Young's modulus of 150 MPa in the linear region of the TLF stress-strain response [19]. This material property was assigned to the PLF model, with variation in model form according to the study design. A Poisson's ratio of 0.495, representing near-incompressibility, was used for both the fibers and ground substance. To the authors' knowledge, no study has specifically investigated the properties of the ground substance embedding the long fibers. Berardo *et al.* (2024) reported elastic modulus in the range of 12.8–24.9 MPa for the nearby thoracic fascia along the craniocaudal and mediolateral anatomical axes, respectively [25]. Since these would not align explicitly with any fiber direction, it provides insight into a possible upper limit for the ground substance elasticity. Properties of the spine, erector spinae, and tendons remained as described in the previously validated FE spine model [24]. LD muscle fibers in the virtual connection representing the LD attachment were assigned a Young's modulus of 36 kPa and Poisson's ratio of 0.495 [26].

4.4.4 Loading and Boundary Conditions

Flexural rotation of the spine was evaluated under loading and boundary conditions as illustrated in Figure 4.4.3, for the two model forms and a base case without the PLF. As indicated by the hatched geometry in Figure 4.4.3(a), the PLF was fixed about the sacrum and iliac crests.

Also highlighted in teal in Figure 4.4.3(a) is the virtual connection to the LD muscle, simulating the smooth transition of PLF fibers into muscle fibers. LD muscle geometry was overlaid in three dimensions with the FE model. The geometry was cut off where the muscle's curvature moves it out of plane of the thoracic region of the PLF sheet, indicated by the dashed line in Figure 4.4.3(a). The PLF fibers above horizontal were extended onto the muscle and two-point, tension-only, LINK180 elements were defined between the lateral end of the PLF fibers and the LD cut-off. Nodes were fixed at the lateral end. This method allows the virtual LD fibers to move with the spine in flexion, while providing resistance in tension. Each muscle fiber defining this boundary was assigned a fraction of the total muscle cross-sectional area at the cut-off line.

As indicated in Figure 4.4.3(b), pure flexion moments of 7.5 Nm were imposed on the superior end plate of T9 and L1, reflecting the approach of Murray and Driscoll (2024) [24]. In combined loading, a follower load of 500 N was also applied to the lumbar spine to represent body weight and, indirectly, the presence of stabilizing muscle forces. Loading was equivalent in all cases, such that rotational lumbar stiffness can be inferred from the magnitude of net L1-S1 rotation, with less rotation indicating a stiffer response. A sliding, no separation contact was defined between the contiguous erector spinae and TLF surfaces.

To address the uncertainty in ground substance elasticity, sensitivity of the results to Young's modulus in the ground substance was analyzed. Within the fiber-embedded TLF model, this input was varied from 10 MPa to 30 MPa in increments of 5 MPa.

4.4.4.1 Abdominal Muscle Force

To demonstrate and quantify the myofascial force transmission potential from the lateral abdominal muscles to the spine through the PLF, lumbar stiffness was evaluated over a range of lateral force applied to the PLF on each side. This is visualized in Figure 4.4.3(c). Since TrA activation is most strongly correlated to IAP, the applied force range is defined by TrA muscle activation consistent with electromyography (EMG) measurements during lifting, typically around 10% of maximum voluntary contraction (MVC) from intramuscular EMG measurements [27], [28]. Muscle force was calculated according to Equation 4.4.1 [29].

$$F = \sigma_{max} \cdot A \cdot n_{EMG}, \tag{4.4.1}$$

where A [mm^2] represents the physiological cross-sectional area of the muscle, n_{EMG} is normalized EMG expressed as % MVC, and σ_{max} [MPa] is the maximum muscle stress, being 0.99 MPa and 0.91 MPa, as computed by Ghezelbash *et al.* (2018) for the RA and OI muscles respectively [30]. Maximum muscle stress in TrA is assumed identical to OI. Functional cross-sectional area was assigned as 500 mm^2, using values reported by McGill *et al.* (1988) [31], in combination with fiber orientation relative to the transverse plane of 10° [32]. Force from TrA activation up to 20% MVC was applied to the PLF. From Equation 4.4.1, this corresponded with a force range of 0–90 N. This may be an overestimate in comparison to Barker *et al.*, who estimated that a 20 N force at the lateral raphe would represent 50% MVC in the TrA.

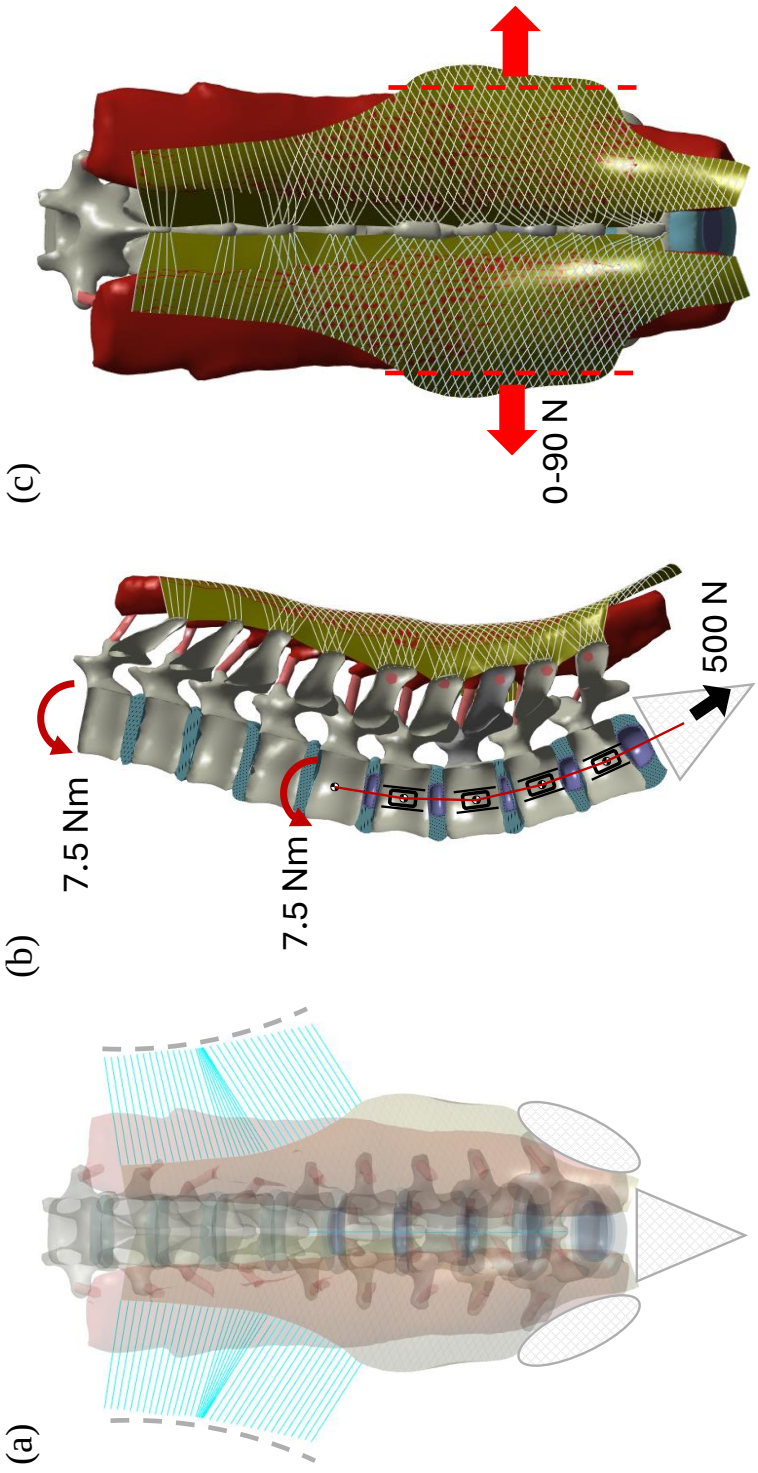

Figure 4.4.3: Loading and boundary conditions. (a) Fixed boundary conditions are indicated by the hatched geometry and the virtual connections to the LD muscle are highlighted in teal. (b) The loading conditions for all trials are superimposed on the model geometry. (c) The loading direction and range of force from abdominal muscle contraction associated with IAP is indicated.

4.5 Results

Table 4.5.1 summarizes measurements of thickness in the volumetric TLF model from segmentation and compares to published values. Good alignment was observed at each level where *in vivo* measurements were taken via ultrasound. At L4, the model lies outside one standard deviation of the available data, but the comparator is disproportionately higher than other levels. The model lies closer to the expectation and further investigation of TLF thickness near the sacrum may be needed.

Table 4.5.1: Thoracolumbar fascia thickness from segmentation by lumbar level.

Lumbar level	L1	L2	L3	L4	L5
TLF thickness [mm] in model	1.24	1.10	1.61	2.78	1.78
TLF thickness [mm] in literature	-	1.83 [33] (0.75–4.15)	1.75 [4] (0.85)	3.55 [34] (0.69)	-

Figure 4.5.1 compares the net lumbar rotation for each of the three model conditions studied, showing a 52% reduction with the addition of the fiber-embedded fascia model to the baseline spine and erector spinae. Changing model form from the fiber-embedded to the isotropic variation without fibers, under the equivalent loading profile, rotation was further reduced by an additional 61%.

Within the fiber-embedded model, the results were sensitive to Young's modulus of the ground substance. Figure 4.5.2(a) highlights this relationship. As the ground substance modulus increased, rotation of the spine decreased. At the low end of the range of ground substance moduli, a steeper slope indicated more sensitivity of lumbar rotation to this parameter of unknown exact magnitude. At the high end, the relationship appeared to approach a plateau beyond 30 MPa.

Applying a lateral force of 45 N, consistent with 10% MVC of the TrA muscle according to Equation 4.4.1, shifted the curve downward, adding stiffness from muscle contraction. Rotations were reduced by an average 8.9%, within the range 10.6%–7.7%, when increasing the modulus from 10 MPa to 30 MPa, respectively. Figure 4.5.2(b) focuses in on the effect of TrA contraction. TrA force was varied from 0–90 N (0–20% MVC) for a given ground substance modulus of 15 MPa. An approximately linear relationship was observed between TrA force and L1-S1 rotation, with the outcome variable decreasing from 10° to 8.4°, or by 16.1%. However, a larger initial drop is shown at the onset under less than 5 N (1% MVC) lateral force. It is not clear whether this initial response has physiological significance or is an artifact of the computational methodology.

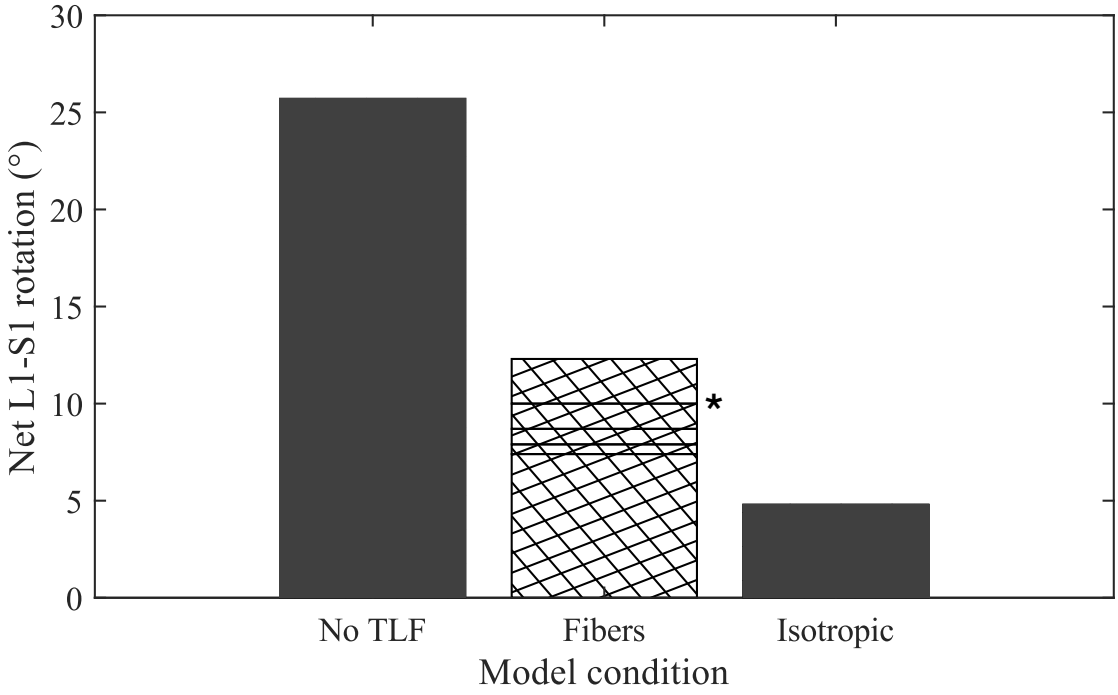

*Figure 4.5.1: Net L1-S1 lumbar spine rotation for each of the three model conditions described. *In descending order along the vertical axis, horizontal lines in the "Fibers" condition represent variations in ground substance Young's modulus from 10* MPa *to 30* MPa*, in increments of 5* MPa*.*

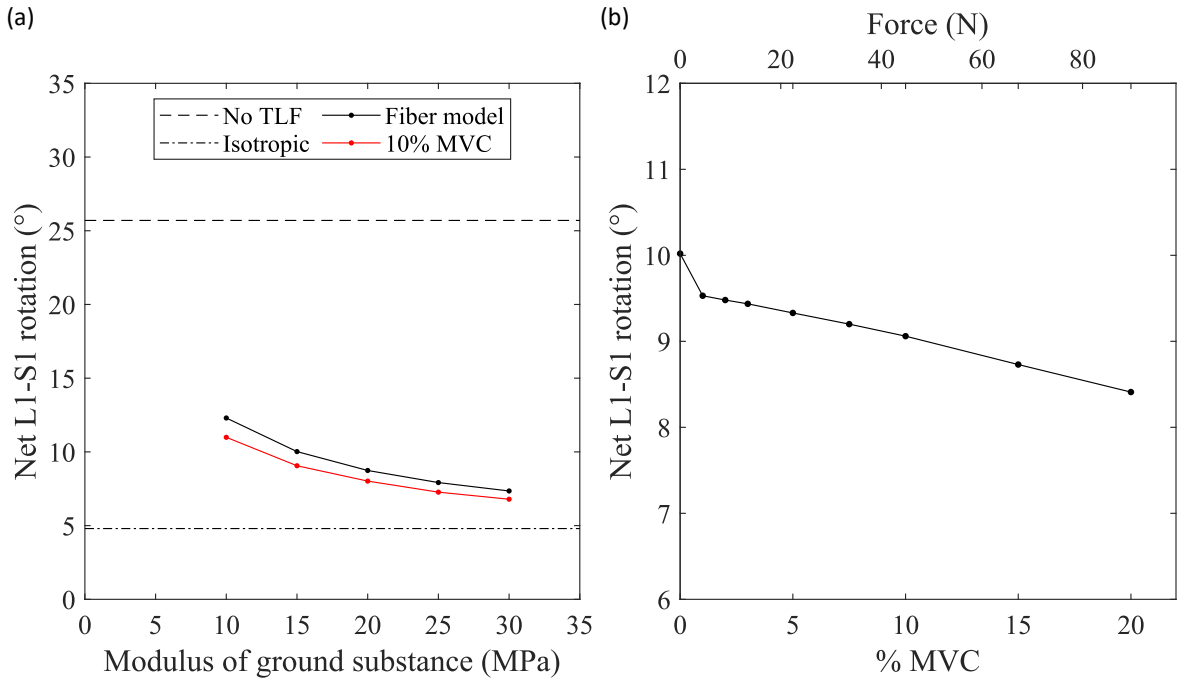

Figure 4.5.2: Sensitivity of net lumbar rotation to (a) Young's modulus of the TLF ground substance, and (b) lateral force on the PLF. The force is equivalently labelled by its magnitude and its estimated TrA contraction, according to Equation 4.4.1.

4.6 Discussion

The TLF has recently gained attention for its important and understudied contribution to spine biomechanics. It is, however, a particularly difficult tissue to study due to its thin structure, complex anatomy, laminate construction, and complex boundary conditions. The latter point makes it such that *ex vivo* testing cannot be done to an intact TLF in simulated human body conditions, without retaining parts of the various muscles inserting in or originating from it. Specifically, continuities with the LD, oblique abdominals, gluteal fascia, and ilium would need to be retained, at minimum, to completely represent the PLF behaviour. The attempts by Ranger *et al.* and Barker *et al.*, for instance, have not respected these continuities [11], [12]. Tesh *et al.* (1987) used foam plastic dowels in an attempt to recreate the boundary with the paraspinal muscle compartment [16]. Similarly, Vleeming *et al.* (2014) substituted inflatable tubes to gain control over the compartment pressure [35].

Numerical investigations can provide unique insight into the behaviour and properties of the anatomically complex tissue, avoiding the difficult cadaveric testing conditions. In light this, the present findings show that simple changes to model form can significantly vary quantification of its role on spine biomechanics. The results indicate particular attention is needed in accurately representing the fiber-based structure when evaluating the function of the TLF. This should be considered in future computational studies when weighing engineering decisions and assumptions.

The biomechanical advantage of the long fiber structure is highlighted, as it can relay tensional forces from muscles, while reducing the cost of added intrinsic flexural stiffness. As shown in Figure 4.5.2(a), low elasticity of the ground substance leaves room for the fibers to move relative to one another without perceived restriction. It is assumed that as the Young's modulus approaches 150 MPa, the behaviour of the fiber-embedded model would match that of the isotropic model. At the low end, the shape of the curve suggests that in the absence of stiffness in the ground substance, the fibers alone may not contribute much to the intrinsic stiffness. However, for both convergence of the computational model and integrity of the biological tissue, a ground substance must exist with some amount of stiffness. In this way it is comparable to any engineering composite material. Further, it is useful to consider a range of elasticity in the ground substance as this may be reflective of changes to tissue properties brought on by adhesions resulting from LBP and associated tissue fibrosis.

Increased flexural stiffness from the PLF imposes greater loading demands to achieve a target flexion angle. Co-contraction of the spine flexors and extensors increases compressive forces to maintain stability via the active system. The passive stabilizing mechanisms of the spine are well adapted to create a neutral zone where lower stiffness facilitates a healthy range of motion adapted

to the requirements of daily activities [36]. Beyond this zone, stiffness rapidly increases to counter hypermobility and instability. The TLF appears to be an important passive stabilizer through its consequential effect on lumbar stiffness. The collagenous fiber structure of the tissue is shown to reduce the demand for flexor muscle forces, in comparison to a variant with direction-independent stiffness. By extension of the reduced flexor muscle demands, the tissue's construction mitigates excessive compressive forces resulting from extensor muscle co-contraction necessary to balance any additional demand for flexural torque to maintain stability. Thus, the fiber-based structure contributes to preserving a safety margin in the IVDs and overall stability.

The TrA could be an important low back stabilizing muscle despite not interfacing directly with the spine. Its active fibers are oriented nearly horizontal, offering efficient geometry for adding stability without the penalty of compressive loads on the spine. During Valsalva maneuver, or forced maximal abdominal pressurization, TrA activation may reach magnitudes of approximately 75% MVC [32], [37]. Commonly, however, it remains around 10% in typical lifting conditions [27], [28]. An approximately linear relationship between lateral muscle force and the decrease in L1-S1 angular displacement was identified from Figure 4.5.2(b). This demonstrates the myofascial force transfer potential of abdominal muscles. TrA contraction at only 20% of the maximum muscle force can increase lumbar stiffness by as much as 16.1%, providing a mechanism for neuromuscular modulation of spine stability through the active motor unit. Further, Vleeming *et al.* and El-Monajjed and Driscoll (2020) have each confirmed, respectively via cadaveric and computational methodologies, that tension through the PLF can vary with paraspinal muscle compartment pressure [35], [38]. This pressure maintains the geometry and optimal line of action of the PLF fibers from their muscle origins to their spinous attachments. The present study, in contrast to Barker *et al.* [12] and Ranger *et al.* [11], has represented this essential interface. The influence of varying the compartment pressure has not been evaluated, however.

By focusing on loads from the TrA, a link can be made to IAP. The muscular contraction is targeted toward generating IAP and the force is representative of IAP magnitudes in lifting conditions. Thus, in addition to buttressing [28] and offloading effects [39], IAP is shown to contribute to spine stability indirectly by inciting abdominal muscle activity and increasing hoop stresses around the abdomen. Contraction of lateral abdominal wall muscles, particularly TrA and OI, can be highly efficient in augmenting stiffness without added physiological cost due to its simultaneous effects on pressurizing the compartment and tensioning the TLF.

Newell and Driscoll first evaluated the stress-shielding effect of TLF remodelling induced by nonspecific LBP using a FE model [18]. Identifying a notable reduction of stress in the erector spinae muscle group, the authors confirmed the findings through cadaveric testing, placing paral-

lel fibers of both the TLF and erector spinae in tension to evaluate the stress distribution between them [19]. Results of the present study highlight how realistic boundary conditions and effective anisotropy from fiber orientation likely alter the mechanical environment of the spine in flexion. Thus, it would be interesting to quantify the stress-shielding potential of the TLF with a more physiologically representative model, compared to the isometric formulation used in the computational study.

Clinically, it can also be interpreted that to regain healthy biomechanics, care should be taken to avoid altering TLF fiber structure and form during operation and suturing. TLF dissection is necessary to access the spine for various surgical objectives including interbody fusion, decompression, microdisectomy, and others [40], [41]. With the rise of minimally invasive procedures, it can be more challenging to reconstruct the fascia with a reduced footprint and surgeons often don't have the time to optimize their approach [41]. Haupt *et al.* (2022) showed that dissection of the TLF can markedly alter resistance to flexion, but suturing is critical to not only support healing, but also reduce loss of passive stability in the spine [42]. The need for fascia suturing after posterior spine surgery is clear and suturing techniques should consider fiber alignment where possible. This should be balanced against competing surgical objectives. For example, Suter *et al.* (2019) identified a cross stitch pattern as optimal for watertightness in the TLF [43]. Synthetic meshes could be an alternative to suturing with the potential to minimize fiber dislocation [44].

4.6.1 Limitations

The study is subject to various limitations and conclusions are drawn within their implicit boundaries. Most importantly, the TLF is a laminate material and fibers lie in different directions in each lamina. The model employed in the present study has considered the effect of fiber orientation and shown how this variable of model form could markedly change its implications on surrounding biomechanical systems. However, the fibers have been compressed to a single sheet of uniform thickness, representing the combination of both the deep and superficial laminae. Likely, the results are an overestimate of the TLF's contribution toward increasing intrinsic stiffness of the spine. In a multi-laminae model, the planes would be free to glide or shear relative to each other, adding degrees of freedom. This added stiffness would further support conclusions on the importance of capturing TLF form. In the single lamina variation, fibers are individualized, but nodes are forced to merge where fibers cross, increasing the effective tissue-level anisotropy. The hypothesized reduced passive stiffness could benefit the tissue's stabilizing potential, by further mitigating the risk of excess compressive forces resulting from co-contraction of flexion-extension muscles. It is more relevant to accurately represent its mechanics so as to define the baseline healthy joint stiffness. From there, it is possible to consider musculoskeletal and neuromuscular risks that may

shift this operating point. The multi-laminae structure may also further linearize the pathway for myofascial force transfer from abdominal muscles and LD.

Similarly, the sliding, no separation contact approximates the physiological loose bonding between the TLF and erector spinae [10]. However, the actual contact is more complex, with a layer of muscle epimysium dividing muscle and fascia. The PLF–erector spinae adhesion is loose enough to be pulled apart without cutting tools, an act that reveals a delicate, filamentous network [10]. Myofascial force transfer occurs not only in series connections, but also in parallel interfaces through shear, creating a force gradient across distal and proximal muscle ends [15]. While it would not be feasible to model every loose fibril of the contiguous interface between the deep PLF and the erector spinae muscles, an effective frictional force would be apparent. It is not clear how this would impact the results discussed. Further, El-Monajjed and Driscoll found a relationship between pressure in the paraspinal muscle compartment and tensile force through the PLF [38]. This pressure was not directly measured in the present study and sensitivity to this variable was not evaluated. This could be controlled either indirectly by varying follower load magnitude or directly by employing an hydrostatic pressure muscle model as described by El Bojairami *et al.* (2020) [45].

Attachment of the collagen fibers in the TLF to the posterior spinous process should be further investigated. Left and right PLF sheets were individualized, while in actuality continuity is believed to exist across the midline [10]. Thus, this remains a point of uncertainty in the study, wherein the PLF was assumed to bond directly with the spinous processes at locations where the extension of a fiber meets the bone. The fascia may blend instead with other collagenous soft tissues in the posterior aspect of the spine, such as the supraspinous ligaments, and the connections could be looser than what is represented in the model.

Finally, while nonlinear deformations and contacts were considered, material properties of the TLF fibers and ground substance were linear. From observation of tensile testing of the thoracic fascia reported by Berardo *et al.* [25], there is a well-defined defined toe-in region of the stress-strain response. In the lumbar region, material testing reported by Yahia *et al.* shows only a small toe-in region [20] and it is not visible in a single sample stress-strain plot of the TLF from Newell and Driscoll [19]. This toe-in behaviour in a biological material is attributed to uncrimping of the collagen fibrils. Both TLF studies had applied a small pre-stress to ensure tension in the samples, which may have eliminated this initial nonlinearity. The presence of this toe-in region in the TLF elastic response would likely alter the shape of the TrA force–flexural stiffness relationship from Figure 4.5.2(b). The abdominal myofascial force transfer may not be apparent at very low contraction magnitudes. On the other hand, pre-stress conditions *in vivo* would likely

negate this effect.

4.7 Conclusion

The fiber-based structure of the TLF was shown to lower the baseline intrinsic stiffness of the lumbar spine, in comparison to an alternative isotropic extreme of model form. Via inclusion of the erector spinae with a no separation contact at the interface of the PLF and paraspinal muscle, as well as continuities with surrounding musculature, the FE methodology alleviated many of the challenges inherent to studying TLF as an important contributor to spine stability and the multifactorial pathomechanism of LBP. It also motivated the need to accurately reflect these boundary conditions and the fiber-based structure of the complex tissue in future computational investigations. A mechanism for active modulation of spine stability though IAP and its associated abdominal hoop-stress was also supported. Lumbar rotation in flexion was sensitive to tension relayed to the PLF from the lateral abdominal wall musculature, at magnitudes relevant to generating IAP during lifting. The case-control methodology with sensitivity analyses yielded results from one-to-one comparison of directly controlled input variables to support the conclusions regarding model form, its effects toward spine stability, and interpretations for clinical practice.

4.8 Declarations

4.8.1 Funding

This study was funded by the Fonds de Recherche du Québec – Nature et Technologies (FRQNT) [grant no. 335748]; the National Sciences and Engineering Research Council of Canada (NSERC) [grant no. 2024-04173]; and McGill University.

4.8.2 Conflicts of Interest

The authors declare that they have no known competing financial interests or personal relationships that could have appeared to influence the work reported in this paper.

4.9 References

[1] M. Driscoll, "Fascia – the unsung hero of spine biomechanics," *J. Bodyw. Mov. Ther.*, vol. 22, no. 1, pp. 90–91, 2018. DOI: 10.1016/j.jbmt.2017.10.014.

[2] G. Casato, C. Stecco, and R. Busin, "Role of fasciae in nonspecific low back pain," *Eur. J. Transl. Myol.*, vol. 29, no. 3, pp. 159–163, 2019. DOI: 10.4081/ejtm.2019.8330.

[3] H. M. Langevin *et al.*, "Ultrasound evidence of altered lumbar connective tissue structure in human subjects with chronic low back pain," *BMC Musculoskelet. Disord.*, vol. 10, no. 151, 2009. DOI: 10.1186/1471-2474-10-151.

[4] C. Pirri *et al.*, "Ultrasound imaging of thoracolumbar fascia thickness: Chronic non-specific lower back pain versus healthy subjects; a sign of a "frozen back"?" *Diagnostics*, vol. 13, no. 8, 2023. DOI: 10.3390/diagnostics13081436.

[5] C. Pirri, N. Pirri, V. Macchi, Pozionato, R. A. De Caro, and C. Stecco, "Ultrasound imaging review of thoracolumbar fascia: A systematic review," *Medicina*, vol. 60, no. 1090, 2024. DOI: 10.3390/medicina60071090.

[6] H. M. Langevin, "Potential role of fascia in chronic musculoskeletal pain," in *Clinical anatomy of the spine, spinal cord, and ANS*. Humana Press, 2008, pp. 123–130.

[7] F. Kondrup, N. Gaudreault, and G. Venne, "The deep fascia and its role in chronic pain and pathological conditions: A review," *Clin. Anat.*, vol. 35, no. 5, pp. 649–659, 2022. DOI: 10.1002/ca.23882.

[8] R. Eberlein, G. A. Holzapfel, and M. Fr ohlich, "Multi-segment fea of the human lumbar spine including the heterogeneity of the annulus fibrosus," *Comp. Mechs.*, vol. 34, pp. 147–163, 2004. DOI: 10.1007/s00466-004-0563-3.

[9] A. Shirazi-Adl, A. M. Ahmed, and S. C. Shrivastava, "Mechanical response of alumbar motion segment in axial torque alone and combined with compression," *Spine*, vol. 11, no. 9, pp. 914–927, 1986.

[10] F. H. Willard, A. Vleeming, M. D. Schuenke, L. Danneels, and R. Schleip, "The thoracolumbar fascia: Anatomy, function and clinical considerations," *J. Anat.*, vol. 221, no. 6, pp. 507–536, 2012. DOI: 10.1111/j.1469-7580.2012.01511.x.

[11] T. Ranger, N. Newell, C. A. Grant, P. J. Barker, and M. J. Pearcy, "Role of the middle lumbar fascia on spinal mechanics: A human biomechanical assessment," *Spine*, vol. 42, no. 8, E459–E465, 2017. DOI: 10.1097/BRS.0000000000001854.

[12] P. J. Barker *et al.*, "Effects of tensioning the lumbar fasciae on segmental stiffness during flexion and extension: Young investigator award winner," *Spine*, vol. 31, no. 4, pp. 397–405, 2006. DOI: 10.1097/01.brs.0000195869.18844.56.

[13] C. Fan *et al.*, "Anatomical and functional relationships between external abdominal oblique muscle and posterior layer of thoracolumbar fascia," *Clin. Anat.*, vol. 31, no. 7, pp. 1092–1098, 2018. DOI: 10.1002/ca.23248.

[14] P. Barker and C. A. Briggs, "Attachments of the posterior layer of lumbar fascia," *Spine*, vol. 24, no. 17, pp. 1757–1764, 1999.

[15] J. Wilke, R. Schleip, C. A. Yucesoy, and W. Banzer, "Not merely a protective packing organ? a review of fascia and its force transmission capacity," *J. Appl. Physiol.*, vol. 124, no. 1, pp. 234–244, 2018. DOI: 10.1152/japplphysiol.00565.2017.

[16] K. M. Tesh, J. S. Dunn, and J. H. Evans, "The abdominal muscles and vertebral stability," *Spine (Phila Pa 1976)*, vol. 12, no. 5, pp. 501–508, 1987. DOI: 10.1097/00007632-198706000-00014.

[17] I. El Bojairami and M. Driscoll, "Coordination between trunk muscles, thoracolumbar fascia, and intra-abdominal pressure toward static spine stability," *Spine*, vol. 47, no. 9, E423–E431, 2022. DOI: 10.1097/BRS.0000000000004223.

[18] E. Newell and M. Driscoll, "Investigation of physiological stress shielding within lumbar spinal tissue as a contributor to unilateral low back pain: A finite element study," *Comput. Biol. Med.*, vol. 133, p. 104 351, 2021. DOI: 10.1016/j.compbiomed.2021.104351.

[19] E. Newell and M. Driscoll, "Mechanical evaluation of human cadaveric lumbar soft tissues suggests possible physiological stress shielding within musculoskeletal soft tissues by the thoracolumbar fascia," *IEEE Trans. Biomed. Eng.*, vol. 71, no. 9, pp. 2678–2683, 2024. DOI: 10.1109/TBME.2024.3387343.

[20] L. H. Yahia, P. Pigeon, and A. E. DesRosiers, "Viscoelastic properties of the human lumbodorsal fascia," *J. Biomed. Eng.*, vol. 15, pp. 425–429, 1993.

[21] M. J. Ackerman, "The visible human poject: A resource for education," *Acad. Med.*, vol. 74, no. 6, pp. 667–670, 1999.

[22] W. R. J. Funnell, http://audilab.bme.mcgill.ca/sw/fie.html.

[23] R. Kikinis, S. D. Pieper, and K. G. Vosburgh, "3D Slicer: A Platform for subject-specific image analysis, visualization, and clinical support," in *Intraoperative Imaging and Image-Guided Therapy*, F. A. Jolesz, Ed. New York, NY: Springer New York, 2014, pp. 277–289. DOI: 10.1007/978-1-4614-7657-3_19.

[24] S. Murray and M. Driscoll, "Finite element evaluation of the contribution of intra-abdominal pressure toward dynamic spine stability," *Comput. Biol. Med.*, 2024, Under review.

[25] A. Berardo, L. Bonaldi, C. Stecco, and C. G. Fontanell, "Biomechanical properties of the human superficial fascia: Site-specific variability and anisotropy of abdominal and thoracic regions," *J. Mech. Behav. Biomed. Mater.*, vol. 157, no. 106637, 2024. DOI: 10.1016/j.jmbbm.2024.106637.

[26] I. El Bojairami, N. Jacobson, and M. Driscoll, "Development and evaluation of a numerical spine model comprising intra-abdominal pressure for use in assessing physiological changes on abdominal compliance and spinal stability," *Clin. Biomech.*, vol. 97, no. 105689, 2022. DOI: 10.1016/j.clinbiomech.2022.105689.

[27] D. Juker, S. Mcgill, P. Kropf, and T. Steffen, "Quantitative intramuscular myoelectric activity of lumbar portions of psoas and the abdominal wall during a wide variety of tasks," *Med. Sci. Sports Exerc.*, vol. 30, no. 2, pp. 301–310, 1998.

[28] M. Essendrop and B. Schibye, "Intra-abdominal pressure and activation of abdominal muscles in highly trained participants during sudden heavy trunk loading," *Spine*, vol. 29, no. 21, pp. 2445–2451, 2004. DOI: 10.1097/01.brs.0000143622.80004.bf.

[29] F. Ghezelbash, A. Shahvarpour, C. Larivière, and A. Shirazi-Adl, "Evaluating stability of human spine in static tasks: A combined in vivo-computational study," *Comput. Methods Biomech. Biomed. Eng.*, vol. 25, no. 10, pp. 1156–1168, 2022. DOI: 10.1080/10255842.2021.2004399.

[30] F. Ghezelbash, Z. El Ouaaid, A. Shirazi-Adl, A. Plamondon, and N. Arjmand, "Trunk musculoskeletal response in maximum voluntary exertions: A combined measurement-modeling investigation," *J. Biomech.*, vol. 70, pp. 124–133, 2018. DOI: 10.1016/j.jbiomech.2017.11.007.

[31] S. M. McGill, N. Patt, and R. W. Norman, "Measurement of the trunk musculature of active males using ct scan radiography: Implications for force and moment generating capacity about the l4l5 joint," *J. Biomech.*, vol. 21, no. 4, pp. 329–341, 1988, ISSN: 0021-9290. DOI: 10.1016/0021-9290(88)90262-X.

[32] A. Jourdan *et al.*, "Numerical investigation of a finite element abdominal wall model during breathing and muscular contration," *Comput. Methods Programs Biomed.*, vol. 244, no. 107985, 2024. DOI: 10.1016/j.cmpb.2023.107985.

[33] J. Wilke, V. Macchi, R. De Caro, and C. Stecco, "Fascia thickness, aging and flexibility: Is there an association?" *J. Anat.*, vol. 234, no. 1, pp. 43–49, 2019. DOI: 10.1111/joa.12902.

[34] C. Larivière, R. Preuss, D. H. Gagnon, H. Mecheri, and S. M. Henry, "Structural remodelling of the lumbar multifidus, thoracolumbar fascia and lateral abdominal wall perimuscular connective tissues: A cross-sectional and comparative ultrasound study," *J. Bodyw. Mov. Ther.*, vol. 24, no. 4, pp. 293–302, 2020. DOI: 10.1016/j.jbmt.2020.07.009.

[35] A. Vleeming, M. D. Schuenke, L. Daneels, and F. H. Willard, "The functional coupling of the deep abdominal and paraspinal muscles: The effects of simulated paraspinal muscle contraction on force transfer to the middle and posterior layer of the thoracolumbar fascia," *J. Anat.*, vol. 255, no. 4, pp. 447–462, 2014. DOI: 10.1111/joa.12227.

[36] M. M. Panjabi, "Clinical spinal instability and low back pain," *J. Electromyogr. Kinesiol.*, vol. 13, no. 4, pp. 371–379, 2003. DOI: 10.1016/S1050-6411(03)00044-0.

[37] A. G. Cresswell, H. Grundström, and A. Thorstensson, "Observations on intra-abdominal pressure and patterns of abdominal intra-muscular activity in man," *Acta. Physiol. Scand.*, vol. 144, pp. 409–418, 1992.

[38] K. El-Monajjed and M. Driscoll, "A finite element analysis of the intra-abdominal pressure and paraspinalmuscle compartment pressure interaction through the thoracolumbar fascia," *Comput. Methods Biomech. Biomed. Eng.*, vol. 23, no. 10, pp. 585–596, 2020. DOI: 10.1080/10255842.2020.1752682.

[39] P. W. Hodges, A. G. Cresswell, K. Daggfeldt, and A. Thorstensson, "In vivo measurement of the effect of intra-abdominal pressure on the human spine," *J. Biomech.*, vol. 34, no. 3, pp. 347–353, 2001. DOI: 10.1016/s0021-9290(00)00206-2.

[40] E. Yilmaz *et al.*, "Is there an optimal wound closure technique for major posterior spine surgery? a systematic review," *Global Spine J.*, vol. 8, no. 5, pp. 535–544, 2018. DOI: 10.1177/2192568218774323.

[41] L. M. Tumialán, R. Ponton, and A. Riccio, "Arthroscopic techniques in minimally invasive spine surgery: Closure of the lumbar fascia: Surgical technique," *Neurosurgery*, vol. 68, no. 4, pp. 1092–1095, 2011. DOI: 10.1227/NEU.0b013e318208f160.

[42] S. Haupt, F. Cornaz, A. L. Falkowski, J. Widmer, and M. Farshad, "Biomechanical considerations of the posterior surgical approach to the lumbar spine," *Spine J.*, vol. 22, no. 12, pp. 2066–2071, 2022. DOI: 10.1016/j.spinee.2022.08.006.

[43] A. Suter *et al.*, "Watertightness of wound closure in lumbar spine—a comparison of different techniques," *J. Spine Surg.*, vol. 5, no. 3, 2019. DOI: 10.21037/jss.2019.08.01.

[44] T. Jentzsch, J. Geiger, and M. W. Clément, "Synthetic meshes in the treatment of postoperative fascial dehiscence of the spine," *J. Back. Musculoskelet. Rehabil.*, vol. 30, pp. 153–162, 2017. DOI: 10.3233/BMR-160728.

[45] I. El Bojairami, K. El-Monajjed, and M. Driscoll, "Development and validation of a timely and representative finite element human spine model for biomechanical simulations," *Sci. Rep.*, vol. 20, no. 21519, Dec. 2020. DOI: 10.1038/s41598-020-77469-1.

5 General Discussion

No model has captured all three mechanisms by which IAP can contribute to stabilizing the spine: offloading, buttressing, and hoop stresses. This can be attributed to a few factors. First, the discourse on IAP has been influenced by the assumption that IAP is generated by contraction of the RA muscle. This muscle has a craniocaudal line of action, inducing compressive forces on the spine [152]. Following this line of thought, any stability gain from IAP would be offset by the cost of additional compressive loading on the spine [124]. This remains true, but studies have highlighted a greater correlation of TrA and OI myoelectric activity with larger IAP magnitudes [89], [91]. These lateral abdominal wall muscles have their lines of action curved around the hoop-like geometry of the abdomen and are oriented near-parallel with the transverse plane, or perpendicular to the spine. McGill (2016) discusses how abdominal muscle contraction can be targeted to specific muscles, but this ability is not trivial and is attainable through either training or genetic ability [153].

Second, cadaveric models are distinctly unsuited to studying IAP. The internal compartment pressure is dependent on stiffness of the abdominal wall. Due to the fluidic nature of the compartment, from the high water content of internal organs, stiffness is lost rapidly with decay and the sealed compartment loses the structure that maintains a baseline pressure. Further, IAP is measured from adjacent cavities, representing a force relayed through the near-incompressible fluid. Thus, pressure generated inside the compartment may not reflect the reality of force transfer pathways. Similarly, in animal and *in vivo* testing, IAP cannot be directly controlled, only measured. These measurements are valid, but the lack of input control creates uncertainty in conclusions relating outputs back to a single change of input. One study has succeeded at indirectly controlling IAP by electrically stimulating the diaphragm in live human subjects [72]. This has offered the strongest evidence to support the offloading mechanism for spine stability.

Third, advances in computational modelling have only recently began to facilitate capturing the fluid-like behaviour of the abdominal compartment. Earlier attempts have mathematically related pressure to the curvature of the spine, but this relies on many assumptions and ignores abdominal muscle involvement altogether. Past studies have also drawn conclusions based on simplified geometry representing the abdominal wall [87], [145]. El Bojairami *et al.* started to expand beyond the spine to capture the stability effects of adjacent systems [147]. The current analysis represents a further development on this initial work, providing more in depth insight into potential stability gains. To the author's knowledge, the spine and trunk model discussed in this report includes the most physiologically representative model of the abdominal compartment. This

approach avoids assumptions on the exact interaction of the hydrostatic pressure with the spine by modelling realistic geometry.

As discussed in Chapter 3.2, the method of directly controlling IAP ignores hoop stresses, as one of the three mechanisms identified for stability from IAP. This was a principle motivating factor in the study design discussed through Chapter 4.2. Direct IAP control capitalizes on an advantage of FE modelling, bypassing limitations imposed by the study of live subjects. However, to represent the three mechanisms simultaneously, the model should include active fiber contraction of the abdominal muscles. This approach would need to capture radial expansion from longitudinal contraction along the fiber direction to induce pressurization of the abdominal compartment in sync with tension at the posterior aspect of the muscle. Incompressibility of the abdominal compartment limits displacement of the abdominal wall toward the midline, forcing the longitudinal stress to maintain a curved line of action. Chapter 4.2 quantifies the extension of abdominal muscle tension from its arched pathway to influence spine stiffness.

Without the active fibers, intrinsic stiffness of the abdominal wall is still represented. Instead, with direct pressure control, the wall behaves as an elastic band resisting displacement. Distributed loads are then contained through muscle stiffness so as to force displacement of the lumabr spine. Comparing to the data of Hodges *et al.* (2001), this approach was shown to accurately represent the offloading effect of IAP [72].

A framework for integrating all three pathways into a comprehensive IAP model using active muscle fibers was explored. The method used an extension of the standard phenomenological Hill-type muscle model in three dimensions, originally proposed by Martins *et al.* (2006). Briefly, the approach takes force-length and force-velocity relationships, as well as EMG activation curve as inputs to drive myoelectric contraction of fibers aligned at their respective pennation angle. The key benefit to this FE formulation is that the active fibers affect the strain energy density formulation of the volumetric element, without node-to-node mapping [67], [154], [155]. Thus, the stress matrix is a sum of passive and active components while incompressibility transforms contractile strain into transverse expansion of the element. Anisotropy from fiber orientation is a tool used extensively in biological modelling, as evidenced in the TLF model of Chapter 4.2. However, for a volumetric body, the nodal independence is also critical since extensive manual labour would be needed to ensure a node is located at each point along the desired line of action in a volumetric body. This would make it challenging within the scope of a thesis. In testing, this method was shown not to be feasible for the current application, despite showing promise for future implementation. A twofold justification is presented. First, testing with a simple fusiform muscle geometry was efficient, but when extending to more complex geometry, computation time

increased dramatically. It appeared likely that geometrical modifications to enable meshing by hexahedron element types only could be done to maintain workable convergence times. However this contrasted against the initial objectives of the study which were aimed at capturing the anatomy as accurately as possible. Second, an element formulation for the volumetric Hill-type active fibers exists as an integrated material type in the FE solver LS-DYNA, but not in ANSYS. ANSYS Transient Structural was used to facilitate integration of components of past work in the Musculoskeletal Biomechanics Research Lab and to ensure consistency in model development. A user-defined material subroutine could be created to programmatically construct a custom element formulation in ANSYS, but the V&V requirements of this task alone would constitute its own research objective. This approach would further facilitate comparison between the effects of IAP and each individual muscle. This comparison could be done in a way to isolate the muscle stiffness effects from the overall contribution of IAP and determine the percentage contribution of each individual component.

Only flexion rotations were considered in evaluating lumbar stiffness in both Chapters 3.2 and 4.2. This was in line with objectives to evaluate the stability potential of IAP during lifting movements through the various pathways discussed. Further, in the study of the stabilizing role of the TLF throughout Chapter 4.2, this approach was coordinated with the *ex vivo* testing of Barker *et al.* [77] and the *in silico* approach of Newell and Driscoll [14]. Specifically, this evaluated the potential gain introduced by an oblique tension that would be expected to minimally add to spinal compressive loads. With regards to fascia modelling, a study limited to flexional rotation was adequate to support emphasis on accurately representing the tissue structure in engineering investigations. However, lateral bending and axial twisting stiffness could be significantly affected by this tension as well. This is evident considering the oblique fiber directions with respect to the craniocaudal axis. Tesh *et al.* (1987) identified that the lateral continuity of the TLF with the oblique abdominal muscles has a large moment arm with respect to the center of rotation along the lumbar anteroposterior axis, potentially offering an important source for lateral stability [127]. Further modelling studies should expand on movement patterns studied in this thesis to evaluate the contributions of IAP and TLF to vertebral stability in all vertebral degrees of freedom.

5.1 Context on Verification and Validation

ASME V&V 40 was published in 2018 to standardize V&V requirements on computational models in medical practice based on their context of use and, as a result, the model influence and decision consequence [156]. Combined, these two factors can be used to approximate model risk. This thesis aimed both to develop a FE model to represent the mechanics of IAP with the spine, and to validate that model within its clinical context of use. The spine and trunk model, as

discussed in Chapter 3.2 was applied toward justifying further modelling in this domain, as well as motivating *in vivo* testing that controls for movement speed and IAP (indirectly). It also augments clinical understanding of IAP and movement speed as factors affecting spine stability, with poor stability during lifting being a risk factor for low back injury. With supporting evidence from *in vivo* and *in silico* investigations, the conclusions could be applied toward clinical decision-making on rehabilitative recommendations and informed guesses regarding cause of injury for non-specific LBP patients. The model is not applied directly toward influencing invasive medical practice and should not be relied on in isolation to inform clinical decision-making. Within the framework established by V&V 40, the model risk would therefore be low.

The same exercise can be applied to the TLF model discussed in Chapter 4.2. In this case, more emphasis is placed on potential applications in clinical decision-making, particularly with respect to fascia closure in operation. However, the study acknowledges further investigation, with volumetric and laminate modelling, is needed. The decision consequence remains low as the argument favors more care in fascia closure to target the pre-operative or healthy baseline fiber structure of the tissue and, further, the closure technique of choice should be weighed against any competing surgical objectives. The study discussion makes reference to mesh closure over suturing, but only to motivate further investigation in this area and not to favor this largely unstudied approach. Model risk therefore remains low in both cases.

With model risk established, V&V efforts can be evaluated in this light, as suggested by the 2018 standard [156]. The spine and trunk model of Chapter 3.2 was shown not to be remarkably sensitive to discretization error, where applicable. It was more sensitive to model inputs with large uncertainty of 50% applied to all shell body thicknesses. This resulted in deviations in the parameters of interest of less than 9%. Similarly, varying material inputs by 20% resulted in no more than 3.4% deviation from the baseline. The largest response, however, was in the peritoneum enclosing the abdominal compartment. This fascial tissue, contiguous with the diaphragm, was modelled to fully enclose the abdomen for maintaining pressure and transferring hydrostatic load through the compartment. Thus, it is relevant to the IAP model. These values add context to the model, as they are not a result of modelling decisions, but rather a reflection of areas that may require attention in future developments. For example, since the model is relatively more sensitive to the thickness and properties of the peritoneum of the abdominal wall, this tissue could be the focus of a future study similar to the TLF investigation in Chapter 4.2 quantifying the effect of variations in model form. V&V 40 establishes targets for rigor of comparison and agreement of model outputs, associated with a level of model risk. For the low risk models presented, good agreement was shown to the cadaveric and *in vivo* comparators used throughout. This is above the

level expected for the defined context of use.

Evaluating model form, the TLF investigation of Chapter 4.2 touches on a key aspect of computational model validation. In this case, it is not a validation task, but rather a variable under analysis. In doing so, sensitivity to this variable, specifically fiber structure in the PLF, and all future TLF modelling can assume this sensitivity to hold true. This will guide future work and their applications as it establishes a point by which they can be evaluated with reference to V&V 40.

Stott *et al.* (2023) evaluated comparators used for V&V tasks in numerical spine models, placing biological specimens, clinical subjects, laboratory subjects and synthetic specimens on a two-axis plot of fidelity and control [157]. Due to the challenges discussed that have delayed in depth investigation of IAP mechanics, the FE method is a suitable alternative, offering the most control of input variables. However, it falls low on the scale of fidelity to a live human subject in everyday life. This critical perspective places this thesis in a borader context, with its enclosed descriptions of computational models applied toward understanding spine stability. The modelling approach is necessary to work around the inherent shortcomings of other scientific methods, but V&V 40 would suggest that it should be included as part of a greater body of evidence when being considered to influence clinical decision-making.

5.2 Applications

Many applications of the models have been discussed throughout this thesis, including development towards a comprehensive general application dynamic model of the spine and trunk, motivation for passive external orthoses to support IAP, training toward targeted muscle activation to generate IAP without undue physiological cost, and fascia closure targeting fiber alignment in posterior spine surgery. There are more broad applications of IAP and its effect on stability during lifting motion that should be addressed.

The models were initially motivated by LBP, particularly in occupational settings. Pregnancy, however, is a common source of non-specific LBP outside of the workplace. Although the model is built from male image data sources, conclusions can still be extended to female anatomy. Although it is not relevant in a conversation about pathologies, it is equally relevant to discuss the biomechanical implications of pregnancy, of which there are many risks that particularly affect spine stability. In pregnancy, abdominal soft tissues are stretched and the result is a lower stiffness of abdominal muscles and fascia post-partum. This negatively impacts the ability to generate IAP in both static and dynamic conditions, as the hoop-like geometry is not maintained.

Studies have compared steady-state IAP magnitudes in women during pregnancy and post-partum as well as peak transient IAP during various activities. It has been shown, most relevantly,

that peak IAP during lifting increases day-by-day after birth [71], [158], [159]. The effect, reported by Hsu *et al.* (2018), was slow (0.21 cmH_2O/day) but significant ($p = 0.005$) [159]. Comparison of IAP magnitudes while lifting pre- and post-pregnancy have not been reported, to the authors' knowledge. The spine and trunk model could be used to evaluate the effect on stability, but in its present state IAP is directly controlled. Thus, IAP measurements from laboratory subjects would be required. It may be additionally relevant in this context to tie the conclusions to muscle activation, after integrating volumetric Hill-type abdominal muscles into the generalized model. This way, direct input of IAP measurements would not be needed, and IAP effects from estimates of tissue elasticity changes post-partum could be quantified.

The present thesis highlights the importance of the transient effects of IAP for maintaining stability in occupational lifting and thus avoiding injury and subsequent LBP. In this light, it would be beneficial for reducing risk of LBP to track IAP in the workplace as a biomarker for spine stability. Presently, accepted methods for measuring IAP involve invasively probing adjacent compartments, namely the stomach and rectum. In women, it is also possible to estimate IAP from measurement of intra-vaginal pressure. Using a device developed by Coleman *et al.* (2012), this can be done outside of laboratory settings [70], [71]. Non-invasively, Jacobson and Driscoll (2022) have validated a device to measure IAP based on abdominal wall compliance [160]. Its main advantage is the approach of external measurement over the skin, but in contrast to Coleman *et al.*, the device can estimate only baseline static IAP magnitude. A non-invasive, dynamic pressure measurement device, suitable for both sexes and deployable in daily life, would be immensely beneficial for furthering IAP studies. Ultrasound-based technologies show promise for this application [29], [161]. Within the context of this thesis, it could be used to build a database of IAP and and its relationship to injury risk in the workplace. This can also be extended to other high-risk lifting scenarios such as moving car seats post-partum.

The study of TLF model form in Chapter 4.2 yielded a deeper understanding of the role toward spine biomechanics and stiffness of the tissue's composite construction and fiber structure. This could also be extended to motivate biomimetic designs of orthoses to augment stability simultaneously through the buttressing effect and by amplifying the hoop-stress tension. Bernier *et al.* (2025) recently tested a back support orthotic, which drew inspiration from fascia. The authors found the device could increase IAP passively while reducing muscle demand [162]. Combining conclusions from the two studies discussed in this thesis, this could be taken further by replicating the PLF model form using high-stiffness fibers within a low-stiffness ground substance in an otherwise comparable orthotic device. A larger moment arm, from the device's external operation, could offer a biomechanical advantage to further reduce muscle demand in lifting tasks.

Further developments on the TLF model, as proposed in Chapter 4.2 would enable a multitude of impactful *in silico* studies. This could include an investigation related to the effect of paraspinal muscle compartment pressure, similar to Vleeming *et al.* [128] and El-Monajjed and Driscoll [129], but extended to the full lumbar spine rather than a single vertebral slab. In the two previous studies, along with the study of Chapter 4.2, tension was applied based on assumed relationships between IAP and lateral abdominal muscle forces. These assumptions could be eliminated by implementing the TLF model with the comprehensive spine and trunk model. This proposed application would require further development toward a multi-layer TLF model by adding geometry and fiber orientations of the middle layer to the existing PLF layer. The methodology of Chapter 4.2 could also be applied to investigate a similar myofascial force transfer pathway through the PLF from the LD. Finally, the potential strength of synthetic meshes to mitigate the risk of altering fiber structure in TLF suturing was briefly introduced. With further development toward a multi-laminae PLF FE model, as discussed above, the biomechanics of this approach could be further studied.

6 Conclusion

In conclusion, transient stabilizing mechanisms of IAP have been investigated, quantified, and discussed. Relevant background information was introduced through a literature review that covered the broad anatomical base of knowledge required to investigate beyond the spine by including adjacent tissues and compartments. IAP and the mechanisms by which it impacts spine stability were discussed as part of a review of the scientific discourse and the various methods used to quantify it. Finally, the most applicable literature in FE modelling as it pertains to the spine and occupational factors that predispose the musculoskeletal structure to risk and instability were discussed. Adjacently, FE modelling studies specifically targeting stiffness through the interplay of IAP and TLF were underlined. IAP and velocity were presented as important biomechanical factors relating to spine stability in occupational lifting, where LBP imposes vast health and economic burdens.

Thus, the first objective was to develop and validate a model to quantify the influence toward stability of these two interconnected variables, with IAP being transient and proportional to lifting velocity. This was addressed through Chapter 3. A nonlinear, transient FE model of the spine and trunk was developed with an anatomically accurate abdominal compartment enclosed by soft tissue and bone relevant in loading the spine via IAP. The compartment pressure was shown to have strong potential to contribute to spine stability through two of the three pathways discussed, while velocity did not have a notable effect when evaluated against the moving trajectory. However, to benefit stability, the quantified intrinsic stiffness gains must be achieved through targeted muscle activation or external orthoses. Future improvements to this IAP and spine model would focus on evaluating co-contraction of abdominal muscles to quantify stiffness with more specific attention on physiological penalties incurred by the active unit.

The three mechanisms were not included in one comprehensive model of IAP, but future work can implement components from both studies to accomplish this. The second objective addressed this limitation of the first study, which lacked anatomically realistic geometry for the TLF. Beyond this, the literature review identified no quantification of the impact of the TLF's long fiber structure from which engineering decisions on TLF model form could be assessed. Thus, Chapter 4 succeeded in studying this variable and assessing stiffness of the spine with the novel anatomy-derived TLF geometry. This was done with and without myofascial force transfer from abdominal contraction tied to generating IAP. The chapter yielded evidence in support of TLF as a key passive stabilizer of the spine as well as having a critical role in active stability through IAP. Future work can build off the segmentation while investigating deeper into the complex structure

of the TLF by modelling the separate lamina and their contact mechanics through gliding or shear. Altogether, the three mechanisms by which IAP can impact stability were supported with numeric data and could be integrated into a single, more comprehensive model in the future.

References

[1] M. L. Ferreira *et al.*, "Global, regional, and national burden of low back pain, 1990–2020, its attributable risk factors, and projections to 2050: A systematic analysis of the global burden of disease study 2021," *Lancet Rheumatol.*, vol. 5, no. 6, e316–e329, 2023. DOI: 10.1016/S2665-9913(23)00098-X.

[2] D. P. Gross *et al.*, "A population-based survey of back pain beliefs in canada," *Spine (Phila Pa 1976)*, vol. 31, no. 18, pp. 2142–2145, 2006. DOI: 10.1097/01.brs.0000231771.14965.e4.

[3] M. Krismer and M. van Tulder, "Low back pain (non-specific)," *Best Pract. Res. Clin. Rheumatol.*, vol. 21, no. 1, pp. 77–91, 2007. DOI: 10.1016/j.berh.2006.08.004.

[4] M. Laffont *et al.*, "The non-silent epidemic: Low back pain as a primary cause of hospitalisation," *Rheumatol. Int.*, vol. 36, pp. 673–677, 2016. DOI: 10.1007/s00296-015-3421-z.

[5] J. N. Katz, "Lumbar disc disorders and low-back pain: Socioeconomic factors and consequences," *J. Bone Joint. Surg.*, vol. 88-A, no. Supplement 2, pp. 21–24, 2006. DOI: 10.2106/JBJS.E.01273.

[6] T. Driscoll *et al.*, "The global burden of occupationally related low back pain: Estimates from the global burden of disease 2010 study," *Ann. Rheum. Dis.*, vol. 73, no. 6, pp. 975–981, 2014. DOI: 10.1136/annrheumdis-2013-204631.

[7] National Institute for Occupational Safety and Health (NIOSH), "Work practices guide for manual lifting," U.S. Department of Health and Human Services (DHHS), Washington, DC, 1981, NIOSH Publication No. 81-122.

[8] R. Norman *et al.*, "A comparison of peak vs cumulative physical work exposure risk factors for the reporting of low back pain in the automotive industry," *Clin. Biomech.*, vol. 13, no. 8, pp. 561–573, 1998. DOI: 10.1016/s0268-0033(98)00020-5.

[9] S. M. McGill, "Chapter 6 - lbd risk assessment," in *Low back disorders: evidence-based prevention and rehabilitation*, 3rd ed. Human Kinetics, 2016, pp. 167–175.

[10] E. Yelin, S. Weinstein, and T. King, "The burden of musculoskeletal diseases in the united states," *Semin. Arthritis Rheum.*, vol. 46, no. 3, pp. 259–260, 2016. DOI: 10.1016/j.semarthrit.2016.07.013.

[11] M. M. Panjabi, "Clinical spinal instability and low back pain," *J. Electromyogr. Kinesiol.*, vol. 13, no. 4, pp. 371–379, 2003. DOI: 10.1016/S1050-6411(03)00044-0.

[12] S. Haupt, F. Cornaz, A. L. Falkowski, J. Widmer, and M. Farshad, "Biomechanical considerations of the posterior surgical approach to the lumbar spine," *Spine J.*, vol. 22, no. 12, pp. 2066–2071, 2022. DOI: 10.1016/j.spinee.2022.08.006.

[13] H. W. Choi and Y. E. Kim, "Effect of lumbar fasciae on the stability of the lower lumbar spine," *Comput. Methods Biomech. Biomed. Eng.*, vol. 20, no. 13, pp. 1431–1437, 2017. DOI: 10.1080/10255842.2017.1370459.

[14] E. Newell and M. Driscoll, "Investigation of physiological stress shielding within lumbar spinal tissue as a contributor to unilateral low back pain: A finite element study," *Comput. Biol. Med.*, vol. 133, p. 104 351, 2021. DOI: 10.1016/j.compbiomed.2021.104351.

[15] T. Ranger, N. Newell, C. A. Grant, P. J. Barker, and M. J. Pearcy, "Role of the middle lumbar fascia on spinal mechanics: A human biomechanical assessment," *Spine*, vol. 42, no. 8, E459–E465, 2017. DOI: 10.1097/BRS.0000000000001854.

[16] P. J. Barker *et al.*, "Effects of tensioning the lumbar fasciae on segmental stiffness during flexion and extension: Young investigator award winner," *Spine*, vol. 31, no. 4, pp. 397–405, 2006. DOI: 10.1097/01.brs.0000195869.18844.56.

[17] N. Bogduk, "Chapter 32 - functional anatomy of the spine," in *Neuroimaging Part II*, ser. Handbook of Clinical Neurology, J. C. Masdeu and R. G. González, Eds., vol. 136, Elsevier, 2016, pp. 675–688. DOI: 10.1016/B978-0-444-53486-6.00032-6.

[18] M. M. Panjabi and A. A. White III, "Basic biomechanics of the spine," *Neurosurgery*, vol. 7, no. 1, pp. 76–93, 1980. DOI: 10.1227/00006123-198007000-00014.

[19] S. Stranding, "Chapter 46 - Back," in *Gray's anatomy: The anatomical basis of clinical practice*. Elsevier, 2021, pp. 814–855.

[20] H. V. Carter and H. Gray, *File:gray 111 - vertebral column-coloured.png*. [Online]. Available: https://commons.wikimedia.org/wiki/File:Gray_111_-_Vertebral_column-coloured.png (visited on 12/11/2024).

[21] V. Palepu, S. D. Rayaprolu, and S. Nagaraja, "Differences in trabecular bone, cortical shell, and endplate microstructure across the lumbar spine," *Int. J. Spine Surg.*, vol. 13, no. 4, pp. 361–370, 2019. DOI: 10.14444/6049.

[22] F. Alonso and D. J. Hart, "Intervertebral disk," *Encyclopedia of the Neurological Sciences*, vol. 2, pp. 724–729, 2014.

[23] Y. Yeni, M. Dix, A. Xiao, D. J. Oravec, and M. J. Flynn, "Measuring the thickness of vertebral endplate and shell using digital tomosynthesis," *Bone*, vol. 157, no. 116341, 2022. DOI: 10.1016/j.bone.2022.116341.

[24] S. A. Holcombe, Y. S. Kang, B. A. Derstine, S. C. Wang, and A. M. Agnew, "Regional maps of cortical bone thickness and cross-sectional area," *J. Anat.*, vol. 235, no. 5, pp. 883–891, 2019. DOI: 10.1111/joa.13045.

[25] M. Mohr, E. Abrams, C. Engel, W. B. Long, and M. Bottlang, "Geometry of human ribs pertinent to orthopedic chest-wall reconstruction," *J. Biomech.*, vol. 40, no. 6, pp. 1310–1317, 2007. DOI: 10.1016/j.jbiomech.2006.05.017.

[26] Z. Li *et al.*, "Rib fractures under anterior–posterior dynamic loads: Experimental and finite-element study," *J. Biomech.*, vol. 43, no. 2, pp. 228–234, 2010. DOI: 10.1016/j.jbiomech.2009.08.040.

[27] N. Newell, D. Carpanen, G. Grigoriadis, J. P. Little, and S. D. Masouros, "Material properties of human lumbar intervertebral discs across strain rates," *Spine J.*, vol. 19, no. 12, pp. 2013–2014, 2019. DOI: 10.1016/j.spinee.2019.07.012.

[28] M. J. Katzenberger, D. L. Albert, A. M. Agnew, and A. R. Kemper, "Effects of age, sex, and two loading rates on the tensile properties of human rib cortical bone," *J. Mech. Behav. Biomed. Mater.*, vol. 102, no. 103410, 2020. DOI: 10.1016/j.jmbbm.2019.103410.

[29] C.-P. Jiang, A. P. Wibisono, and T. Pasang, "Selective laser melting of stainless steel 316l with face-centered-cubic-based lattice structures to produce rib implants," *Materials*, vol. 14, no. 20, 2021. DOI: 10.3390/ma14205962.

[30] A. R. Kemper *et al.*, "The biomechanics of human ribs: Material and structural properties from dynamic tension and bending tests," *Stapp Car Crash J.*, vol. 51, pp. 235–273, 2007.

[31] C. Öhman-Mägi, O. Holub, D. Wu, R. M. Hall, and C. Persson, "Density and mechanical properties of vertebral trabecular bone—a review," *JOR Spine*, vol. 4, no. 4, e1176, 2021. DOI: 10.1002/jsp2.1176.

[32] J. Cassidy, "Hierarchal structure of the intervertebral disc," *Connective tissue research*, vol. 23, pp. 75–88, 1989.

[33] N. Newell *et al.*, "Biomechanics of the human intervertebral disc: A review of testing techniques and results," *J. Mech. Behav. Biomed. Mater.*, vol. 69, pp. 420–434, 2017. DOI: 10.1016/j.jmbbm.2017.01.037.

[34] B. Yang, M. F. Wendland, and G. D. O'Connell, "Direct quantification of intervertebral disc water content using mri," *J. Magn. Reson. Imaging*, vol. 52, no. 4, pp. 1152–1162, 2020. DOI: 10.1002/jmri.27171.

[35] P. J. Mansfield and D. A. Neumann, "Structure and function of the vertebral column," in *Essentials of Kinesiology for the Physical Therapist Assistant (Third Edition)*. Elsevier, 2019, ch. 8, pp. 178–232.

[36] B. L. Showalter *et al.*, "Comparison of animal discs used in disc research to human lumbar disc: Torsion mechanics and collagen content," *Spine (Phila Pa 1976)*, vol. 37, no. 15, E900–E907, 2012. DOI: 10.1097/BRS.0b013e31824d911c.

[37] D. W. McMillan, G. Garbutt, and M. A. Adams, "Effect of sustained loading on the water content of intervertebral discs: Implications for disc metabolism.," *Ann. Rheum. Dis*, vol. 55, no. 12, pp. 880–887, 1996. DOI: 10.1136/ard.55.12.880.

[38] J. S. Pooni, D. W. L. Hukins, P. F. Harris, R. C. Hilton, and K. E. Davies, "Comparison of the structure of human intervertebral discs in the cervical, thoracic and lumbar regions of the spine," *Surgical and Radiologic Anatomy*, vol. 8, pp. 175–182, 1986.

[39] N. Bogduk, "Chapter 4 - The ligaments of the lumbar spine," in *Clinical and radiological anatomy of the lumbar spine*. Elsevier, 2012, pp. 39–47.

[40] B. Yang, Y. Lu, C. Um, and G. O'Connell, "Relative nucleus pulposus area and psoition alter disk joint mechanics," *Journal of Biomechanical Engineering*, vol. 141, no. 5, 2019. DOI: 10.1115/1.4043029.

[41] Y. Du *et al.*, "Sensitivity of intervertebral disc finite element models to internal geometric and non-geometric parameters," *Front. Bioeng. Biotechnol.*, vol. 9, no. 660013, 2021. DOI: 10.3389/fbioe.2021.660013.

[42] G. D. O'Connell, E. J. Vresilovic, and D. Elliot, "Comparison of animals used in disx research to human lumbar disc geometry," *Spine*, vol. 32, no. 3, pp. 328–333, 2007. DOI: 10.1097/01.brs.0000253961.40910.c1.

[43] N. T. Jacobs, D. H. Cortes, J. M. Peloquin, E. J. Vresilovic, and D. M. Elliott, "Validation and application of an intervertebral disc finite element model utilizing independently constructed tissue-level constitutive formulations that are nonlinear, anisotropic, and time-dependent," *J. Biomech.*, vol. 47, no. 11, pp. 2540–2546, 2014. DOI: 10.1016/j.jbiomech.2014.06.008.

[44] M. Bashkuev, S. Reitmaier, and H. Schmidt, "Effect of disc degeneration on the mechanical behavior of the human lumbar spine: A probabilistic finite element study," *Spine J.*, vol. 18, no. 10, pp. 1910–1920, 2018. DOI: 10.1016/j.spinee.2018.05.046.

[45] O. Perey, "Fracture of the vertebral end-plate in the lumbar spine: An experimental biomechanical investigation," *Acta Orthop. Scand.*, vol. 28, no. sup25, pp. 1–101, 1957. DOI: 10.3109/ort.1957.28.suppl-25.01.

[46] W. Zhong *et al.*, "In vivo morphological features of human lumbar discs," *Medicine (Baltimore)*, vol. 93, no. 28, e333, 2014. DOI: 10.1097/MD.0000000000000333.

[47] P. Little J, M. J. Pearcy, and G. J. Pettet, "Parametric equations to represent the profile of the human intervertebral disc in the transverse plane," *Med. Biol. Eng. Comput.*, vol. 45, pp. 939–945, 2007. DOI: 10.1007/s11517-007-0242-6.

[48] A. Sharma, K. Lagerstrand, H. Brisby, and H. Hebelka, "Interpretation of morphological details of nondegenerated lumbar intervertebral discs on magnetic resonance imaging: Insights from a comparison between computed tomography discograms and magnetic resonance imaging," *J. Comput. Assist. Tomogr.*, vol. 46, no. 3, pp. 487–491, 2022. DOI: 10.1097/RCT.0000000000001292.

[49] J. Iwanaga *et al.*, "Anatomical and biomechanical study of the lumbar interspinous ligament," *A. J. Neurosurg.*, vol. 14, no. 4, pp. 1203–1206, 2019.

[50] H. V. Carter and H. Gray, *File:gray301.png*. [Online]. Available: https://en.m.wikipedia.org/wiki/File:Gray301.png (visited on 12/11/2024).

[51] H. V. Carter and H. Gray, *File:Gray319.png*. [Online]. Available: https://en.m.wikipedia.org/wiki/File:Gray319.png (visited on 12/11/2024).

[52] A. Kiapour *et al.*, "Biomechanics of the sacroiliac joint: Anatomy, function, biomechanics, sexual dimorphism, and causes of pain," *Int. J. Spine Surg.*, vol. 14, no. 1, S3–S13, 2020.

[53] N. Hammer *et al.*, "Description of the iliolumbar ligament for computer-assisted reconstruction," *Ann. Anat.*, vol. 192, no. 3, pp. 162–167, 2010. DOI: 10.1016/j.aanat.2010.02.003.

[54] P. Hanson and B. Sonesson, "The anatomy of the iliolumbar ligament," *Arch. Phys. Med. Rehabil.*, vol. 75, no. 11, pp. 1245–1246, 1994.

[55] Y. Guan *et al.*, "Moment–rotation responses of the human lumbosacral spinal column," *J. Biomech.*, vol. 40, pp. 1975–1980, 2007. DOI: 10.1016/j.jbiomech.2006.09.027.

[56] M. M. Panjabi, T. R. Oxland, I. Yamamoto, and J. J. Crisco, "Mechanical behavior of the human lumbar and lumbosacral spine as shown by three-dimensional load-displacement curves," *J. Bone Joint Surg.*, vol. 76, no. 3, pp. 413–424, 1994.

[57] M. Dreischarf *et al.*, "Comparison of eight published static finite element models of the intact lumbar spine: Predictive power of models improves when combined together," *J. Biomech.*, vol. 47, pp. 1757–1766, 2014. DOI: 10.1016/j.jbiomech.2014.04.002.

[58] K. Wong, J. C. Leong, M.-k. Chan, K. D. Luk, and W. W. Lu, "The flexion-extension profile of lumbar spine in 100 healthy volunteers," *Spine*, vol. 29, no. 15, pp. 1636–1641, 2004. DOI: 10.1097/01.BRS.0000132320.39297.6C.

[59] I. R. A. Punekar, J. S. Khouri, M. Catanzaro, A. L. Shaik, and H. N. Langstein, "Redefining the rectus sheath: Implications for abdominal wall repair," *Plast. Reconstr. Surg.*, vol. 141, no. 2, pp. 473–479, 2018. DOI: 10.1097/PRS.0000000000004043.

[60] J. Wilke, R. Schleip, C. A. Yucesoy, and W. Banzer, "Not merely a protective packing organ? a review of fascia and its force transmission capacity," *J. Appl. Physiol.*, vol. 124, no. 1, pp. 234–244, 2018. DOI: 10.1152/japplphysiol.00565.2017.

[61] S. M. McGill, *Low Back Disorders Evidence-Based Prevention and Rehabilitation*. Human Kinetics, 2002.

[62] R. Rai *et al.*, "Tendinous inscriptions of the rectus abdominis: A comprehensive review," *Cureus*, vol. 10, no. 8, 2018. DOI: 10.7759/cureus.3100.

[63] J. M. Broyles *et al.*, "Defining the anatomy of the tendinous intersections of the rectus abdominis muscle and their clinical implications in functional muscle neurotization," *Ann. Plast. Surg.*, vol. 80, no. 1, pp. 50–53, 2018. DOI: 10.1097/SAP.0000000000001193.

[64] G. Lehman and S. M. McGill, "Quantification of the differences in emg magnitude between upper and lower rectus abdominis during selected trunk exercises," *Phys. Ther.*, vol. 81, no. 5, pp. 1096–1101, 2001.

[65] H. V. Carter and H. Gray, *File:gray399.svg*. [Online]. Available: https://commons.wikimedia.org/wiki/File:Gray399.svg?uselang=fr (visited on 12/11/2024).

[66] D. M. Urquhart, P. J. Barker, P. W. Hodges, I. H. Story, and C. A. Briggs, "Regional morphology of the transversus abdominis and obliquus internus and externus abdominis muscles," *Clin. Biomech.*, vol. 20, no. 3, pp. 233–241, 2005. DOI: 10.1016/j.clinbiomech.2004.11.007.

[67] A. Jourdan *et al.*, "Numerical investigation of a finite element abdominal wall model during breathing and muscular contration," *Comput. Methods Programs Biomed.*, vol. 244, no. 107985, 2024. DOI: 10.1016/j.cmpb.2023.107985.

[68] I. A. Stokes and M. Gardner-Morse, "Quantitative anatomy of the lumbar musculature," *J. Biomech.*, vol. 32, no. 3, pp. 311–316, 1999. DOI: 10.1016/S0021-9290(98)00164-X.

[69] S. M. McGill, "A revised anatomical model of the abdominal musculature for torso flexion efforts," *J. Biomech.*, vol. 29, no. 7, pp. 973–977, 1996. DOI: 10.1016/0021-9290(95)00148-4.

[70] T. J. Coleman *et al.*, "Development of a wireless intra-vaginal transducer for monitoring intra-abdominal pressure in women," *Biomed. Microdevices*, vol. 14, no. 2, pp. 347–355, 2012. DOI: 10.1007/s10544-011-9611-x..

[71] T. J. Coleman *et al.*, "Effects of walking speeds and carrying techniques on intra-abdominal pressure in women," *Int. Urogynecol. J.*, vol. 26, pp. 967–974, 2015. DOI: 10.1007/s00192-014-2593-5.

[72] P. W. Hodges, A. G. Cresswell, K. Daggfeldt, and A. Thorstensson, "In vivo measurement of the effect of intra-abdominal pressure on the human spine," *J. Biomech.*, vol. 34, no. 3, pp. 347–353, 2001. DOI: 10.1016/s0021-9290(00)00206-2.

[73] M. Paiva *et al.*, "Mechanical implications of in vivo human diaphragm shape," *J. Appl. Physiol. (1985)*, vol. 72, no. 4, pp. 1407–1412, 1992. DOI: 10.1152/jappl.1992.72.4.1407.

[74] J. I. Seok, S. Y. Kim, F. O. Walker, S. G. Kwak, and D. H. Kwon, "Ultrasonographic findings of the normal diaphragm: Thickness and contractility," *Ann. Clin. Neurophysiol.*, vol. 19, no. 2, pp. 131–135, 2017. DOI: 10.14253/kjcn.2017.19.2.131.

[75] M. Driscoll, "Fascia – the unsung hero of spine biomechanics," *J. Bodyw. Mov. Ther.*, vol. 22, no. 1, pp. 90–91, 2018. DOI: 10.1016/j.jbmt.2017.10.014.

[76] F. H. Willard, A. Vleeming, M. D. Schuenke, L. Danneels, and R. Schleip, "The thoracolumbar fascia: Anatomy, function and clinical considerations," *J. Anat.*, vol. 221, no. 6, pp. 507–536, 2012. DOI: 10.1111/j.1469-7580.2012.01511.x.

[77] P. Barker and C. A. Briggs, "Attachments of the posterior layer of lumbar fascia," *Spine*, vol. 24, no. 17, pp. 1757–1764, 1999.

[78] E. Newell and M. Driscoll, "Mechanical evaluation of human cadaveric lumbar soft tissues suggests possible physiological stress shielding within musculoskeletal soft tissues by the thoracolumbar fascia," *IEEE Trans. Biomed. Eng.*, vol. 71, no. 9, pp. 2678–2683, 2024. DOI: 10.1109/TBME.2024.3387343.

[79] M. Kirilova, S. Stoytchev, D. Pashkouleva, and V. Kavardzhikov, "Experimental study of the mechanical properties of human abdominal fascia," *Med. Eng. Phys.*, vol. 33, no. 1, pp. 1–6, 2011. DOI: 10.1016/j.medengphy.2010.07.017.

[80] A. Berardo, L. Bonaldi, C. Stecco, and C. G. Fontanell, "Biomechanical properties of the human superficial fascia: Site-specific variability and anisotropy of abdominal and thoracic regions," *J. Mech. Behav. Biomed. Mater.*, vol. 157, no. 106637, 2024. DOI: 10.1016/j.jmbbm.2024.106637.

[81] *Intra-abdominal hypertension and the abdominal compartment syndrome: updated consensus definitions and clinical practice guidelines from the World Society of the Abdominal Compartment Syndrome*, vol. 39, 7, The Abdominal Compartment Society, 2013, pp. 1190–1206. DOI: 10.1007/s00134-013-2906-z.

[82] M. L. Malbrain *et al.*, "The role of abdominal compliance, the neglected parameter in critically ill patients — a consensus review of 16. part 1: Definitions and pathophysiology," *Anaesthesiol. Intensive Ther.*, vol. 46, no. 5, pp. 392–405, 2014. DOI: 10.5603/AIT.2014.0062.

[83] G. E. Tzelepis, L. Nasiff, F. D. McCool, and J. Hammond, "Transmission of pressure within the abdomen," *J. Appl. Physiol. (1985)*, vol. 81, no. 3, pp. 1111–1114, 1996. DOI: 10.1152/jappl.1996.81.3.1111.

[84] M. Hagins, M. Pietrek, A. Sheikhzadeh, M. Nordin, and K. Axen, "The effects of breath control on intra-abdominal pressure during lifting tasks," *Spine*, vol. 29, no. 4, pp. 464–469, 2004. DOI: 10.1097/01.brs.0000092368.90019.d8.

[85] M. Kawabata, N. Shima, and H. Nishizono, "Regular change in spontaneous preparative behaviour on intra-abdominal pressure and breathing during dynamic lifting," *Eur. J. Appl. Physiol.*, vol. 114, no. 11, pp. 2233–2239, 2014. DOI: 10.1007/s00421-014-2944-4.

[86] S. M. McGill and R. Norman, "Reassessment of the role of intra-abdominal pressure in spinal compression," *Ergonomics*, vol. 30, no. 11, pp. 1565–1588, 1987. DOI: 10.1080/00140138708966048.

[87] K. Daggfeldt and A. Thorstensson, "The role of intra-abdominal pressure in spinal unloading," *J. Biomech.*, vol. 30, no. 11, pp. 1149–1155, 1997. DOI: 10.1016/S0021-9290(97)00096-1.

[88] S. M. McGill and M. T. Sharratt, "Relationship between intra-abdominal pressure and trunk emg," *Clin. Biomech.*, vol. 5, pp. 59–67, 1990.

[89] A. G. Cresswell, H. Grundström, and A. Thorstensson, "Observations on intra-abdominal pressure and patterns of abdominal intra-muscular activity in man," *Acta. Physiol. Scand.*, vol. 144, pp. 409–418, 1992.

[90] D. A. Hackett and C. M. Chow, "The valsalva maneuver: Its effect on intra-abdominal pressure and safety issues during resistance exercise," *J. Strength Cond. Res.*, vol. 27, no. 8, pp. 2338–2345, 2013. DOI: 10.1519/JSC.0b013e31827de07d.

[91] M. Essendrop and B. Schibye, "Intra-abdominal pressure and activation of abdominal muscles in highly trained participants during sudden heavy trunk loading," *Spine*, vol. 29, no. 21, pp. 2445–2451, 2004. DOI: 10.1097/01.brs.0000143622.80004.bf.

[92] D. Juker, S. Mcgill, P. Kropf, and T. Steffen, "Quantitative intramuscular myoelectric activity of lumbar portions of psoas and the abdominal wall during a wide variety of tasks," *Med. Sci. Sports Exerc.*, vol. 30, no. 2, pp. 301–310, 1998.

[93] A. G. Cresswell and A. Thorstensson, "Changes in intra-abdominal pressure, trunk muscle activation," *Eur. J. Appl. Physiol. Occup. Physiol.*, vol. 68, no. 4, pp. 315–321, 1994. DOI: 10.1007/BF00571450.

[94] W. S. Cobb *et al.*, "Normal intraabdominal pressure in healthy adults," *J. Surg. Res.*, vol. 129, no. 2, pp. 231–235, 2005. DOI: 10.1016/j.jss.2005.06.015.

[95] F. Ghezelbash, A. Shirazi-Adl, M. Sharifi, N. Arjmand, and B. Bazrgari, "Chapter 4 - computational stability of human musculoskeletal systems," in *Digital Human Modeling and Medicine*, G. Paul and M. Hamdy Doweidar, Eds., Acad. Press, 2023, pp. 85–105. DOI: 10.1016/B978-0-12-823913-1.00025-7.

[96] M. M. Panjabi, "The stabilizing system of the spine," *J. Spinal Disord.*, vol. 5, no. 4, pp. 383–389, 1992. DOI: 10.1097/00002517-199212000-00001.

[97] S. M. McGill, "Low back stability: From formal description to issues for performance and rehabilitation," *Exerc. Sport Sci. Rev.*, vol. 29, no. 1, pp. 26–31, 2001. DOI: 10.1097/00003677-200101000-00006.

[98] E. Bourdon, R. B. Graham, and J. van Diëen, "A comparison of methods to quantify control of the spine," *J. Biomech.*, vol. 96, no. 109344, 2019. DOI: 10.1016/j.jbiomech.2019.109344.

[99] N. P. Reeves, K. S. Narendra, and J. Cholewicki, "Spine stability: The six blind men and the elephant," *Clin Biomech (Bristol)*, vol. 22, no. 3, pp. 266–274, 2007. DOI: 10.1016/j.clinbiomech.2006.11.011.

[100] V. K. goel, S. Goyal, C. Clark, K. Nishiyama, and T. Nye, "Whole lumbar spine: Effect of discectomy," *Spine*, vol. 10, no. 6, pp. 543–554, 1985.

[101] A. Rohlmann, S. Neller, L. Claes, G. Bergmann, and H.-J. Wilke, "Influence of a follower load on intradiscal pressure and intersegmental rotation of the lumbar spine," *Spine*, vol. 26, no. 24, E557–E561, 2001. DOI: 10.1097/00007632-200112150-00014.

[102] R. E. Kearney, R. B. Stein, and L. Parameswaran, "Identification of intrinsic and reflex contributions to human ankle stiffness dynamics," *IEEE Trans. Biomed. Eng.*, vol. 44, no. 6, pp. 493–504, 1997. DOI: 10.1109/10.581944.

[103] K. P. Granata, G. P. Slota, and B. C. Bennett, "Paraspinal muscle reflex dynamics," *J. Biomech.*, vol. 37, no. 2, pp. 241–247, 2004. DOI: 10.1016/s0021-9290(03)00249-5.

[104] F. De Groote, J. L. Allen, and L. H. Ting, "Contribution of muscle short-range stiffness to initial changes in joint kinetics and kinematics during perturbations to standing balance: A simulation study," *J. Biomech.*, vol. 55, pp. 71–77, 2017. DOI: 10.1016/j.jbiomech.2017.02.008.

[105] E. Maaswinkel, M. Griffioen, R. S. G. M. Perez, and J. H. van Dieën, "Methods for assessment of trunk stabilization, a systematic review," *J. Electromyogr. Kinesiol.*, vol. 26, pp. 18–35, 2016. DOI: 10.1016/j.jelekin.2015.12.010.

[106] M. Solomonow, "Time dependent spine stability: The wise old man and the six blind elephants," *Clinical Biomechanics*, vol. 26, no. 3, pp. 219–228, 2011. DOI: 10.1016/j.clinbiomech.2010.10.010.

[107] J. Cholewicki and S. M. McGill, "Mechanical stability of the in viva lumbar spine: Implications for injury and chronic low back pain," *Clin. Biomech. (Bristol)*, vol. 11, no. 1, pp. 1–15, 1996. DOI: 10.1016/0268-0033(95)00035-6.

[108] F. Ghezelbash, A. Shahvarpour, C. Larivière, and A. Shirazi-Adl, "Evaluating stability of human spine in static tasks: A combined in vivo-computational study," *Comput. Methods Biomech. Biomed. Eng.*, vol. 25, no. 10, pp. 1156–1168, 2022. DOI: 10.1080/10255842.2021.2004399.

[109] A. Bergmark, "Stability of the lumbar spine," *Acta Orthop. Scand.*, vol. 60, no. sup230, pp. 1–54, 1989. DOI: 10.3109/17453678909154177.

[110] B. Bazrgari, A. Shirazi-Adl, M. Trottier, and P. Mathieu, "Computation of trunk equilibrium and stability in free flexion-extension movements at different velocities," *J. Biomech.*, vol. 41, no. 2, pp. 412–421, 2008. DOI: 10.1016/j.jbiomech.2007.08.010.

[111] Z. El Ouaaid, A. Shirazi-Adl, and A. Plamondon, "Effects of variation in external pulling force magnitude, elevation, and orientation on trunk muscle forces, spinal loads and stability," *J. Biomech.*, vol. 49, no. 6, pp. 946–952, 2016. DOI: 10.1016/j.jbiomech.2015.09.036.

[112] C. Larivière *et al.*, "Identification of intrinsic and reflexive contributions to low-back stiffness: Medium-term reliability and construct validity," *J. Biomech.*, vol. 48, no. 2, pp. 254–261, 2015. DOI: 10.1016/j.jbiomech.2014.11.036.

[113] M. Lortie and R. E. Kearney, "Identification of physiological systems: Estimation of linear time-varying dynamics with non-white inputs and noisy outputs," *Med. Biol. Eng. Comput.*, vol. 39, no. 3, pp. 381–390, 2001. DOI: 10.1007/BF02345295.

[114] D. L. Guarín and R. E. Kearney, "Estimation of time-varying, intrinsic and reflex dynamic joint stiffness during movement," *Front. Comput. Neurosci.*, vol. 11, no. 51, 2017. DOI: 10.3389/fncom.2017.00051.

[115] K. P. Granata and S. A. England, "Stability of dynamic trunk movement," *Spine*, vol. 31, no. 10, E271–E276, 2006. DOI: 10.1097/01.brs.0000216445.28943.d1.

[116] R. B. Graham and S. H. Brown, "Local dynamic stability of spine muscle activation and stiffness patterns during repetitive lifting," *J. Biomech. Eng.*, vol. 136, no. 12, p. 121 006, 2014. DOI: 10.1115/1.4028818.

[117] I. A. Stokes, "Mechanical function of facet joints in the lumbar spine," *Clin. Biomech.*, vol. 3, no. 2, pp. 101–105, 1988. DOI: 10.1016/0268-0033(88)90052-6.

[118] A. B. Schultz, D. N. Warwick, M. H. Berkson, and A. L. Nachemson, "Mechanical properties of human lumbar spine motion segments—part i: Responses in flexion, extension, lateral bending, and torsion," *J. Biomech. Eng.*, vol. 101, no. 1, pp. 46–52, 1979. DOI: 10.1115/1.3426223.

[119] M. Pope and M. Panjabi, "Biomechanical definitions of spinal instability," *Spine*, vol. 10, no. 3, pp. 255–256, 1985.

[120] I. El Bojairami, "Assessment of static spinal stability and muscle activation strategies: A comprehensive approach via a novel validated finite element spine model inclusive of thoracolumbar fascia, intramuscular pressure, and intra-abdominal pressure," Ph.D. dissertation, McGill University, 2021.

[121] A. G. Patwardhan, R. M. Havey, K. P. Meade, B. Lee, and B. Dunlap, "A follower load increases the load-carrying capacity of the lumbar spine in compression," *Spine*, vol. 24, no. 10, pp. 1003–1009, 1999.

[122] M. Rao, "Explicit finite element modeling of the human lumbar spine," Ph.D. dissertation, University of Denver, 2012.

[123] A. Rohlmann, T. Zander, M. Rao, and G. Bergmann, "Realistic loading conditions for upper body bending," *J. Biomech.*, vol. 42, pp. 884–890, 2009. DOI: 10.1016/j.jbiomech.2009.01.017.

[124] J. Cholewicki, K. Juluru, and S. M. McGill, "Intra-abdominal pressure mechanism for stabilizing the lumbar spine," *J. Biomech.*, vol. 32, no. 1, pp. 13–17, 1999. DOI: 10.1016/S0021-9290(98)00129-8.

[125] C. Lariviére, J.-A. Boucher, H. Mecheri, and D. Ludvig, "Maintaining lumbar spine stability: A study of the specific and combined effects of abdominal activation and lumbosacral orthosis on lumbar intrinsic stiffness," *J. Orthop. Sports. Phys. Ther.*, vol. 49, no. 4, pp. 262–271, 2019. DOI: 10.2519/jospt.2019.8565.

[126] J. Cholewicki, K. Juluru, A. Radebold, M. M. Panjabi, and S. M. McGill, "Lumbar spine stability can be augmented with an abdominal belt and/or increased intra-abdominal pressure," *E. Spine J.*, vol. 8, pp. 388–395, 1999. DOI: 10.1007/s005860050192.

[127] K. M. Tesh, J. S. Dunn, and J. H. Evans, "The abdominal muscles and vertebral stability," *Spine (Phila Pa 1976)*, vol. 12, no. 5, pp. 501–508, 1987. DOI: 10.1097/00007632-198706000-00014.

[128] A. Vleeming, M. D. Schuenke, L. Daneels, and F. H. Willard, "The functional coupling of the deep abdominal and paraspinal muscles: The effects of simulated paraspinal muscle contraction on force transfer to the middle and posterior layer of the thoracolumbar fascia," *J. Anat.*, vol. 255, no. 4, pp. 447–462, 2014. DOI: 10.1111/joa.12227.

[129] K. El-Monajjed and M. Driscoll, "A finite element analysis of the intra-abdominal pressure and paraspinalmuscle compartment pressure interaction through the thoracolumbar fascia," *Comput. Methods Biomech. Biomed. Eng.*, vol. 23, no. 10, pp. 585–596, 2020. DOI: 10.1080/10255842.2020.1752682.

[130] S. A. Ferguson and W. S. Marras, "A literature review of low back disorder surveillance measures and risk factors," *Clin. Biomech.*, vol. 12, no. 4, pp. 211–226, 1997. DOI: 10.1016/S0268-0033(96)00073-3.

[131] W. S. Marras *et al.*, "The role of dynamic three-dimensional trunk motion in occupationally-related low back disorders," *Spine*, vol. 18, no. 5, pp. 617–628, 1993. DOI: 10.1097/00007632-199304000-00015.

[132] W. S. Marras *et al.*, "Biomechanical risk factors for occupationally related low back disorder," *Ergonomics*, vol. 38, no. 2, pp. 377–410, 1995. DOI: 10.1080/00140139508925111.

[133] S. M. McGill, "Chapter 2 - Epidemiological studies and what they really mean," in *Low back disorders: evidence-based prevention and rehabilitation*, 3rd ed. Human Kinetics, 2016, pp. 29–48.

[134] A. H. McGregor, I. D. McCarthy, and S. P. Hughes, "Motion characteristics of the lumbar spine in the normal population," *Spine*, vol. 20, no. 22, pp. 2421–2428, 1995.

[135] D. R. McIntyre, L. H. Glover, M. C. Conino, R. H. Seeds, and J. A. Levene, "A comparison of the characteristics of preferred low-back motion of normal subjects and low-back-pain patients," *J. Spinal Disord.*, vol. 4, no. 1, pp. 90–95, 1991.

[136] L. Johnen, M. Schaub, A. Mertens, V. Nitsch, and C. Brandl, "Can cumulative loading estimates be used to assess the collective occupational risk of msd? evaluation of calculation methods for spinal cumulative loading," *Int. J. Ind. Ergon.*, vol. 92, no. 103361, 2022. DOI: 10.1016/j.ergon.2022.103361.

[137] E. Wagnac, P.-J. Arnoux, A. Garo, and C.-E. Aubin, "Finite element analysis of the influence of loading rate on a model of the full lumbar spine under dynamic loading conditions," *Med. Biol. Eng. Comput.*, vol. 50, pp. 903–915, 2012. DOI: 10.1007/s11517-012-0908-6.

[138] J. L. Wang, M. Parnianpour, A. Shirazi-Adl, A. E. Engin, S. Li, and A. Patwardhan, "Development and validation of a viscoelastic finite element model of an l2/l3 motion segment," *Theor. Appl. Fract. Mec.*, vol. 28, pp. 81–93, 1997.

[139] N. Arjmand and A. Shirazi-Adl, "Model and in vivo studies on human trunk load partitioning and stability in isometric forward flexions," *J. Biomech.*, vol. 39, pp. 510–521, 2006. DOI: 10.1016/j.jbiomech.2004.11.030.

[140] B. Bazrgari and A. Shirazi-Adl, "Spinal stability and role of passive stiffness in dynamic squat and stoop lifts," *Comput. Methods Biomech. Biomed. Eng.*, vol. 10, no. 5, pp. 351–360, 2007. DOI: 10.1080/10255840701436974.

[141] A. Plamondon, C. Lariviére, A. Delisle, D. Denis, and D. Gagnon, "Relative importance of expertise, lifting height and weight lifted on posture and lumbar external loading during a transfer task in manual material handling," *Ergonomics*, vol. 55, no. 1, pp. 87–102, 2012. DOI: 10.1080/00140139.2011.634031.

[142] F. Ghezelbash, Z. El Ouaaid, A. Shirazi-Adl, A. Plamondon, and N. Arjmand, "Trunk musculoskeletal response in maximum voluntary exertions: A combined measurement-modeling investigation," *J. Biomech.*, vol. 70, pp. 124–133, 2018. DOI: 10.1016/j.jbiomech.2017.11.007.

[143] J. Cholewicki, S. M. McGill, and R. W. Norman, "Comparison of muscle forces and joint load from an optimization and emg assisted lumbar spine model: Towards development of a hybrid approach," *J. Biomech.*, vol. 28, no. 3, pp. 321–331, 1995.

[144] R. Remus, S. Selkmann, A. Lipphaus, M. Neumann, and B. Bender, "Muscle-driven forward dynamic active hybrid model of the lumbosacral spine: Combined fem and multibody simulation," *Front. Bioeng. Biotechnol.*, vol. 11, pp. 1–23, 2023. DOI: 10.3389/fbioe.2023.1223007.

[145] A. A. Stokes, M. Gardner-Morse, and S. M. Henry, "Intra-abdominal pressure and abdominal wall muscular function: Spinal unloading mechanism," *Clin. Biomech.*, vol. 25, pp. 859–866, 2010. DOI: 10.1016/j.clinbiomech.2010.06.018.

[146] J. Guo, W. Duo, and G. Ren, "Embodiment of intra-abdominal pressure in flexible multibody model of the trunk and the spinal unloading effects during static lifting tasks," *Biomech. Model. Mechanobiol.*, vol. 20, pp. 1599–1626, 2021. DOI: 10.1007/s10237-021-01465-1.

[147] I. El Bojairami, K. El-Monajjed, and M. Driscoll, "Development and validation of a timely and representative finite element human spine model for biomechanical simulations," *Sci. Rep.*, vol. 20, no. 21519, Dec. 2020. DOI: 10.1038/s41598-020-77469-1.

[148] E. Bernier and M. Driscoll, "Numerical investigation of intra-abdominal pressure and spinal load-sharing upon the application of an abdominal belt," *J. Biomech.*, vol. 161, no. 111863, 2023. DOI: 10.1016/j.jbiomech.2023.111863.

[149] I. El Bojairami and M. Driscoll, "Coordination between trunk muscles, thoracolumbar fascia, and intra-abdominal pressure toward static spine stability," *Spine*, vol. 47, no. 9, E423–E431, 2022. DOI: 10.1097/BRS.0000000000004223.

[150] H. M. Langevin *et al.*, "Ultrasound evidence of altered lumbar connective tissue structure in human subjects with chronic low back pain," *BMC Musculoskelet. Disord.*, vol. 10, no. 151, 2009. DOI: 10.1186/1471-2474-10-151.

[151] C. Pirri *et al.*, "Ultrasound imaging of thoracolumbar fascia thickness: Chronic non-specific lower back pain versus healthy subjects; a sign of a "frozen back"?" *Diagnostics*, vol. 13, no. 8, 2023. DOI: 10.3390/diagnostics13081436.

[152] S. M. McGill, "Chapter 4 - normal and injury mechanics of the lumbar spine," in *Low back disorders: evidence-based prevention and rehabilitation*, 3rd ed. Human Kinetics, 2016, pp. 97–151.

[153] S. M. McGill, "Chapter 3 - Functional anatomy of the lumbar spine," in *Low back disorders: evidence-based prevention and rehabilitation*, 3rd ed. Human Kinetics, 2016, pp. 49–83.

[154] J. A. C. Martins, M. P. M. Pato, and E. B. Pires, "A finite element model of skeletal muscles," *Virtual Phys. Prototyp.*, vol. 1, no. 3, pp. 159–170, 2006. DOI: 10.1080/17452750601040626.

[155] W. Zeng *et al.*, "Modeling of active skeletal muscles: A 3d continuum approach incorporating multiple muscle interactions," *Front. Bioeng. Biotechnol.*, vol. 11, no. 1153692, 2023. DOI: 10.3389/fbioe.2023.1153692.

[156] "V&V 40 – Assessing credibility of computational modeling through verification and validation: application to medical devices," *ASME*, 2018.

[157] Stott *et al.*, "A critical comparison of comparators used to demonstrate credibility of physics-based numerical spine models," *Annals of Biomedical Engineering*, vol. 51, no. 1, pp. 150–162, 2023. DOI: 10.1007/s10439-022-03069-x.

[158] A. S. E. Staelens, "Intra-abdominal pressure measurements in term pregnancy and postpartum: An observational study," *PLoS One*, vol. 9, no. 8, e104782, 2014. DOI: 10.1371/journal.pone.0104782.

[159] Y. Hsu *et al.*, "Variables affecting intra-abdominal pressure during lifting in the early postpartum period," *Female Pelvic Med. Reconstr. Surg.*, vol. 24, no. 4, pp. 287–291, 2018. DOI: 10.1097/SPV.0000000000000462.

[160] N. Jacobson and M. Driscoll, "Validity and reliability of a novel, non-invasive tool and method to measure intra-abdominal pressure in vivo," *J. Biomech.*, vol. 137, p. 111 096, 2022. DOI: 10.1016/j.jbiomech.2022.111096.

[161] Wang *et al.*, "Bioadhesive ultrasound for long-term continuous imaging of diverse organs," *Science*, vol. 377, no. 6605, pp. 517–523, 2022. DOI: 10.1126/science.abo2542.

[162] E. Bernier, A. Mithani, A. Aoude, and M. Driscoll, "Feasibility of a novel back support device to improve spine stability and muscular activity during trunk flexion: A prospective cross-sectional study with healthy controls and low back pain subjects - preliminary," *Clin. Biomech.*, vol. 122, p. 106 414, 2025. DOI: 10.1016/j.clinbiomech.2024.106414.

[163] S. M. McGill, *Low back disorders: evidence-based prevention and rehabilitation*, 3rd ed. Human Kinetics, 2016.

Appendices

A Supporting Figures for the Spine Model

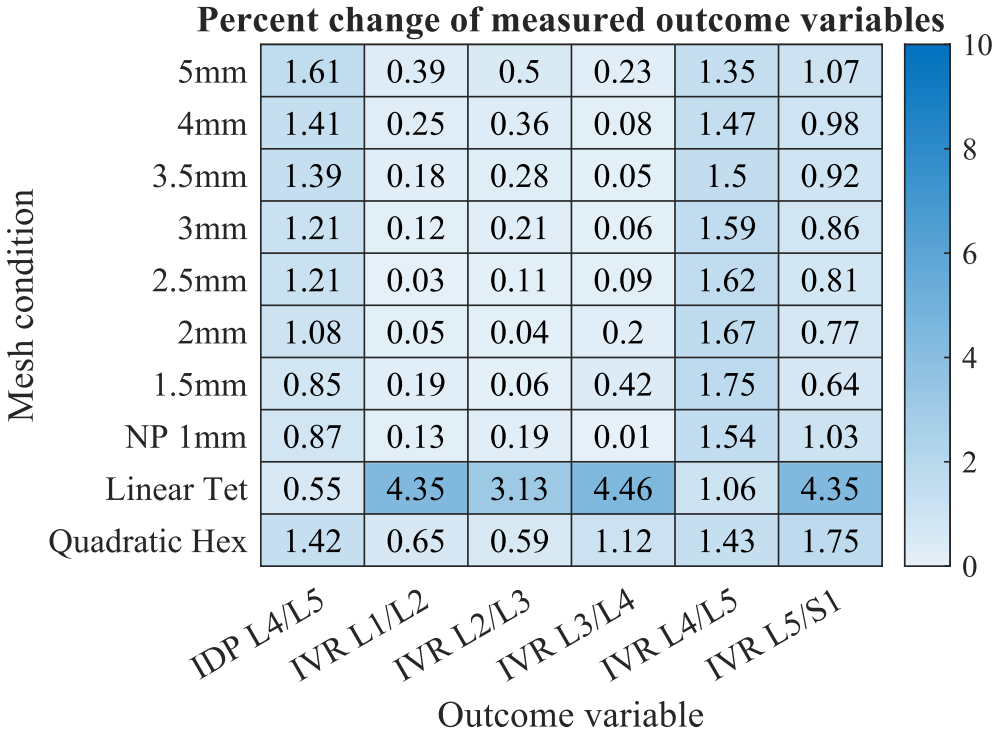

Figure A.0.1: Sensitivity analysis results for variations of the intervertebral disc.

$$IVR_{(t)} = \left[\theta_{L_i} - \theta_{L_{i-1}}\right]_{(t)} + \left[\theta_{L_i} - \theta_{L_{i-1}}\right]_{(t-1)}$$

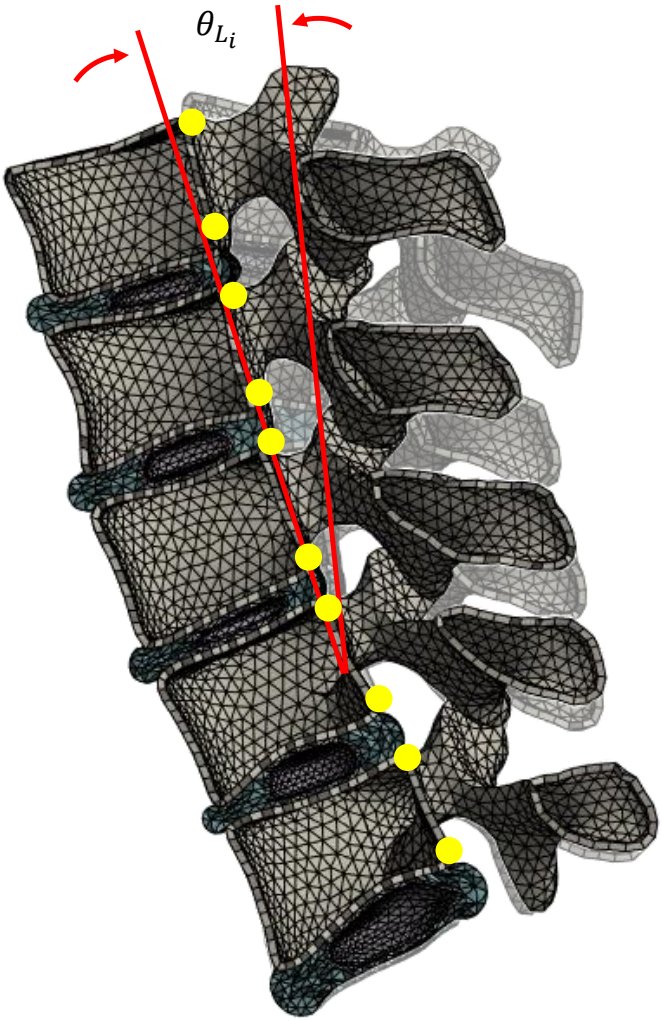

Figure A.0.2: Graphical representation of the script created to measure intervertebral rotations (IVRs).